283075

JPRS-CST-86-033

18 AUGUST 1986

China Report

SCIENCE AND TECHNOLOGY

19981021 107

DTIC QUALITY INSPECTED 4

FBIS **FOREIGN BROADCAST INFORMATION SERVICE**

134
A07

NOTE

JPRS publications contain information primarily from foreign
newspapers, periodicals and books, but also from news agency
transmissions and broadcasts. Materials from foreign-language
sources are translated; those from English-language sources
are transcribed or reprinted, with the original phrasing and
other characteristics retained.

Headlines, editorial reports, and material enclosed in brackets
[] are supplied by JPRS. Processing indicators such as [Text]
or [Excerpt] in the first line of each item, or following the
last line of a brief, indicate how the original information was
processed. Where no processing indicator is given, the infor-
mation was summarized or extracted.

Unfamiliar names rendered phonetically or transliterated are
enclosed in parentheses. Words or names preceded by a ques-
tion mark and enclosed in parentheses were not clear in the
original but have been supplied as appropriate in context.
Other unattributed parenthetical notes within the body of an
item originate with the source. Times within items are as
given by source.

The contents of this publication in no way represent the poli-
cies, views or attitudes of the U.S. Government.

PROCUREMENT OF PUBLICATIONS

JPRS publications may be ordered from the National Technical
Information Service, Springfield, Virginia 22161. In order-
ing, it is recommended that the JPRS number, title, date and
author, if applicable, of publication be cited.

Current JPRS publications are announced in Government Reports
Announcements issued semi-monthly by the National Technical
Information Service, and are listed in the Monthly Catalog of
U.S. Government Publications issued by the Superintendent of
Documents, U.S. Government Printing Office, Washington, D.C.
20402.

Correspondence pertaining to matters other than procurement
may be addressed to Joint Publications Research Service,
1000 North Glebe Road, Arlington, Virginia 22201.

CHINA REPORT

SCIENCE AND TECHNOLOGY

CONTENTS

ABSTRACTS

/7310

.

GROUP OFFICIALLY FORMED IN 1985 FOR CHARACTER CODING STANDARD

Beijing ZHONGGUO BIAOZHUNHUA [CHINA STANDARDIZATION] in Chinese No 8, Aug 85 p 1

[Jointly issued notice by the State Council Office of the Leading Group for Promotion of Electronics, the State Science and Technology Commission, and the State Bureau of Standards: "Circular Regarding Developing Technical Appraisals of Chinese Character Input Coding"]

[Text] The State Council Office of the Leading Group for Promotion of Electronics, the State Science and Technology Commission, and the State Bureau of Standards recently joined to issue the "Circular Regarding Developing Technical Appraisals of Chinese Character Input Coding" in hope that all relevant areas would take heed and support it.

The "Circular" points out that Chinese characters make up the working language of this country, and proper resolution of Chinese character data processing technologies is a key to the universal application of computers in China. In recent years, there has been much work done domestically on Chinese character input coding, many methods have been proposed, there have been many different plans for coding, and the optimization of these plans has become a problem in urgent need of resolution for the dissemination and application of data processing technologies. To enhance leadership and to do the work well, it is intended that the State Bureau of Standards take the lead and join with the China Chinese Language Information Research Conference to comprise a "Chinese Character Input Plan Evaluation Group" (the working group to depend upon the Institute of Information Categorization and Coding of the State Bureau of Standards).

The "Circular" states that the responsibilities of the working group will be: to assume responsibility for the overall plan and organization for the optimization of Chinese character input coding plans, and to progressively develop relevant standardization; to rely upon societies, to organize specialists to unify evaluation standards, and to integrate evaluation activities in organizing and coordinating relevant units in optimizing a feasible Chinese character input coding plan that suits our national situation, the results to be reported to the state for approval; and to be responsible for the collection and management of domestic Chinese character input plans.

The "Circular" requires that to review experiences and keep the work moving, a national appraisal activity is scheduled to be organized in October of this year [1985]. Chinese character input coding plans developed by departments, regions, or individuals may be volunteered or recommended for participation, for which request support from relevant sources. The optimized plan to be put forward during appraisal will be recommended for inclusion in the "National Exhibit of Computer Applications" to be held in 1986, for which relevant areas are requested to prepare well.

12586
CSO: 4008/1072

CHINESE CHARACTER TYPE MATRIX STANDARDS ISSUED

Beijing ZHONGGUO BIAOZHUNHUA [CHINA STANDARDIZATION] in Chinese No 8, Aug 85 pp 1-2

[Text] The State Bureau of Standards held a news conference 21 May [1985] in Beijing regarding Chinese written language information processing standards. At the conference, State Bureau of Standards Deputy Director Zhong Ming [6988 2494] issued two standards for Chinese written language information handling, the GB5007.1~2-85 "Character Matrix Sets and Data Sets for Information Exchange Using a 24 X 24 Matrix" and the GB5199.1~2-85 "Character Matrix Sets and Data Sets for Information Exchange Using a 15 X 16 Matrix." These two national standards began implementation on 1 June 1985 and 1 October 1985, respectively. At the same time, the State Bureau of Standards formally authorized the Department of Information at the Yanshan Computer Applications Research Center to be responsible for providing floppy disks and fixed-mask ROM (MASKROM) that have the complete dot matrix character matrix data sets, together with indexes, which will guarantee the accurate implementation of standards.

With the rapid development and application of our computer technology, many industrial and applications departments are in urgent need of a set of high quality, standardized Chinese character type matrices and type matrix data. Based on the requirements of national tasking regarding the scientific and technical problem of Chinese character type matrix sets and data sets, by recommendation of the Ministry of the Electronics Industry, units of the Information Department of the Yanshan Computer Applications Research Center and the Shanghai Institute of Printing Technology jointly developed standards for "24 X 24" and "15 X 16" dot matrices, and with the close cooperation of specialists and 2 years of thorough study and repeated experience, that task has been outstandingly accomplished. These two standards meet relevant regulations regarding national standards for the exchange coding of our Chinese characters; the two sets of type matrices use the publishing Song typeface scheme, the character shape dot matrices are accurate, the core is stable, strokes are fluid, and they suit relevant national scales for the written language. When comparing these character shapes with similar ones both in this country and abroad, the former are of a higher standard. Because of uniform writing of the standard and assigned provision of the standard product, not only will this lay the technical foundation for the unification of Chinese character output shapes in this country, for the development of

3

Chinese character optical recognition technologies, and the production of Chinese character terminals, but will also bring major economic and social results to the development of information technology in this country.

Finally, Deputy Director Zhong Ming made a concise policy explanation regarding the problem of protecting international cooperation in standardizing scientific and technical projects and protecting standardization rights. Based on the spirit of the "Resolution by the CPC Central Committee Regarding Restructuring of the Science and Technology System," the State Bureau of Standards intends to gradually develop international technical cooperation in information technology, including development of the standardization of science and technology projects such as Chinese character information technologies, and will as well have test sites. Particular affairs concerning the open door policy and cooperation with national standardization of science and technology will be the responsibility of the China Association of Standardization. He pointed out that if foreign companies want to directly use major Chinese research achievements in technology standardization, they must respect our rights. In addition, he also announced that based on the regulations in Item 3 of Section 2 of the "Standardized Inspection and Control Methods for the Import of Technology and Equipment" as jointly issued by the State Bureau of Standards, the State Planning Commission, the State Economics Commission, the State Science and Technology Commission, and the Ministry of Foreign Economic Relations and Trade, the State Bureau of Standards will join with relevant departments to undertake standardized inspections of computer equipment imported in lots in order to strengthen the uniform management of the technical standardization of information processing.

12586
CSO: 4008/1072

STANDARDS PLANNING MANAGEMENT SOFTWARE DESCRIBED

[Article by Zhan Yinghao [6124 5391 3185]: "A Computer Management System for Standards Planning"]

[Text] At present, to suit development of the national economy, many standards management departments have produced plans for formulation and revision of standards based on actual conditions. Because all departments are responsible for so many different standards and there are so many and they cover so much area, it is very troublesome to manually search out from planning how many of a certain kind of standard ought to be worked out in a given year from planning. Consequently, since computers have the capacity for high speed processing of data, if they are used to accomplish this work, then that will be very convenient and quick.

After a computer retrieval system was established for standards documents, we began a computer management system for standards planning in early 1985, which put automation of standards planning and management into effect in a timely manner.

I. The Overall Structure of the Computer Management System for Standards Planning

The standards planning computer management system is composed of the following four independent subsystems (see diagram):

Standards Planning Management System
|
↓
password OK
|
↓

```
  ┌─────────────────────────────────┬──────────────────────────┐
  ↓                 ↓                ↓                          ↓
subsystem for    subsystem for    subsystem to              subsystem to
setting up and   database search  generate inverted         generate reports
renewing database                 files
  ↓                 ↓                ↓                          ↓
```
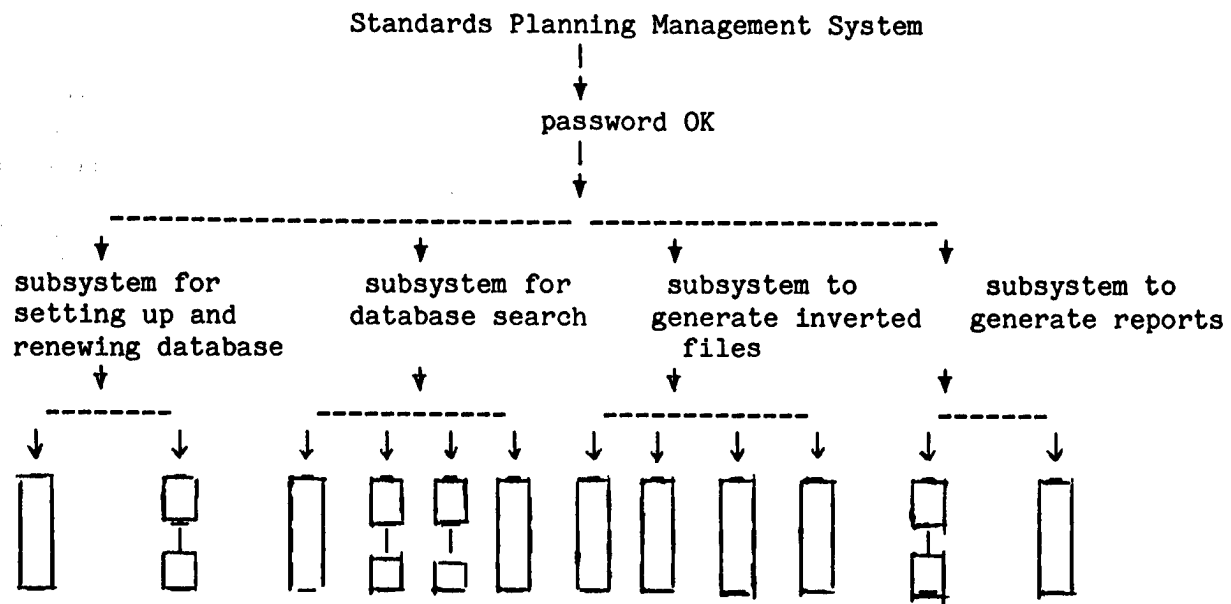
Overall Diagram of Standards Planning Management

Each subsystem is composed of mutually independent function modules, and these function modules are in turn comprised of several related or parallel subsystems.

1. Subsystem to establish and renew the database.

Taking practical use into consideration, database records are composed of a number, name of standard, number of document category for the standard, date of drafting, date of approval, level of the standard, number of standards, drafting unit, and managing unit, and each record has a fixed length of 256 bytes. The main file of the database is the set of these various records.

In the subsystem to establish and renew the database, a series of operations may be performed on the main file of the database, such as setting up, revising, inserting, and deleting.

2. Subsystem for database searching.

Because the management system for standards planning caters to standardization management personnel, to free these people from a lot of retrieval and statistics work, five different paths have been established in the database retrieval subsystem: retrieval and statistics by category, retrieval and statistics by date of drafting, retrieval and statistics by date of approval, retrieval and statistics by drafting unit, and retrieval and statistics by combinations.

a. The path of retrieval and statistics by category. The categorizing methods we have used are the "Methods for Categorizing China's Standards Documents (provisional)", which in the future is certain to be well known by

standards management personnel in this country, and which will then have greater practical use.

b.   The path of linked retrieval and statistics. This path does an arbitrary logical combination of the five data items: standards document category number, drafting unit, managing department, date of drafting, and date of approval, and the computer can find standards plans that satisfy the logical expression from the main file of the database. For example, it can retrieve certain kinds of standards through this path by the particular year and drafting unit.

c.   The path of retrieval and statistics by date of drafting. This path retrieves standards by date drafting began through drafting date inverted files and the database main file, which is of great convenience to standards management departments when formulating annual planning.

d.   The path of retrieval and statistics by date of approval. Through retrieval of date of drafting inverted files and the database main file, management personnel can be aware of standards sent for approval each year and their numbers, which consequently allows for approval according to a rational arrangement by date.

e.   The path of retrieval and statistics by drafting unit. Through a computer search of drafting unit inverted files and the database main file, this allows people to know the standards drafted by a particular unit and their numbers.

The five retrieval paths each set up its own counter so that all can compile the numbers of the standards plans that satisfy retrieval requirements.

3.   Subsystem for generation of inverted files.

There are four inverted files in the standards planning management system. They are categorical inverted files, drafting unit inverted files, drafting date inverted files, and approval date inverted files. These inverted files are automatically generated as the main file of the database is set up, they are the core files for retrieval, and it is they through which rapid retrieval according to the four modes of category, drafting unit, drafting date, and approval date is realized.

4.   Subsystem for report generation.

To satisfy different management requirements, the standards planning management system includes a report generation subsystem. In reports from the report generation subsystem, the report formats may be arbitrarily changed, and management personnel may interactively define report output formats to their own satisfaction. Standards plans that satisfy retrieval requirements may be output on a printer or a terminal.

II. Software Design Characteristics of the Standards Planning Management System

1. Using an advanced database management system (DBMS).

Having used a database management system to write the standards planning management system software allows the data to be least redundant, so that it can serve in many applications in the optimal format: data may be shared; data storage is independent of using its application program, that is, data is independent.

2. Quick response time.

Because the advanced techniques of B+ tree search organizational structure and inverted files has been used in the standards planning management system software, this allows the computer to access any file in the database within 2 seconds.

3. Varied retrieval and statistics paths.

The standards planning management system software sets up the five retrieval and statistics paths: standards document categories, standards drafting units, standards drafted year, standards approval year, and combinations. It is especially the semi-programming techniques in the combination searches of macro substitutions, reverse Polish exchange, and intermediary code generation that allows the user to undertake various logical combinations (AND, OR, NOT) of the five data items: standards document category, standards drafting unit, standards management unit, standards drafted year, and standards approval year. The number of logical expressions that can be formed is given in:

$$C^1 + 3C^2 + 3^2C^3 + 3^3C^4 + 3^4C^5 = 5 + 30 + 90 + 135 + 81 = 341$$

That is, there are 341 different ways to search the main file of the database using the combination retrieval and statistics path, and it may be said that with so many changes, this will be very convenient for various kinds of users.

4. User defined report formats.

Because the standards planning management system software has used a database management system (DBMS), this basically solves the deficiency in file management systems whereby data cannot be interchanged, for the software can combine various different data files for report output, and the user can define the report output format that he needs in the report generation subsystem. The computer will then print out reports based on this format.

III. Conclusions

Currently, the standards planning management system software is running regularly on a Cromemco computer. Because the currently domestically popular Great Wall 0520, IBM-PC/XT, and compatibles are all available with a database management system similar to that of the Cromemco, the standards planning management system software can be transferred to the IBM-PC/XT and compatibles

with nearly no changes. This gives the software a strong hardware adaptability.

The standards planning management system has just been established, there are many areas that need more work, and so we will continue to be diligent so that we can make new contributions to modernizing our standardization work.

12586
CSO: 4008/1072

APPLIED SCIENCES

COMPUTER USE IN CALCULATING POWER SUPPLY NETWORK LOSSES

Xian DIANLI DIANZI JISHU [POWER ELECTRONICS] in Chinese No 1, 1 Feb 86 pp 44-48

[Article by Shen Qingyue [3088 1987 6460]]

[Text] Computers are increasingly used today in engineering calculations, and
because of their speed, large memory capacity, precision, and the availability
of external recording devices, they have greatly increased the efficiency with
which engineering calculations can be performed. In particular, the availabil-
ity of pocket calculators and microcomputers has opened up new areas in applied
computing.

Computers are widely employed in electric power systems, and the calculation
of network losses is only one of many possible applications. However, it is
an important one because power networks are widely used in both urban and rural
areas. Since the calculations are both useful and flexible, we will illustrate
them here by discussing a program for calculating network losses using a
PC-1500 pocket calculator. The PC-1500 has an 8-bit central processing unit
and comes with 16K of firmware for supporting the BASIC language. The internal
storage can be increased ty 26K, although one 8K memory module suffices for our
application. The computer has a one-line liquid crystal display and cassette
for external storage. The microprinter available for the PC-1500 is of partic-
ular note--it is four-directional, prints in four colors, and has two operating
modes; moreover, it can handle Chinese-language databases and produce output in
Chinese characters, and it is equipped with internal memory which is reserved
for printing applications. Only a CE-158 interface cable is needed to permit
the printer to communicate with the microcomputer. The PC-1500 is well suited
for calculating network losses when the total number of calculations is not
too great and a high degree of flexibility is desired.

1. Algorithm for Calculating Network Losses

There are two methods that are widely used to calculate electric power losses
in networks--one uses the average value of the electric current, while the
other (current-squared) method requires sampling the current at regular inter-
vals and forming the sum of the squares. Either method is suitable for
computer implementation, and the choice depends on the properties of the
computer and the characteristics of the power grid.

10

Before the calculations can be carried out, initial data must be input to the computer. These data should be measured as accurately as possible, with sources of human error eliminated; however, the meters themselves have a finite error which must also be taken into account. In the current-squared method, the parameters characterizing the environment do not have to be supplemented by additional correction parameters, and neither voltage values nor electric meters are required. Although the hourly current readings for a given day must be processed to give a representative daily current and derive a network loss figure valid for that day, the required calculations are easily carried out on a computer.

In the time-squared method, the network current is calculated in terms of certain parameters K_i called the current drop ratios. Since the currents in the various parts of the network depend on user demand, which is easily measured, the total current withdrawn from successive stages of the network can be found and the corresponding drops K_i calculated. Since the power is proportional to I^2R, the equivalent resistance for stage i of the circuit from which a known current is withdrawn is given by multiplying the resistance R_i of the section by $K_i{}^2$. The output resistance is the sum of the equivalent resistances for each stage.

In addition to the losses in the wires, networks also suffer from ac power losses and from losses in power meters and lines connecting the grid to the users. The ac losses are calculated in terms of the nominal parameter values but can be corrected (if the grid and meter voltages differ significantly) by taking the ratio of the grid and meter voltages; the other losses can be calculated by taking appropriate ratios of the total electricity passing through the various stages of the network.

The detailed steps for calculating the daily losses are as follows:

(1) First, calculate the equivalent resistance $R_i' = R_iK_i$ of the i-th stage; here R_i is the resistance of stage i and

$$K_i = \frac{A_i + A_{i+1} + \cdots\cdots\cdots + An}{A_1 + A_2 + \cdots\cdots + A_1 + \cdots\cdots + An}$$

where A_i is the time-integrated current (charge) flowing through stage i.

(2) The output resistance is then given by the sum

$$R = R_1' + R_2' + \cdots\cdots + Rn' = \sum_{i=1}^{n} R_i'$$

where n is the number of stages in the network.

(3) One then computes the sum of the squares

$$I = I_1^2 + I_2^2 + \cdots\cdots + I_{24}^2 = \sum_{i=1}^{24} I_1{}^2$$

11

of the daily current readings; here I_i is the output current sampled at time $t = i$ hours.

(4) The loss rate in the network wires is then given by

$$\Delta A_d \text{ percent} = \frac{I \cdot 3R \cdot 10^{-3}}{A_{ds}} \times 100$$

where A_{ds} is the total electricity supplied per day.

(5) The power loss in the wires is then

$$\Delta A_L = A_s \cdot \Delta A \cdot \text{percent} \cdot (P_{ma}/P_{da}) \cdot K_R/100$$

where A_s is the average electricity delivered per month; P_{ma} and P_{da} are the monthly and daily average loads; T_m and T_d are the number of hours during the month or day when electricity is supplied; the factor K_R corrects for ambient temperature (see Table 1).

Table 1.

Type	Quarter 1	2	3	4	Yearly total
Loss in network wires	0.95	1.05	1.1	1.0	1.05
Loss in transformer windings	1.0	1.10	1.15	1.05	1.1

(6) The equivalent resistance for the ac losses is given by

$$R_T = P_T \cdot 10^3 / (S \cdot 0.0577)^2$$

$$P_T = P_1 + P_2 + \cdots\cdots + Pn = \sum_{i=1}^{n} P_i$$

$$S = S_1 + S_2 + \cdots\cdots + Sn = \sum_{i=1}^{n} S_i$$

where P_i is the power loss in the transformer (copper loss) for stage i of the network, and S_i is the corresponding rated capacitance of the transformer.

(7) The power delivered at low voltage to the user is described by

$$K_D = \frac{A_1 + A_2 + \cdots\cdots + An - A_{HV}}{A_1 + A_2 + \cdots\cdots + An}$$

where A_{HV} is the electricity supplied at high voltage.

(8) The copper losses in the transformers are given by the product

$$\Delta A_c = (I \cdot K_D \cdot 10^{-3} \cdot R_T \circ (P_{ma}/P_{da})^2 \cdot (T_m/T_d) \cdot K_R$$

(9) The losses in the transformer cores are

$$\Delta A_I = B \cdot T_m$$

$$B = B_1 + B_2 + \cdots\cdots + Bn = \sum_{i=1}^{n} B_i$$

where B_i is the rated core loss for transformer i.

(10) The remaining losses caused by connecting the users to the grid and the losses from other sources are given by

$$\Delta Au = A_{ms} \cdot K_D \cdot 1 \text{ percent}$$

(11) The total network loss is given by the sum

$$\Delta A = \Delta A_L + \Delta A_C + \Delta A_I + \Delta A_\nu$$

2. Program

The program for calculating the losses breaks into two main parts which compute the wire losses and the transformer, user connection, and other losses, respectively. The losses in the network wires comprise a large fraction of the total losses and the principal step in their calculation is to find the equivalent resistances R_i'. In accordance with the structure of the network, this portion of the program is divided into two parts which describe the main power lines and their branches, respectively.

The initial values needed in the calculations are input interactively by the user. However, since this method makes it impossible to correct input errors, the program also lists the values. If inspection reveals an error, the incorrect value(s) can be changed. The data are arranged as matrices; each matrix corresponding to a specific physical parameter, and each matrix element gives the value of the parameter for a specific stage of the network. The data used to calculate the transformer losses are organized in the same way, so that the calculations primarily involve matrix operations.

The computed results can be output in tabular form or schematically, in which the network is represented by a sequence of nodes with the equivalent resistances displayed. After the program has terminated, the results can be output in either of these two forms as many times as desired. The tables are provided with Chinese-language captions to make them easier to interpret. The Chinese characters are printed out in graphics mode; each time a character is to be printed, a printer subroutine is called which outputs the numeric codes corresponding to the dot pattern stored in graphics memory for the character.

3. A flowchart of the program is presented. We will illustrate it by going through a specific example of which we calculate the network losses for a farming village on the outskirts of a city. Because the primary network contains some branch lines which are little-used (or else are so short that they have little influence on the total losses), the network model is first simplified by incorporating these branches into others; the branches and the corresponding parameters of the resulting network are shown in Figure 2.
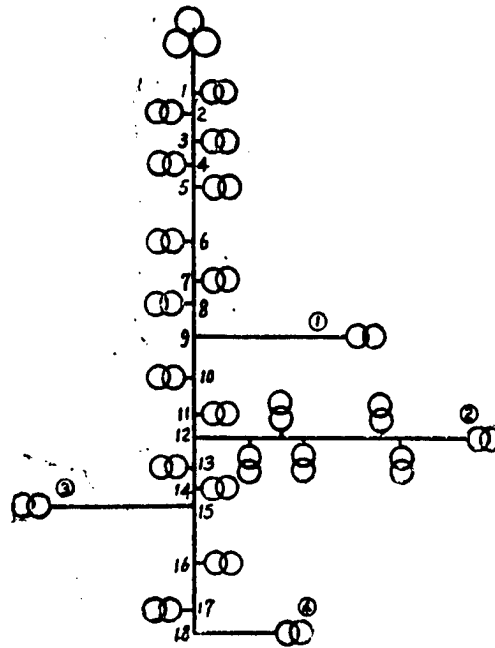
Figure 2.

Table 2.

Node	kwh	Resistance	Node	kwh	Resistance
1	4,608	0.63	Branch 1:		
2	7,693	0.11	1	38,828	2
3	600	0.37	Branch 2:		
4	7,266	0.2	1	6,879	0.77
5	3,560	0.2	2	3,096	0.36
6	12,630	0.6	3	23,419	1.28
7	18,355	0.38	4	22,023	0.42
8	10,275	0.1	5	9,754	0.18
9	38,828	0.3	6	50,733	1.28
10	18,896	0.31			
11	3,500	0.37	Branch 3:		
12	115,904	0.16	1	57,295	2.4
13	6,895	0.26	Branch 4:		
14	7,154	0.11	1	55,298	1.7
15	57,295	0.1			
16	1,155	0.61			
17	9,543	0.3			
18	55,298	0.07			

```
                          ( Start )
                             |
         / Node current    A_t(I)                        /
        /  Resistance of stage I    R(I)                /
                             |
                          ( Is
                          there a )---------------- N ----------+
                          branch?)                              |
                             |                                  |
        / Input parameters, Node current  B(I, J)   /           |
       /  for branch J  :   resistance    BR(I, J) /            |
                             |<-------------------------------- +
                    [ A_3 = ΣA1(I) + ΣB1(I) ]
                             |
    +------------------------------------------------------+
    |  Compute...    A_2 = A_2 - A_1(I-1)                   |
    |  for the       RD(I) = R(I)*(A^2 1A3)**2             |
    |  main line     RD = RD + RD(I)                        |
    +------------------------------------------------------+
      |                      |
      |     N --------( Done? )
      +---------------------->| Y
    +------------------------------------------------------+
    |  Compute...    B_2 = B_2 - B1(I, J)                   |
    |  for the       BD(I, J) = BR(I, J)*(B_2/A_3)**2      |
    |  branches      BD = BD + BD(I, J)                     |
    +------------------------------------------------------+
      |                      |
      |     N --------( Done? )
      +---------------------->|
                  / Input the output                 /
                 /  parameters of the network       /
                             |
    +------------------------------------------------------+
    | Calculate    IS =  I_1                                |
    | the          A percent = IS*3*RD*10^- /AD             |
    | losses       A = AM*A percent*(PM/PD)*KR              |
    +------------------------------------------------------+
                             |
                  / Input parameters                  /
                 /  for the transformers             /
                             |
    +------------------------------------------------------+
    | Calculate     RT = TC/(TS*0.0577)**2                 |
    | transformer,  KD = (A_3 - A_H)/A                      |
    | user-         AC=IS*KD*RT*(PM/PD)II2I(KR+0.05)*       |
    | connection,   AI = TI*TM              (TM/TD)         |
    | and other     AT = AC*AI                              |
    | losses...     AU = AM*KP*0.01                         |
    +------------------------------------------------------+
                             |
              [ Output results in tabular form ]
                             |
                    ( Schematic )----- N -----( Stop )
                    ( desired?  )
                             | Y
              +--------------------------------+
              | Print circles ⊖                |
              | showing node position          |
              +--------------------------------+
                             |
              [ Print RD(I) for main line I ]
                             |
                    ( Any        )----- N ----+
                    ( branches?  )            |
                             |                |
              +--------------------------------+
              | Print BD(I, J) for branch J    |
              | of main line                   |
              +--------------------------------+
                             |<---------------+
              N ------( Done? )
                             | Y
                          ( Stop )
```
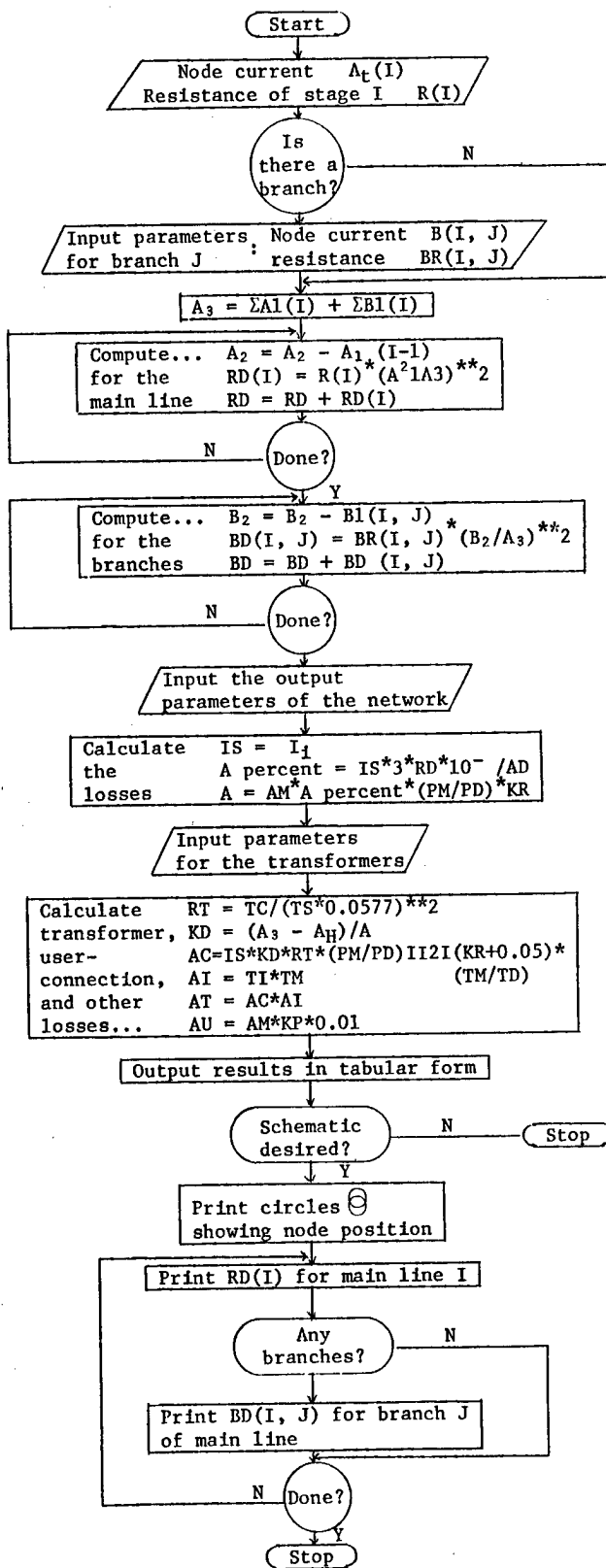
Figure 1.

The hourly output currents are listed in Table 3, while Table 4 lists the transformer characteristics (the capacitance, the number of step-down transformers, and the type of losses). The parameters listed in the three tables must all be input to the computer, which prompts the operator with a question mark "?," after which the value is entered. After each phase of data entry, the values are displayed on the screen for review and possible correction (to correct a value one presses Y on the keyboard; otherwise, the program continues).

Once all the data have been entered the calculations begin, and after a while the printer outputs the results as a table of numbers. If the operator wants a simplified schematic of the network with the calculated currents and equivalent resistances displayed on it, the Y key is pressed in response to a prompt and a multicolored schematic is printed out. To print out data in tabular form one types the instruction GOTO 500, while to get a simplified schematic one types GOTO 620 (there is no need to run the program twice). The results are displayed as shown in Table 5.

Table 3. Hourly Currents for a 24 Hour Period

Time	1	2	3	4	5	6	7	8	9	10	11	12	13	14	15	16	17	18	19	20	21	22	23	24
Current	10	8	25	27	52	30	54	55	58	65	55	65	62	65	60	72	68	63	48	45	38	30	30	30

Daily supply (kwh)	No of hours electricity is supplied	Monthly supply (kwh)	No of hours per month electricity is supplied	No of kwh supplied on high voltage lines
16,800	24	423,200	673	74,722

Table 4.

Type of losses \ Capacitance kVA	20	30	50
Number of step down transformers	20	14	27
Nominal core losses, kw	0.21	0.3	0.44
Copper losses in the windings, kw	0.62	0.85	1.33

Table 5.

Node	kwh	Resistance	Equivalent resistance
1	4,608	0.68	0.68
2	7,693	0.11	0.11
3	600	0.37	0.35
4	7,266	0.2	0.19
5	3,560	0.2	0.13

[continued]

16

[Continuation of Table 5]

Node	kwh	Resistance	Equivalent resistance
6	12,630	0.6	0.53
7	18,355	0.38	0.31
8	10,275	0.1	0.07
9	38,828	0.3	0.21
10	18,896	0.31	0.16
11	3,500	0.37	0.17
12	115,904	0.16	0.07
13	6,895	0.26	0.03
14	7,154	0.11	0.01
15	57,295	0.1	0.01
16	1,155	0.61	0.02
17	9,543	0.3	0.01
18	55,298	0.07	0

Branch 1:

1	38,828	2	0.02

Branch 2:

1	6,879	0.77	0.07
2	3,096	0.36	0.03
3	23,419	1.28	0.1
4	22,023	0.42	0.02
5	9,754	0.18	0
6	50,733	1.28	0.02

Branch 3:

1	57,295	2.4	0.05

Branch 4:

1	55,298	1.7	0.04

Equivalent resistance of the wires   3.468

I1 + .. + I24 = 65,976
T day = 24
T month = 678
A day = 16,800
A month = 423,200
AL day percent = 4.09
P day = 700
P month = 624.19
    KR = 1.1
Wire losses   16,959.7
    RD t = 3.841
A high = 74,722
AA to = 5,256.478169
AA to = 13,749.84
Transformer losses   19,006.32
Connection wires   3,398.64
Total losses   39,364.6

17
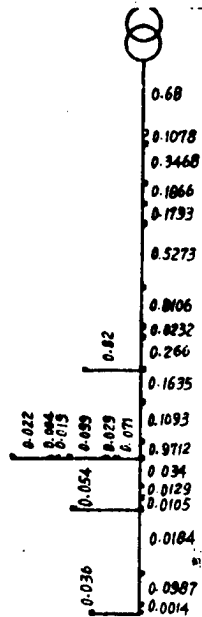
Figure 3. Schematic Showing the
Equivalent Resistances

The program occupies approximately 5 kilobytes of computer memory and is
suitable for calculating network losses in supply networks at voltages below
10 kV. However, the range of values that can be calculated is smaller than
the range of output parameters that can be recorded; in particular, the pro-
gram cannot handle systems in which two or more branches leave a single node.
Apart from this limitation, however, the program is quite general. (Of
course, the finite width of the printer paper limits the size of the simpli-
fied schematics that can be printed; in particular, the number of nodes with
branches must not be too large.)

12617/9365
CSO: 4008/1048

PROBLEMS APPLYING DATABASE TECHNIQUE TO TDC SYSTEM

[Article by Su Yongle [5685 3057 2867], Xian Institute of Industrial Automation Instrumentation: "A Preliminary Study of Two Problems of Applying a Database Technique to a TDC System"]

[Text] Abstract: Database techniques are currently applied in China mainly in information management and enterprise management. Yet, in terms of development, application of database techniques in TDC systems is undoubtedly an important area. This paper explores how to resolve two problems which crop up when applying database techniques in TDC systems, viz., realtime and operating language design.

The Function of Databases

The primary role of a database as part of a TDC system, is first of all to organize different control systems by different processes through database operation; next, through the process parameters, system parameters and related information in the collector control system it conversely acts in the control system to express the controls of the actual object.

The logic relationship of the control system and the database are as illustrated in Figure 1.
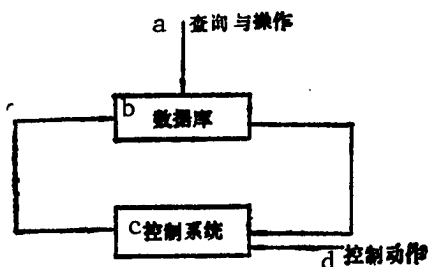
Figure 1

Key:
a. Query and operation
b. Database
c. Control system
d. Control action

On Realtime Problems

In TDC systems, the high realtime demands are one of the most prominent problems. Thus, resolving the realtime problem is a key problem for database technique application in TDC systems. This problem will be discussed below:

1. Process interface

Ordinarily, the logic structure of a database is as illustrated in Figure 2. Using this structure, the user only communicates with

Key:
a. User program 1
b. User program 2
c. User program n
d. View
e. Conceptual database
f. Physical database
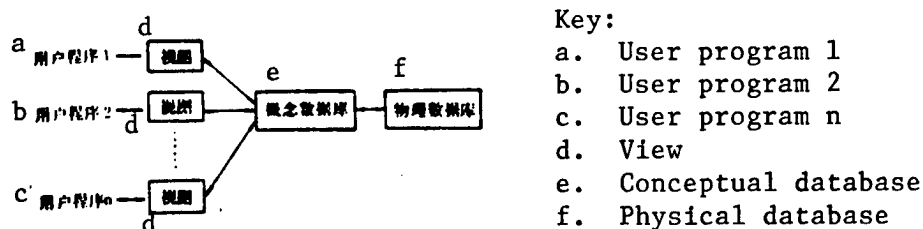
Figure 2

the view and does not communicate directly with the physical database. Thus, each operations command sent from the user's terminal is relayed through several levels to the physical database and then returns from the physical database to the user's terminal, and the time required is rather long. Currently, the computers used in industrial process control are primarily minicomputers and microcomputers and it is very difficult to obtain satisfactory realtime response using this type of database system structure.

To solve this problem, we introduced the concept of the process interface. The process interface is a mechanism through which high demand realtime operation commands and queries are communicated directly with the physical database and do not go through conceptual database conversion. In addition, communication between the physical database and the process control system is also carried out through the process interface so that the process control system is not directly linked to the conceptual database. Changes in process parameters in the control system are frequent, and while these changes cause frequent changes in the physical database, linking the control system and the physical database directly through the process interface without requiring conversion through the conceptual database, can save a great deal of time in order to guarantee realtime.

According to this conception, processing of some operational commands and queries with realtime demands depends on the design of the control system and physical database. The design of the physical database is also restricted by the specfic control system. This influences the independence of the data, that is, we sacrifice some of the data's independence to obtain high realtime. For most control systems, especially medium- or mini-computer dedicated control system, data independence is not an unusually important characteristic. Thus, this type of trade-off is acceptable in a TDC system.

The process interface is essentially a simple mechanism for communication between the user and the physical database and between the process control system and the physical database. After this mechanism has been established in a database system, it forms a database management system (DBMS).

2. System Structure

In a TDC system, in addition to the abovementioned high realtime demand commands and queries, there are also some operations with high realtime demands. For example, for control system maintenance and configuration, including control system makeup and control parameter zhengding [2419 1353], these operations are operations of the control system in the formative process, and still do not initiate realtime control. Thus, the realtime demands of these operations are not high and they can be carried out through design of the conceptual database, so that it has higher data independence.

Summarizing the above, we can divide the operational language of the database into two parts: one part is the high realtime operations and queries, and the other part is the operations which do not have high realtime demands. The execution of the first group of operations are linked directly with the physical database through the process interface; the execution of the second group of operations is by linking the database management system and the physical database through the view and the conceptual database. In addition, the control system also communicates with the physical database through the process interface and does not directly link with the conceptual database. Thus, the logic structure of the TDC system is as illustrated in Figure 3.

This structure both maintains the general features of the database and also guarantees the realtime demands of the process control system.
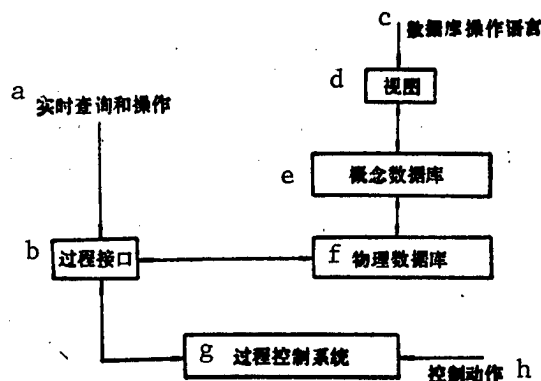
Figure 3

Key:
a. Realtime queries and operations
b. Process interface
c. Database operation language
d. View
e. Conceptual database
f. Physical database
g. Process control system
h. Control action

Database Operation Language

When database techniques are applied to realtime industrial process control, designing a suitable operation language is an important problem. Since a realtime control system user is frequently an operation worker or technician who is familiar with analog instruments, the operation language design should take this situation into consideration. For this, the QBE language first proposed by the IBM Company's M. Zloof in 1975 is clearly superior. However,

QBE language is a two-dimensional list format language, and all the operation and query results are presented in list format. Yet, in TDC systems, some more visual displays (including graphs and flow charts) are required. We feel that on the foundation of the original QBE language, based on the demands of a TDC system, it is appropriate to make suitable expansions in the requirements of conceptual and query function in order to adapt to the needs of control system operation. For basic knowledge concerning the QBE language, please see References [1], [2], and [3].

1. Relational Units Presentation Schema

Suppose that $\{R_i | i=1, \ldots, n\}$ is a database schema. It is the set of all relational schemas in the database, for all i, suppose $S_i=\{A_i \ j=1, \ldots, m\}$ is the set of all attribute domains in R_i, and G_i is a plane figure,

$$t_i : S_i -> G_i$$

is a map so that $t_i(A_i^j,) \subset G_i (j=1, \ldots m)$ is the subset within G_i, thus we say that (G_i, t_i) is the unit presentation schema of the relation R_i. $(i=1, \ldots, n)$

According to this definition, as long as different (G_i, t_i) are defined for different control systems, the same database schema can provide different unit presentation schemas, i.e., provide people a different display form. The unit presentation schema must be defined when the system is formed. Once the unit presentation schema has been defined, there will be no changes in later operation and operation processes. The unit presentation schema is a display form that depends on a specific control system.

Example 1. Suppose that PP is a relation which has control loops (N) and some of its process parameter attributes. This can be expressed as

PP(N,PV,SV,MV)

in which N is the loop number, PV is the measurement value, SV is the given value, and MV is the operations output value. These are all attributes of PP. Defining G and t appropriately can provide the unit presentation schema of the PP relation as illustrated in Figure 4.

At this time, $G=\pi$

t (N field) = field N

t (PV field) = line segment AB;

t (SV field) = line segment EF;

t (MV field) = line segment CD.

To understand the process parameters, we use the query statement

PP	N	PV	SV	MV
	T 101	P.	P.	P.

The query results are as illustrated in Figure 5.
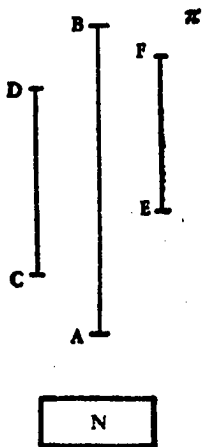
Figure 4
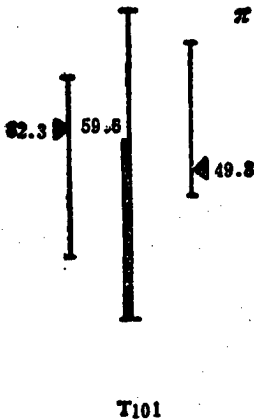
Figure 5

Example 2. Suppose SP is a relation which has a control loop and its system parameter attributes, which we express as:

$$SP\ (NP,P,I,D,T)$$

in which N is the loop number, P is the proportional coefficient, I is the integral coefficient, D is the differential coefficient, and T is the control period. Defining G and t appropriately we can get the unit presentation schema of the SP relation as illustrated in Figure 5.

To understand the relation situation of the system, we use the query statement

SP	N	P	I	D	T
	T 101	P.	P.	P.	P.

The results of the query are as illustrated in Figure 7.

23

$$P = \boxed{P}$$

$$1 = \boxed{I}$$

$$D = \boxed{D}$$

$$T = \boxed{T}$$

$$\boxed{N}$$

Figure 6

$$P = 201.5$$

$$I = 1$$

$$D = 0$$

$$T = 1$$

$$T_{j\emptyset 1}$$

Figure 7

2. Expansion of Query Functions

(1) Presentation Schema of Natural Linkage

To expand the functions of the QBE language, first of all we define the concept of the natural linkage presentation schema. Directly stated, it puts together two views according to a natural mode. It is defined as follows:

Suppose (G_1, t_1), (G_2, t_2) are the unit presentation schema of the relations R_1 and R_2, respectively, and S_1, S_2 are the attribute field set of the relations R_1 and R_2, and supposing that R is the natural linkage of R_1 and R_2, written as: $R=R_1|x|R_1$. Let $G=G_1+G_2$, in which "+" represents the linkage operation of the two views. Suppose $S=\{A_k\}=S_1 \cup S_2$, is the set of all the attribute fields in R_1 and R_2, $t:S\rightarrow G$ is a map, so that

$$t(A_k) = \begin{cases} t_1(A_k) & \text{当 } A_k \in S_1 \\ t_2(A_k) & \text{当 } A_k \in S_2 - S_1 \end{cases}$$

hence it is said that (G,t) is the unit presentation schema of natural linkage R.

From the definition we know that, generally speaking, the unit presentation schema of $R_1|x|R_2$ and $R_2|x|R_1$ is different.

Using the same method, we can define the unit presentation schema of K relational natural linkages. Its definition is as follows:

$$\overset{k}{\underset{j=1}{|\times|}} R_j = (\overset{k-1}{\underset{j=1}{|\times|}} R_j) |\times| R_k$$

24

Example 3. Suppose PP, SP and their unit presentation schemas are as described in Examples 1 and 2. Then the unit presentation schema of the natural linkage

$$R = PP \,|\, x \,|\, SP$$

is as illustrated in Figure 8.

Similarly, the unit presentation schema of $R = SP \,|\, x \,|\, PP$ is as illustrated in Figure 9
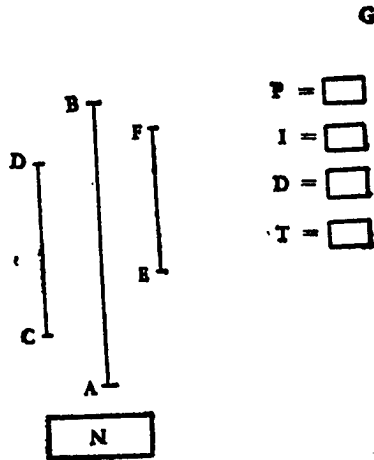
Figure 8
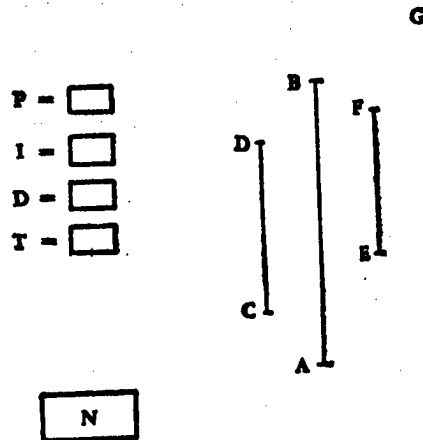
Figure 9

(2) Unconditional Queries

In the QBE language, in the format, a P is prefixed before the example elements of certain attribute ranks. The operation, expresses a query with regard to the attribute in the relation and prints out the result of the query. However, if a P is prefixed to a constant element, the operation is meaningless. Yet, we would like to give this operation a special meaning, i.e., it expresses the unit in the entire database through certain relational queries and in the other relations related to the designated attribute value. Below we describe this operation in detail. See References [2] and [3] for definition of example elements and constant elements.

Suppose the relational database schema:

$R = \{R_i(A_{i1}, \ldots, A_i n_j)\ i=1, \ldots, m\}$, in which $R_j(A_{ij} \ldots, A_i n_j)$ is the relation which has n_i attributes $A_{ij}, \ldots, A_i n_i$. The attributes need not be different for different Rs.

Supposing that R_k is a certain relational schema in a relational database, A_k is an attribute of R_k, and is a constant element, then Operation I:

```
-----------------------------------------------------------------
  R_k      A_{k1}      ...        Ak_3        ...        A_k n_k
-----------------------------------------------------------------
```

$$P.a$$

indicates that first of all relations of all attribute A_{kj} in the database are naturally linked to obtain a new relation expressed as R_A, i.e.,

$$R_A = |x| R_i$$
$$\quad\quad i$$

(in which R_i at least has the attribute A_{ki})

Supposing R_A has 1 attributes A_1, A_2, ..., A_1, let $As = A_k$ ($1 \leq S \leq 1$) then operation I is equivalent to the ordinary sense of the operation in QBE language:

```
-----------------------------------------------------------------
  R_A       A_1        ...        As        ...         A_1
-----------------------------------------------------------------
```

$$P. \qquad\qquad\qquad\qquad a$$

(3) Conditional Query

Sometimes we hope to localize within a certain range the query and the relational unit related to the designated attribute values. This range can be realized through a query with a conditional box.

For example, R_k, A_{kj} etc., are as described in the Second Section, we have the operation II,

```
------------------------------------------------------------------------
  R_k     A_{k1}    ...     A_{kj}    ...    A_k n_k    Condition
------------------------------------------------------------------------
                             P.a                        |x|   R_j
                                                          j
                                                      ({R_j}C{R_1})
```

in which $\{R_j\}C\{R_i\}$ expresses the subset of the relational set of all attributes A_{kj}. Let $R_A' = |x| R_j$, supposing R_A' had $1'$ attributes A_1', A_2'. ..., A_1', supposing $A_t' = A_{kj}$ ($1 \leq t \leq 1'$), then Operation II is equivalent to the sense of the operation in the QBE language:

```
---------------------------------------------------------------------
R´        A´              ...        A´              ...        A´
 A         1                          t                          1
---------------------------------------------------------------------
        P.                                      a
```

Here the sole difference between Operation I and Operation II is that R_A' is given by the condition in the conditional box.

Thus, Operation II will print out all the unit designated by the value a of attribute A_{kj} in R_A'. This is equivalent to finding more detailed information about an entity in a database through a relation R_i.

Example 4. Suppose that in a database only the PP relation in Example 1 and the SP relation in Example 2 have a relation relevant to N (loop number) attributes. In Example 3 we gave the unit presentation schema $R=PP|z|SP$ as illustrated in Figure 8. Then the results of the query of operation;

```
-----------------------------------------------------------------
    PP       N        PV         SV          MV
-----------------------------------------------------------------
        P.T101
```

are as illustrated in Figure 10.

Similarly, the results of the query of operation:

```
-----------------------------------------------------------------
    SP       N        P          I         D         T
-----------------------------------------------------------------
        P.T101
```

are the same.
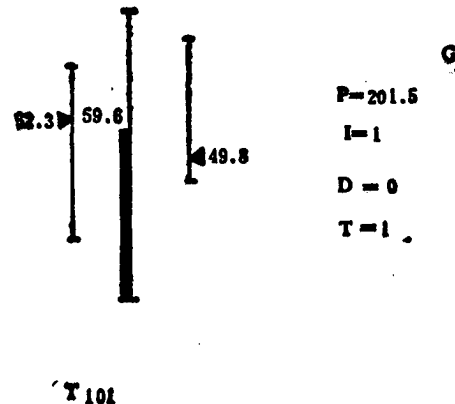
Figure 10

REFERENCES

1. Ullman, J.D., PRINCIPLES OF DATABASE SYSTEMS, Computer Science Press, Potomac, MD 1980.

2. Su Yongle [5685 3057 2867], QBE YUYAN DAOYIN [INTRODUCTION TO QBE LANGUAGE], GONGYE YIBIAO YU ZIDONGHUA ZHUANGZHI [INDUSTRIAL INSTRUMENTATION AND AUTOMATION], 1985, Nos 1,2.

3. M.M. Zloof, QUERY-BY-EXAMPLE: A DATABASE LANGUAGE, IBM System Journal, Vol 16, No 4, 1977.

[About the Author] Su Yongle, male, 47, engineer, graduated from the Department of Mathematics, Beijing University in 1962. He is currently working at the Xian Institute of Industrial Automated Instrumentation, and is a member of the Xian Computer Society and the Shaanxi Instrumentation Society. He has developed JKS-BASIC language and its interpretive system; FORTRAN language compiling system error processing; Xian instrument industry wage management system, etc.

COUPLING FREQUENCIES OF RAMAN FREE-ELECTRON LASERS

[Text] Abstract: Analytical expressions of coupling frequencies of Raman free-electron lasers are deduced based on the physical image of the coupling between negative energy space charge wave and electromagnetic wave. Formulas are presented for different operation schemes. Under certain limiting conditions, these formulas are reduced to the familiar approximate expressions in the literature. Experimental results have borne out our analysis.

I. Introduction

The mechanism of a Raman free electron laser may be regarded as a coupling between the negative energy space charge wave in the electron plasma and the positive energy electromagnetic wave and the resulting cohetent amplification of the latter. In the absence of a static magnetic wiggler (undulation) field in space, the dispersion curves of the negative energy space charge wave and the positive energy electromagnetic wave do not cross and there will be no coherent amplification of the radiation. The role of the wiggler field is to shift the dispersion curve of the space charge toward that of the electromagnetic wave so that they cross each other and result in a coupled amplification. The coupling frequency and the wave number are determined by the position of the intersection.

We analyzed the coupling frequency of the Raman free electron laser under different conditions. Calculations were made for a single energy relativistic electron beam propagating along the guiding magnetic field B_o in the z direction in free space (or in a wave guide tube) and passing through a right-polarized static magnetic wiggler field with a wave number k_w. Naturally, the parameters of the electron beam, the guiding field, and the wiggler must all meet the Raman criteria.[1-3]

Based on the theoretical analysis, we conducted an experimental study of the Raman free electron laser and obtained laser output. Preliminary parametric studies showed that the theory was correct.

II. Dispersion Curve of a Negative Energy Space Charge Wave in a Wiggler Field

Figure 1 shows schematically the phase relationship along the z axis of the wiggler field (or transverse velocity field), the electromagnetic wave and the space charge wave for electromagnetic wave amplification. The energy equation of the interaction between the electromagnetic wave with an electric field component E and the free electron laser with a transverse velocity v is

$$\dot{\gamma} = -\frac{ev_{\perp}E}{c^2 m},$$ (1)

If $\dot{\gamma} < 0$, electromagnetic amplification is obtained. If $v_{\perp}$ and E reach their respective simultaneously at a certain point in space, then, to maintain a maximum negative value of $\dot{\gamma}$, E should have an opposite maximum when the space charge wave passes through one half a period ($\lambda_w/2$) of the wiggler field; that is,

$$\lambda_w/2\lambda = \lambda_w/2\lambda_d - 1/2,$$ (2)

where λ and λ_d are respectively the wavelengths of the electromagnetic wave and the space charge wave. (2) can also be written as

$$k = k_d - k_w,$$ (2)'

where $k \equiv 2\pi/\lambda$, $k_d \equiv 2\pi/\lambda_d$, $k_w \equiv 2\pi/\lambda_w$. (2)' is the relationship between the wavelengths of the electromagnetic radiation and the space charge wave.[1-3] It clearly shows that when the dispersion curve of the space charge wave in the (ω, k_d) coordinate system is replotted in the (ω, k) coordinate system, the curve will be shifted along the k axis by k_w. This translation causes the two nonintersecting curves to cross and leads to the free electron laser radiation.
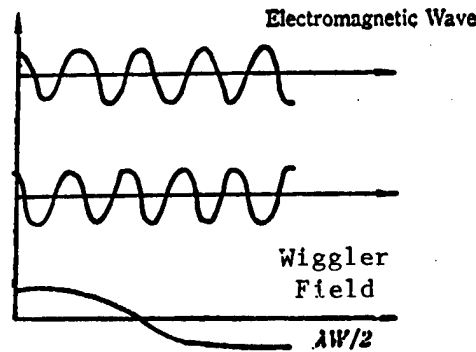
Fig. 1 Schematic of the phase relationship among wiggler field, EM wave and space-charge wave in a free-electron laser

III. Free Space Coupling Frequency Caused by Negative Energy Electrostatic Beam Mode

In the coordinate system (the primed coordinates) of particles moving along the z axis with velocity v_z, the electrostatic beam mode dispersion relation (negative energy branch) of the electron beam plasma[4] is

$$\omega'_d = -\omega_p, \tag{3}$$

where ω'_d is the electrostatic beam mode frequency in the particle coordinates, $\omega_p = \sqrt{4\pi n e^2/\gamma_s m}$ is the plasma characteristic frequency (or response frequency), $\gamma_s \equiv 1/\sqrt{1-\beta_s^2}$ is the relativity factor determined by the v_z velocity of the electron beam, $\beta \equiv v_s/c$; n is the electron density in the laboratory frame of reference, and e and m are respectively the electron charge and mass. From the relativistic Dopper relation

$$\omega'_d = \gamma_s(\omega - v_s k_d), \tag{4}$$

we obtain the dispersion relation of the negative energy electrostatic beam mode in the laboratory frame of reference, shown in Figure 3 as a dotted line:

$$\omega = v_s k + v_s k_w - \omega_p/\gamma_s, \tag{5}$$

On the other hand, the dispersion equation[4] for the right-handed circularly polarized electromagnetic wave propagating along the z axis in the particle frame of reference is

$$\omega'^2 - c^2 k'^2 - \frac{\omega_p^2 \omega'}{\omega' - \Omega_o} = 0, \tag{6}$$

where ω' and k' are respectively the frequency and wave number of the electromagnetic wave in the particle frame, $\Omega_o \equiv eB_0/mc$ is the cyclotron frequency, and B_0 is the guiding field in the z direction.
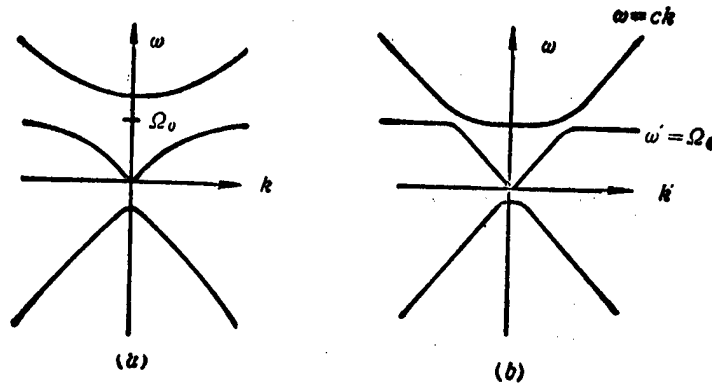
Fig. 2   Dispersion curves of EM wave in particle reference frame

(a) General case $(\omega_p \approx \Omega_0)$;   (b) $\omega_p \ll \Omega_0$

31
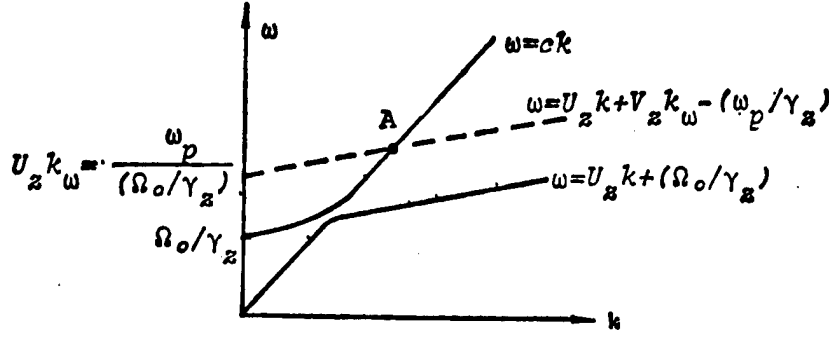
Fig. 3 Dispersion curves of EM wave (solid curve) and negative-energy
space-charge wave (dash curve) in lab reference frame

$$\left(\frac{\Omega_0}{\gamma_s} < \left(v_s k_w - \frac{\omega_p}{\gamma_s}\right), \ \omega_p \ll \Omega_0\right)$$

Figure 2(a) shows the general curve shape of Equation (6). When $\omega_p \ll \Omega_0$ the curve is shown in Figure 2(b) and approaches the three straight line sections of $\omega' = \Omega_0$ and $\omega' = \pm c k'$. Note that $\omega_p \ll \Omega_0$ is not necessarily satisfied, especially at low electron beam energy.

Using the relativistic Dopper equation $\omega' = \gamma_s(\omega - v_s k)$, and $k' = \gamma_s(k - v_s\omega/c^2)$, we obtain the corresponding Equation (6) in the laboratory frame:

$$(\omega^2 - k^2 c^2) - \frac{\omega_p^2(\omega - k v_s)}{(\omega - k v_s - \Omega_0/\gamma_s)} = 0_0 \tag{7}$$

The general shape of (7) is shown as the solid lines in Figure 3, where A is the intersection and its corresponding frequency is the coupling frequency of the Raman free electron laser. It should be pointed out that in our simplified treatment only the real parts of ω and k are involved.

The frequency ω and the corresponding wave number k are found from (7) and (5):

$$\omega = \gamma_s^2 \alpha \pm \gamma_s^2 \alpha \left[1 - \frac{\omega_p^2}{\gamma_s^2 \alpha(\alpha - \Omega_0/\gamma_s)}\right]^{1/2}, \tag{8}$$

$$k = \frac{\beta_s \gamma_s^2 \alpha}{c} \pm \frac{\gamma_s^2 \alpha}{c}\left[1 - \frac{\omega_p^2}{\gamma_s^2 \alpha(\alpha - \Omega_0/\gamma_s)}\right]^{1/2}, \tag{9}$$

where $\alpha \equiv v_s k_w - \omega_p/\gamma_{s0}$. Since the wave is propagating in the positive direction, the positive sign should be chosen in (8) and (9). When the condition $\omega_p^2 \ll \gamma_s \alpha(\alpha - \Omega_0/\gamma_s)$ is satisfied, (8) may be approximated by

$$\omega \approx \frac{v_s k_w - \omega_p/\gamma_s}{1 - \beta_s} - \frac{\omega_p^2 \beta_s}{2\alpha(\alpha - \Omega_0/\gamma_s)}_0 \tag{10}$$

32

Note that the condition implies that ω_p is far less then ω and Ω_0 is far away from the magnetic resonance point $v_z k_x \gamma_z$.

The first term on the right hand side of (10) agrees with the expression derived by Marshall et al.[5] from momentum and energy conservation for an ideal case and for $\omega_p \ll \omega$. The second term is a correction term, which makes the coupling frequency given by (10) slightly greater than that given by Reference 5 when B_0 is large $(\Omega_0 > \gamma_s \alpha)$. Conversely, when $\Omega_0 < \gamma_s \alpha$, the correction term will make the frequency lower. When Ω_0 approaches $\gamma_s \alpha$, the assumption leading to (10) no longer holds true and (8) must be used. $\Omega_0 = \gamma_s \alpha$ is a singularity, as can be seen in Figure 3 as well. At this time the dispersion curve of the negative energy electrostatic beam mode $(\omega = v_s k + \alpha)$ coincides with the asympotote of the electromagnetic dispersion curve $(\omega = v_s k + \Omega_0/\gamma_s)$ and ω and k undergo large change in the vicinity.

It should be noted that the transverse velocity of the electron according to the stable orbit theory[6] is given by

$$v_\perp = \Omega_W v_s / (\Omega_0 - \gamma_s v_s k_W), \tag{11}$$

where $\Omega_W \equiv eB_W/mc_0$. The singularity is also at $\Omega_0 = \gamma_s \alpha$, where $v_\perp \to \infty$. The singularity should be avoided in a real device as it can cause rapid dispersion of the electron beam energy.

IV. Effects of the Waveguide Dispersion on the Coupling Frequency

The derivations above are for an infinite free space whereas the electron beam actually propagates in a waveguide tube, corrections must be made for the electromagnetic dispersion relation. To simly the problem, we assume that $\omega_p^2 \ll \omega^2$ is true and that the singularity point is far away, Equation (7) in the waveguide becomes

$$\omega^2 - c^2 k^2 - \omega_{c0}^2 \approx 0, \tag{12}$$

where $\omega_{c0} \equiv 2\pi c/\lambda_{c0}$ is the waveguide cutoff frequency and λ_{c0} is the cutoff wavelength.

From (5) and (12), it is easy to show that, for the electrostatic beam mode, the free electron laser coupling frequency is

$$\omega = \gamma_s^2 \left(k_W v_s - \frac{\omega_p}{\gamma_s}\right)\left\{1 \pm \left[\beta_s^2 - \frac{\beta_s^2 \omega_{c0}^2}{\left(\frac{\omega_p}{\gamma_s} - k_W v_s\right)^2 \cdot \gamma_s^2}\right]^{1/2}\right\}, \tag{13}$$

When ω_p/γ_s is negligible in comparison to $k_W v_z$, we have the approximate relationship

$$\omega \doteq \gamma_s^2 k_W v_s \left[1 \pm \left(\beta_s^2 - \frac{\omega_{c0}^2}{\gamma_s^2 k_W^2 c^2}\right)^{1/2}\right]. \tag{14}$$

33

This equation shows that, to achieve the coupling between the space charge
wave mode and the electromagnetic mode, the following inequality must be
satisfied:

$$\lambda_{free} < \frac{\lambda_{\infty}}{\gamma_{s}(1+\beta_{s})},$$ (15)

where $\lambda_{free} = 2\pi c/\omega_{free}$ and is the coupling wavelength in free space. When γ_z is
small (low energy electron beam), (15) is not automatically satisifed. In
fact, (15) shows that the "effective" cutoff frequency of the waveguide is
increased by a factor of $\gamma_{s}(1+\beta_{s})$. For example, for an electron beam with
$\gamma = 2$, this factor is almost 4. In assure normal operation, the radius a of
the waveguide often has to be large (because $\omega_{\infty} \propto 1/a$); however, for a double
spiral oscillator, the excitation current I_{w} of the wiggler is directly
proportional to $\exp(5.68a/\lambda_{w})$ for fixed k_{w} and B_{w}, an increase in the radius
will cause a rapid increase in the excitation current I_{w} and lead to technical
difficulties.

Figure 4 shows the variation of the parameter $\lambda_{free} \cdot \gamma_{s}(1+\beta_{s})$ in (15) as a
function of the guiding field B_0 for $\gamma = 3.5$ (accelerator voltage 1.25 MV) and
$\gamma = 2$ (accelerator voltage $\simeq 0.5$ MV). It is clear that a radius drift tube
with a radius $R_{d} = 5.5$ mm works for $\gamma = 3.5$ but not for $\gamma = 2$ over the entire
range of (15). Since we had $\gamma = 2$, we close an $R_{d} = 10$ mm.
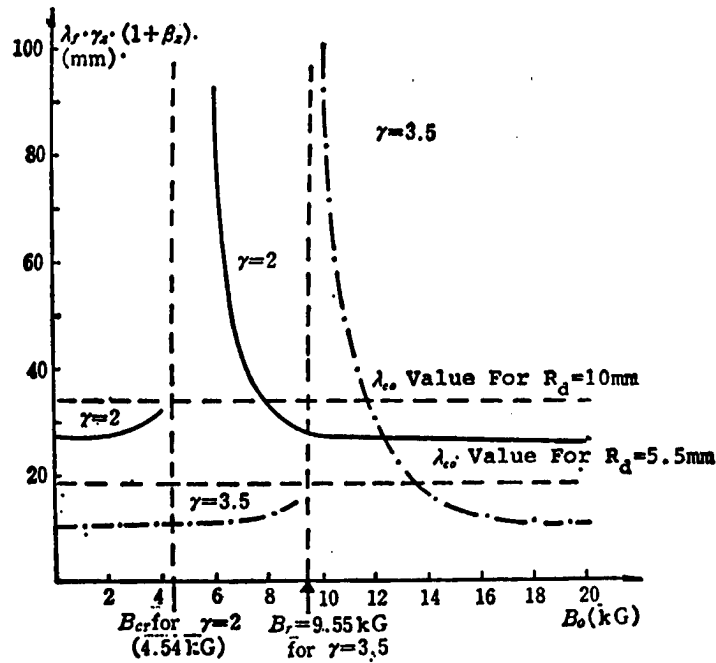
Fig. 4   Parameter $\lambda_{f} \cdot \gamma_{s}(1+\beta_{s})$ versus B_0

$\lambda_{w} = 3$ cm; λ_{∞}–cutoff wavelength for TE_{11} mode; $\gamma = 2$ curve: $B_{w} = 0.5$ kG, $I = 1$ kA;
$\gamma = 3.5$ curve: $B_{w} = 0.63$ kG, $I = 1.2$ kA

34
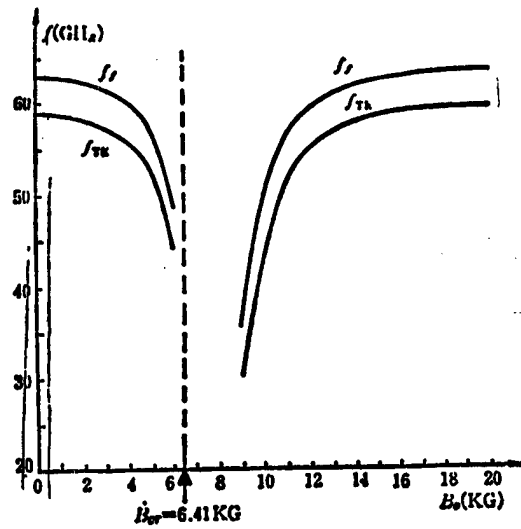
Fig. 5   Coupling frequency in free space f_f
and in waveguide (TE_{11} mode) versus guiding
magnetic field B_0
$(\gamma=2,\ I=1kA,\ r_b=0.3\,cm,\ R_d=1\,cm,$
$\lambda_w=2.25\,cm,\ B_w=0.5\,kG)$

Figure 5 shows the free space coupling frequency f_f and the TE_{11} mode coupling frequency f_{TE} in a 20 mm diameter drift tube versus B_0 for $\gamma = 2$. The difference between f_f and f_{TE} is clearly evident.

Figure 6 shows the effect of the wiggler field B_w on the coupling frequency of the TE_{11} mode when $\gamma = 2$. Figure 7 shows the effect of the wiggler wavelength λ_w on the coupling frequency of the TE_{11} mode and the transverse velocity $\beta_\perp$ of the electron for the case of $\gamma = 2$. In the $\lambda_w < 2.25$ cm region, f_{TE} decreases with decreasing λ_w. This is because that $\beta_\perp$ increases as the magnetic resonance singularity is approached (see Equation (11)). Our experiments were for $\lambda_w = 2.25$ cm and $\lambda = 2.2$ cm.
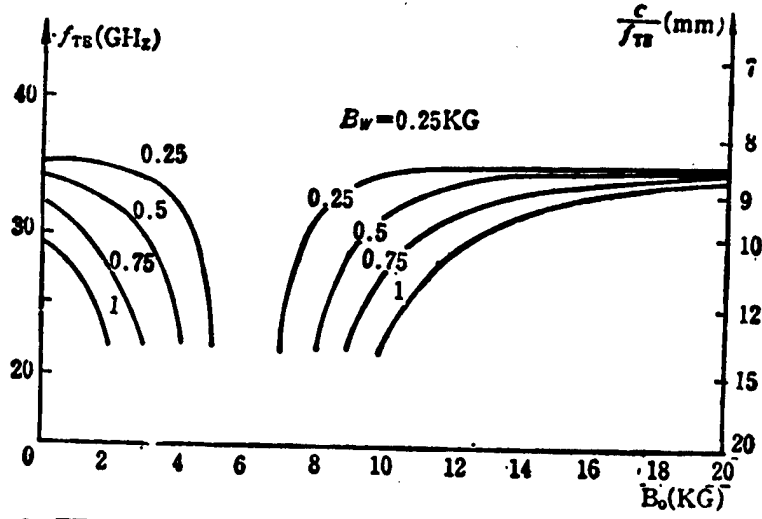
Fig. 6 TE$_{11}$ mode coupling frequency versus B_0 for different wiggler fields
($\gamma=2$, $I=1$ kA, $r_b=0.3$ cm, $R_d=1$ cm, $\lambda_w=3$ cm)
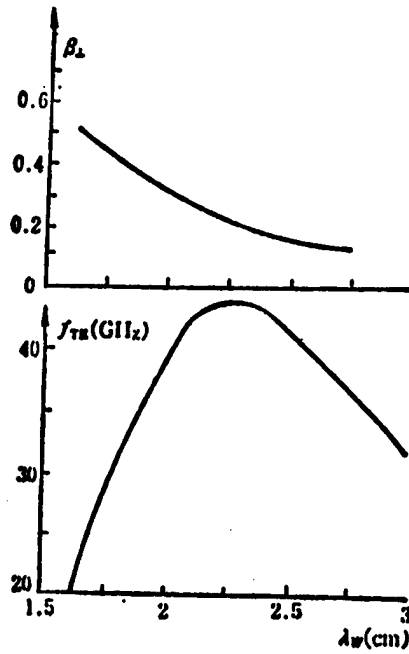
Fig. 7 Transverse velocity of electrons
$\beta_\perp$ and TE$_{11}$ mode coupling frequency
f_{TE} versus wiggler period λ_w
($\gamma=2$, $I=1$ kA, $r_b=0.3$ cm, $R_d=1$ cm,
$B_W=0.5$ kG, $B_0=10$ kG)

As can be seen from Figures 4-7, the coupling frequency is affected by a number of complex factors. In selecting the optimum operating condition of an overall design, the gain calculation must also be brought in. Based on the above theoretical analysis, we conducted an instrument design and testing. A high current electron beam (0.5 MeV, 1 kA) emitted from a carefully designed foil-less diode tube was guided by a strong axial magnetic field and formed a 1 meter tall highly collimated column (or hollow column) in the drift tube. This column of electron beam served as the lasing material. A right-hand circularly polarized double winding wiggler with a period λ_w of 2.2 cm or an axially symmetric iron ring wriggler with a period λ_w of 2.25 cm was used as the pumping source. In both cases free electron laser radiations (coherent radiation amplification mode) were obtained.[7] The laser parameters were measured to be: width at half maximum = 20 ns, average power = 0.5 MW, electron efficiency $\cong$ 0.1 percent, and wavelength of the K_a branch $\cong$ 8 mm.

Preliminary parameteric studies showed that the optimum operating region is in the vicinity of B_o = 9 kG and B_w = 0.5 kG. The results are consistent with Figures 4-7 and the calculated laser wavelength of 7 mm is also in agreement with the measured value. Details of the experiment and the results will be published elsewhere.

References

1. P. Sprangle, et al., in "Infrared and Millimeter Waves," (Academic Press), 1979, 1, chapter 7.

2. H.P. Freund, et al., Phys. Rev. A, 1981, 24, No 4 (Oct), 1965.

3. H.P. Freund, et al., Phys. Rev. A, 1982, 26, No 4 (Oct), 2004.

4. J.D. Lawson, "The Physis of Charged-Particle Beams," (Thomson Ltd.), 1977.

5. T.C. Marshall, et al., in "Advances in Electronis and Electron Physics," ed. L. Marton and C. Marton, 1980, 53.

6. L. Friedland; Phys. Fluids, 1980, 23, No 12 (Dec), 2376.

7. Chu Cheng, et al., ZHONGGUO JIGUANG [CHINESE JOURNAL OF LASERS] Vol 12, No 12, 767(1985).

APPLIED SCIENCES

TRANSFORMATION OF LASER BEAM THROUGH GLASS RING

[Article by Zhang Guoshun [1728 0948 7311], Cheng Fuan [4453 4395 1344], Liu Le [0491 3157] and Wang Keqi [3769 0344 6386]]

[Text] Abstract: A new optical element--a glass ring--is introduced in this paper. The glass ring can transform a laser beam into a plate beam under certain conditions. The transformation is described in detail. The ring works like an optical fiber.

Some conclusions at different angles (from 0° to 90°) are obtained and the future applications are explained.

Introduction

The laser beams produced by a resonance cavity are usually one-dimensional beams with a high degree of directionally. Two-dimensional planar laser beams are more difficult to produce. Two dimensional operation of certain high gain materials has been reported[2,5]; for example, a two-dimensional planar laser beam has been produced by Rhodamin 6G dye in a cylindrical glass cavity and the multiple reflection within the cylinder formed a resonance cavity. Such operation is difficult to achieve in more commonly used lasers. Methods for converting a 1-D laser beam with an optical device into a 360° 2-D planar laser light has never been reported.

The ring lens reported here is a section of optical glass tube with cylindrical inner and outer surfaces. the laser beam enters the glass ring from one side and a planar laser beam is obtained when certain conditions are satisfied by the incidence angle. This device may be applied in situations where a reference plane or a 2-D planar laser is required.

I. Principle and Experiment

Figure 1 shows the propagation of a meridian light in a fiber optics. The angle of incidence β at the interface must exceed the critical angle to ensure total reflection. When the light ray propagates to the curved part, the incidence angle at the inner surface α increases and the incidence angle at the outer

surface β decreses. When β becomes less than the critical angle and if the radius of curvature is small, the totally reflecting meridian ray at the straight section will escape through the outer surface when it reaches the curved section.
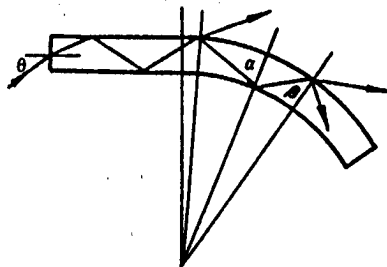
Fig. 1.

Based on the above principle, we conducted the following experiment. A beam of He-Ne laser was first directed toward the center of the glass ring so that the beam is normal to the axis of the ring and coincide with the x axis, as shown in Figure 3. The ring was then moved slowly along the y axis so that the distance H between the incident beam and the x axis varied between 0 and R + d. It was found experimentally that when H fell within a certain range (see next section), the laser beam was transformed into a 2-D planar beam filling up all 360°. When the planar beam was intercepted by a surrounding screen, a closed bright line was observed. In certain regions the bright line consisted of alternating bright and dark dots. When smoke was applied around the ring, the planar laser beam became clearly visible, as shown in Figure 2.
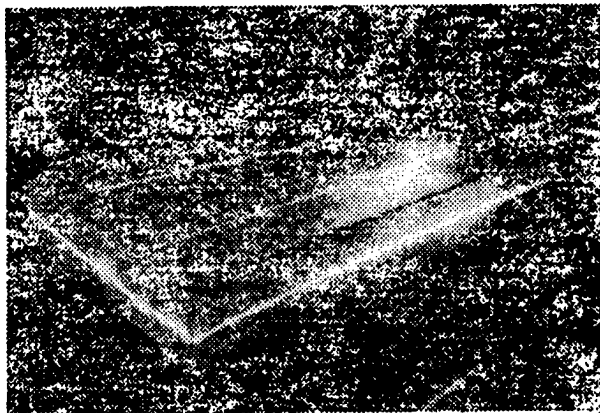
Fig. 2.
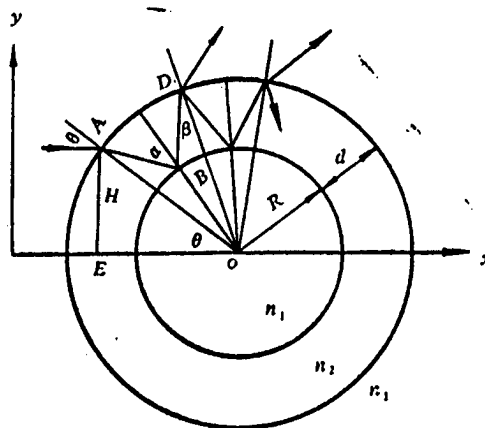
Fig. 3.

II. Optical Path Analysis

The angle α in Fig. 3 is the critical angle and the He-Ne laser beam enters with an incidence angle θ at point A. The inner radius of the ring is R and the outer radius is R + d, where d is the thickness. If the refractive index of the ring is n_2 and the refractive index of the surrounding medium is n_1, then,

$$sin\alpha = \frac{n_1}{n_2} \tag{1}$$

$$sin \angle OAB = \frac{R}{R + d} \cdot sin\alpha = \frac{n_1}{n_2} \cdot \frac{R}{R + d}$$

From $sin\theta = \frac{n_2}{n_1} \cdot sin \angle OAB$.

$$sin\theta = \frac{R}{R + d} \tag{2}$$

For the incidence angle on the inside of the ring to be critical, θ must be equal to $sin^{-1}(R/R+d)$ and this is independent of the refractive index of the material. Since $sin \beta/R = sin \alpha/R+d$, angle β is less than angle α. That is, when the incidence angle on the inner surface is critical, the incidence angle β on the outer surface is less than critical and some light will escape. The laser beam bounces repeatedly between the inner and outer walls of the ring and a planar laser beam is formed by refraction.

In Figure 3 AE = H is the vertical distance from the incidence point to the x axis. From the diagram, $sin \theta = H/R+d$. When α is the critical angle, a comparison with (2) shows that

$$H = R \tag{3}$$

When H increases and the refracted light becomes tangent to the inner circle, as shown in Figure 4, we have

$$sin\theta = \frac{n_2}{n_1} \frac{R}{R+d} \tag{4}$$

Hence, $H = \frac{n_2}{n_1} R$. When the surrounding medium is air (n_1=1), we have

$$H = n_2 R \tag{5}$$

If the glass ring is made of k9 optical glass, H = 1.52R. When the incidence angle θ continuous to increase and H becomes greater than n_2R, we have the

40

situation shown in Fig. 5, where β is less than the critical angle. Therefore, incident rays with H >n_2R will have their refracted rays missing the inner circle. Some light will escape at each reflection and refraction. The maximum reflection angle β is the critical angle, when θ = 90°, β is equal to the critical angle.
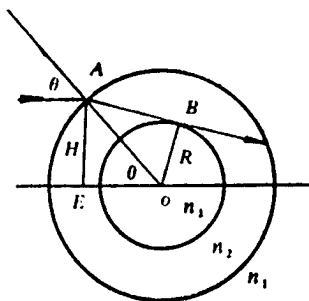
Fig. 4.
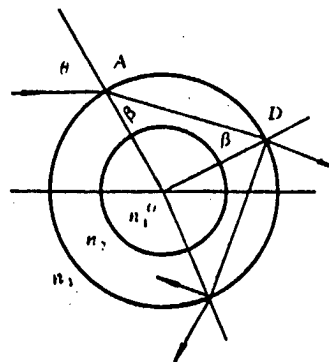
Fig. 5.

Figure 6 shows the optical path for H <R, or small θ. At this time α is less than critical and

$$sin\gamma = \frac{R+d}{R} sin\theta \qquad (6)$$

where $sin\theta < \frac{R}{R+d}$. The light ray entering the ring will undergo multiple reflections and some light will escape at each reflection.
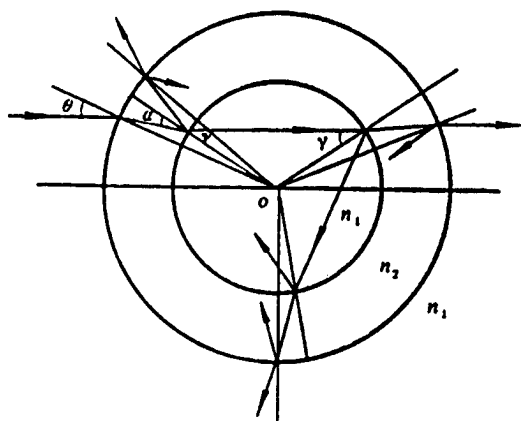
Fig. 6.
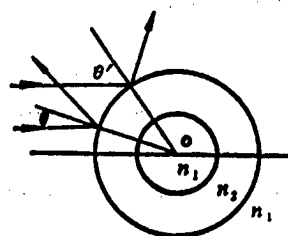
Fig. 7.

This will lead to intensity inhomogeneity of the planar laser beam and should be avoided.

Figure 7 shows the incident light reflecting from the outer surface. Since the incident beam has a finite width, the beam contains different angles of incidence. Reflection at the circular surface causes the reflected rays to propagate in different directions. This also causes intensity variation and measures should be taken to reduce the outer surface reflection. Moreover, rays reflected from the inner and outer surfaces may interfere and form alternating unequally spaced dots[4,6].

For light rays incident on the glass ring perpendicular to the axis of the ring. Figure 6 depicts the situation when $H = 0-R$, Figure 3 shows the condition $H = R$ to n_2R, and Figure 5 shows the condition $(R + d) > H > n_2R$.

Neglecting the actual divergence angle of the beam or the Gaussian characteristics, then the case in Figure 3 is realized when the beam width is equal to $(n_2 - 1)R$ and H is between R and n_2R. The range of the incidence angle is determined by R and d and is independent of n_1 and n_2.

III. Conclusions

A 2-D planar laser beam can be produced by the glass ring. Any application that calls for a planar laser beam may use the glass ring. The ring lens expands the range of application from one dimension to two dimensions.

Velocity measurement by a light net relies on the two signals when a light speed flying object passes two planar light beams. A microprocessor is used to calculate the average velocity between the two planes.

Applications in plane survey--The planar laser beam produced by the ring may be used directly for line drawing in architecture and ship building, indoor remodeling, and alignment of large buildings. With improved manufacturing precess and installation accuracy of the ring, the planar light beam produced may serve as optical standards in accurate plane survey.

Flow field indication--An important task in the research of internal combustion engines in the display of the gas distribution in the cylinder. Since the planar laser beam can clearly show the distribution and flow of small particles in a mist, a number of planar laser beams may be used in the display of the flow field of gas vapors in the cylinders of an internal combustion engine.

In addition, the ring lens may find uses in defense research on light target, multipoint communication, and laser warning system. The ring lens may also be used in laser machining and laser display.

Judging from the experimental results, the ring lens is a valuable optical component. Ring lenses of different precision may be used in different applications. Special components may be designed according to the application.

For future work, the characteristics of the ring lens should be investigated in order to understand the light intensity distribution and the conditions for interference.

REFERENCES

1. Mu Guoguang [3019 0948 0342] and Zhan Yuanling [2069 0337 0109], "Optics," People's Education Publishing Company, Sept 1979.

2. Wang Xipo [3769 6006 0980] and Peng Guifang [1756 2710 5364] of the Changchun Applied Chemistry Institute, article on two dimensional planar laser, Vol 3, No 1, 1983.

3. Xu Daxiong [1776 1129 7160], "Physical Basis of Fiber Optics," Advanced Education Publishing Company, Sept 1978.

4. "Laser Display Experiments," translated by Song Zhufeng [2646 4554 6265], People's Education Publishing Company, 1980.

5. Z. Gy. Horvath, A.A. Malyntin and A.V. Kilpio. Laser Focus 16, 1980, 32.

6. D.C. Brown and T.L. Rome, Am. J. Phys. V 40, p 470 March 72.

COMPOSITION ANALYSIS OF COMBUSTION PRODUCTS OF TOWN GAS AND STUDIES ON CORRESPONDING EQUIPMENT WITH SBC DATA PROCESSING

[English abstract of article by Jin Zhigang [6855 1807 0474], et al.]

[Text] This paper describes a self-designed continuous autoanalysis equipment of combustion products and explains the theoretical approach and technical measures taken. The new equipment has the following advantages:

1. increased precision,

2. considerable reduction of test time,

3. timely printing of combustion parameters: coefficient of excess of air 2, CO content in dry and airfree flue gas $CO_{a=1}$, and ration CO/CO_2,

4. display of combustion parameters.

Results of experiments show that the equipment is a power-ful tool in investigating combustion performance. (Paper received 1 Dec 84.)

REFERENCES

[1] 煤气燃烧及输配测试技术 金志刚 1981. 建工出版社

[2] 支架对液化石油气灶烟气中 CO 浓度的影响 金志刚 李文비 1982.10 "城市煤气情报"

[3] Gas Analysis Instumentation A.Verdin 1973.

Catalysis

INVESTIGATION ON THE ADSORPTION AND REACTION OF n-BUTENE ISOMERS OVER FERRITE SPINELS WITH PULSE AND TPD TECHNIQUES

Beijing CUIHUA XUEBAO [JOURNAL OF CATALYSIS] in Chinese Vol 7, No 1, Mar 86 pp 1-8

[English abstract of article by Qiu Fengyan [6726 7685 3508], et al., of Lanzhou Institute of Chemical Physics, Academia Sinica]

[Text] Adsorption and reaction of n-butene isomers over α-Fe_2O_3, $ZnFe_2O_4$ and $ZnCrFeO_4$ were studied by means of pulse and TPD techniques. It is shown that the three butene isomers are adsorbed on the three oxides at approximately the same amount, but they react quite differently on them. At room temperature, three isomers show almost no reaction on α-Fe_2O_3; meanwhile, double bond migration and selective oxidation to butadiene occur distinctly over the two spinels to different extents. Results with multiple pulses of butenes on the two spinels demonstrate that the butadiene formation in the second pulse is much greater than that in the first, then it lowers again in the subsequent pulses. It is suggested that selective oxidation sites are generated on the two spinels through the action of the first butene pulse. The TPD spectra of butanes adsorbed at room temperature on the three oxides show two well-separated peaks: the low temperature peak (<200°C) consists of butene and butadiene; while the high temperature peak (200-600°C) is also a composite peak and consists of CO_2 only. The butenes retain strongly on the oxides except α-Fe_2O_3. Repeated TPD runs up to 600°C are required to "desorb" thoroughly the retained butenes. CO_2 is the sole project in subsequent TPD runs. Two modes of generation of selective oxidation sites on the spinels (reduction activation and heating activation) are suggested and plausible structures of surface species (both the adsorbed butene and active sites) in selective and total oxidations are discussed. (Paper received 2 Aug 84.)

REFERENCES

〔1〕 Massoth, F. E. & Scarpiello, D. A., J. Catal., 21, 294(1971).
〔2〕 Rennard, R. J. & Kehl, W. L., ibid., 21, 282(1971).
〔3〕 Kung, H. H., Kundalkar, B., Kung, M. C. et al., J. Phys. Chem., 84, 382(1980).
〔4〕 Kung, H. H., Kung, M. C. & Yang, B. L., J. Catal., 69, 506(1981).
〔5〕 汪汉卿, 冯良波, 陈英武等, 中国科学, №9, 875(1979).
〔6〕 徐慧珍, 王肯, 燃料化学学报, 8, 187(1980).
〔7〕 Gibson, M. A. & Hightower, J. W., J. Catal., 41, 420(1976).
〔8〕 Idem., ibid., 41, 431(1976).

SYNCHRONOUS TRACKING TPD AND TPSR OF CO ON Pt/Al$_2$O$_3$ BY TC-GC TECHNIQUE

[English abstract of article by Li Qiyuan [2621 0796 3293], et al., of Research
Institute of Qilu Petrochemical Corporation, Zibo, Shandong]

[Text] CO TPD spectra on Pt/γ-Al$_2$O$_3$ catalysts have been monitored by GC in
step with thermoconductivity (TC) technique. Results showed that the TC-
spectrum of desorbed CO is flat broad profile from 331 to 776K, which is simi-
lar to that reported by other authors. The GC-spectra indicated that there
exist two peaks for CO or CO$_2$, of which the maximum temperatures T_{m1} and T_{m2}
are 237, 384°C and 220, 309°C respectively. The effect of re-adsorption of
CO on the broadening of spectra observed under our experimental conditions may
be neglected, so the broadening of spectra is attributed to the existence of
multi-chemisorption states of CO and CO$_2$. Raising the temperature of heat
treatment of the catalysts in H$_2$ from 500 to 800°C for 6 hours, a considerable
change of behaviors of adsorption and reaction for CO took place. The amount
of adsorbed CO decreased from 96.6 to 68.6ml/g-Pt, but the ratio of CO$_2$ to CO
in desorbed product increased from 0.69 to 2.25. There was only a single peak
of CO$_2$ on the TPSR spectra in O$_2$- He carrier gas, of which the maximum tempera-
ture reduced from 231 to 76°C. From the TPD spectra after a period of CO oxi-
dation in a gaseous mixture containing a major amount of H$_2$, it was found that
the tendency to yield CO$_2$ was markedly enhanced. It is interesting that the
CO reactivity characterized by TPD and TPSR corresponds to the selective oxi-
dation activity measured by steady-state flow method. Under the given reaction
conditions, the measured turnover frequency of CO selective oxidation on sample
treated at 800°C was 3.1 x 10^{-2} mol/site.sec, it is thirty-three times as large
as that on the sample treated at 500°C. However, in H$_2$-Ar carrier gas, TPSR
spectra of adsorbed CO revealed that the methanation to CH$_4$ did not show
obvious different from that of the sample treated at high temperature in H$_2$.
(Paper received 21 Sep 84.)

REFERENCES

(1) Falconer, J. L. & Schwarz, J. A., *Catal. Rev.-Sci. Eng.*, 25 (2), 141(1983).
(2) Fujimoto, K., Kameyama, M. & Kunugi, T., *J. Catal.*, 61, 7(1980).
(3) Takahashi, M. et al., *ibid.*, 45, 15(1976).
(4) 伏义路, 林培琰, 催化学报, 3, 205(1982).
(5) 徐慧珍, 陈惠功, 翁善至, 同上, 4, 185(1983).
(6) Foger, K. & Anderson, J. R., *Appl. Surf. Sci.*, 2, 335(1979).
(7) Herz, R. K. et al., *J. Catal.*, 73, 66(1982).
(8) Tauster, S. J. et al., *J. Amer. Chem. Soc.*, 100, 170(1978).

STUDIES OF $Co_2(CO)_6(PBu_3)_2$ COMPLEX SUPPORTED ON ZrO_2 AND DISPERSED COBALT CATALYSTS

[English abstract of article by Xu Huizhen [1776 1979 3791], et al., of Lanzhou Institute of Chemical Physics, Academia Sinica]

[Text] The decarbonylation of $Co_2(CO_6)(PBu_3)_2$ supported on ZrO_2 and $Zr(OH)_4$, and the adsorbed species of CO on the dispersed cobalt catalysts have been studied by IR spectroscopy, UV diffuse reflectance spectroscopy and temperature-programmed decomposition technique (TPDE). It is found that when the surface complex is heated in vacuum, the intensity of terminal carbonyl diminishes somewhat with increasing temperature, and the intensity of bridged carbonyl increases simultaneously. As the temperature is raised to 300°C, the carbonyl bands disappear completely. However, the C-H frequency bands persist in the IR spectra, showing the phosphine ligands still exist on the catalyst surface. When CO admitted to the dispersed catalysts after decarbonylation of supported complexes, it is noticed that at the time of exposing the catalysts with adsorbed CO to air, the frequency band of CO disappears at once. According to experimental results, two models of the $Co_2(CO)_6(PBu_3)_2$ supported on ZrO_2 and $Zr(OH)_4$ are proposed. The interactions of the $Co_2(CO)_6(PBu_3)_2$ with the surface of ZrO_2 and $Zr(OH)_4$ are also discussed respectively. When supported on ZrO_2, the Co in $Co_2(CO)_6(PBu_3)_2$ interacts with oxygen ions on ZrO_2 surface. $Co_2(CO)_6(PBu_3)_2$ directly interacts with hydroxyl groups on $Zr(OH)_4$ surface when supported on $Zr(OH)_4$, hydrogen bonding occurs between the oxygen atoms of carbonyl ligands and the OH groups. At elevated temperature under vacuum, hydrogen bonding diminishes and partially decarbonylated complex is formed, which is similar to that supported on ZrO_2. (Paper received 25 Aug 84.)

REFERENCES

〔1〕 Nakamura, R., Oomura, A. et al., *Chem. Lett.*, 1463(1982).

〔2〕 Iwasawa, Y., Yamada, M., Sato, Y. et al., *J. Mol. Catal.*, 23, 95(1984).

〔3〕 Schneider, R. L., Howe, R. F. & Watters, K. L., *J. Catal.*, 79, 298(1983).

〔4〕 杨震宇, 罗玉忠, 刘惠德等, 催化学报, 1, 26(1980).

〔5〕 Abrahamson, H. B., Frazier, C. C., Ginley, D. S. et al., *Inorg. Chem.*, 16, 1554(1977).

〔6〕 Levenson, R. A. & Gray, H. B., *J. Amer. Chem. Soc.*, 97, 6042(1975).

〔7〕 Gardner, R. A. & Petrucci, R. H., *ibid.*, 82, 5051(1960).

INFRARED STUDY ON THE CONVERSION OF METHANOL TO HYDROCARBONS ON HZSM-5 ZEOLITE

[English abstract of article by Dong Qingnian [5516 1987 1628] of Shanxi
Institute of Coal Chemistry, Academia Sinica, Taiyuan]

[Text] Description of the catalytic action of HZSM-5 zeolite in published
literatures usually emphasized the contribution of Bronsted acid sites, but
the effect of Lewis acid sites was often neglected. The methanol adsorption
and conversion on HZSM-5 zeolite were studied by means of in situ infrared
spectroscopy. It was found that methanol was bound to Bronsted acid sites
forming weak hydrogen bonds, but it was adsorbed on Lewis acid sites through
strong chemical bonds. Consequently, the dehydration of methanol took place
primarily on the Lewis acid sites to form dimethyl ether, the first inter-
mediate. Therefore, it is obvious the Lewis acid sites also played an impor-
tant role in the conversion of methanol to hydrocarbons. According to the IR
spectra of methanol adsorbed on HZSM-5 zeolite at different temperatures, it
was revealed that methanol reacted further with dimethyl ether thus produced
to form high ether-like species on Bronsted acid sites in the range of 200-
300°C. This implicated the beginning of carbon chain multiplication. Con-
tinuously raising the reaction temperature to above 300°C, polymerization,
cracking and dehydration took place, and different kinds of hydrocarbons were
produced. A proposed reaction scheme for the conversion of methanol was given.
(Paper received 8 Sep 84.)

REFERENCES

〔1〕 Chang, C. D. & Silvestri, A. J., *J. Catal.*, 47, 249(1977).
〔2〕 Derouane, E. G., Nagy, J. B. & Dejaifve, P., *ibid.*, 53, 40(1978).
〔3〕 小野嘉夫等, 触媒(日), 21, 356(1979).
〔4〕 Kagi, D., *J. Catal.*, 69, 242(1981).
〔5〕 Kaeding, W. W. & Butter, S. A., *ibid.*, 61, 155(1980).
〔6〕 郭文珪, 梁娟, 赵素琴等, 催化学报, 5, 11(1984).
〔7〕 张芷, 傅聪忍, 刘裕铭等, 燃料化学学报, 10, 53(1982).
〔8〕 张芷, 傅聪忍, 榭欣欣等, 同上, 12, 193(1984).

〔9〕 Védrine, J. C., Auroux, A. et al., *J. Catal.*, 59, 248(1979).
〔10〕 郭文珪, 辛勤, 张慧等, 催化学报, 2, 113(1981).
〔11〕 王建民, 吕久茹, 石油化工, 11, 656(1982).
〔12〕 Topsøe, N. -Y. et al., *J. Catal.*, 70, 41(1981).
〔13〕 董庆年, 燃料化学学报, 11, 60(1983).
〔14〕 杨玉华, 赖国长, 成都科技大学学报, № 1, 47(1983).
〔15〕 陈国权, 蔡光宇, 王清遐等, 燃料化学学报, 10, 308(1982).
〔16〕 Bellamy, L. J., "The Infrared Spectra of Complex Molecules", Chapman & Hall, London, 3rd Ed., 1975.
〔17〕 Bellamy, L. J., "The Infrared Spectra of Complex Molecules, Vol 2, Advances in Infrared Group Frequencies", Chapman & Hall, London, 2nd Ed., 1980.
〔18〕 Perchard, J. P., *Spectrochim. Acta*, 26A, 707(1970).
〔19〕 Wieser, H. & Laidlaw, W. G., *ibid.*, 24A, 1055(1968).

THE STRUCTURAL CHANGES OF HZSM-5 ZEOLITES TREATED BY HIGH TEMPERATURE STEAM AND THEIR EFFECTS ON THE ALKYLATION OF TOLUENE WITH METHANOL

[English abstract of article by Zeng Zhaohuai [2582 2507 2849], et al., of
Department of Chemistry, Zhongshan University, Guangzhou]

[Text] The structural changes of HZSM-5 zeolites treated by steam at various
temperatures were studied by XRD, XPS, IR, TGA, TPD and vacuum vapor gravimetric
absorption techniques, and the alkylation of toluene with methanol over the
zeolites was examined by continuous-flow microreaction chromatography as well.
Experimental results of HZSM-5 zeolites after steam treatment at 600, 700, 800
and 900°C for 6 hours respectively were as follows: The framework topology of
zeolite samples was not destroyed as shown by the XRD patterns, but a change
from orthorhombic symmetry to apparent monoclinic symmetry was observed. XPS
analysis indicated that the aluminium atoms were removed greatly from the frame-
work. IR spectra and TPD graphs revealed that the surface Bronsted acid sites
and the acidic strength were decreased remarkably, the same conclusion might
also be drawn from the TGA data. Adsorption data showed that the zeolite chan-
nels and pore openings would be twisted and/or contracted slightly.

When the alkylation of toluene with methanol was performed over the steam
treated HZSM-5 zeolite catalyst, a high selectivity for p-xylene was obtained.
This is attributed to the changes of surface acidity and channel structure of
the zeolite, however, the former is the primary factor. It is considered that
the temperature for steam treatment is not necessary to exceed 700°C, and for
the methylation of toluene, the appropriate reaction temperature is 450 to 550°C.
For example, alkylation of toluene over a 600°C steam treated HZSM-5 sample at
a reaction temperature of 500°C gives 81.4 percent selectivity for p-xylene with
a 29.8 percent toluene conversion. (Paper received 9 Jul 84.)

REFERENCES

〔1〕 Yashima, T., Ahmad, H., Yamazaki, K. et al., *J. Catal.*, 16, 273(1970).

〔2〕 Yashima, T., Yamazaki, K., Ahmad, H. et al., *ibid.*, 17, 151(1970).

〔3〕 Kaeding, W. W., Chu, C., Young, L. B., *ibid.*, 67, 159(1981).

〔4〕 *U. S.* 3,965,209(1976).

〔5〕 Yashima, T., Sakaguchi, Y. & Namba, S., "Proceedings of the 7th International Congress on
  Catalysis", (Eds. Seiyama, T. & Tanabe, K.), Kodansha, Tokyo, p. 739, 1981.

〔6〕 曾昭槐、王炽瑜，石油化工，12, 389(1983).

〔7〕 Kerr, G. T., *J. Catal.*, 15, 200(1969).

〔8〕 孟中岳、鲍书林、周日新，催化学报, 2, 209(1981).

〔9〕 *U. S.* 3,702,886(1972).

〔10〕 Wu, E. L., Lawton, S. L., Olson, D. H. et al., *J. Phys. Chem.*, 83, 2777(1979).

〔11〕 郭文珪等，催化学报, 2, 113(1981).

〔12〕 Jacobs, P. A., "Carboniogenic Activity of Zeolites", Elsevier, Amsterdam, p. 168, 1977.

〔13〕 Weisz, P. B., *Pure Appl. Chem.*, 52, 2091(1980).

〔14〕 Wei, J., *J. Catal.*, 76, 433(1982).

STUDIES ON THE ION EXCHANGED ULTRASTABLE Y TYPE (USY) ZEOLITES BY INFRARED
SPECTROSCOPY

[English abstract of article by Zhang Yingzhen [1728 4134 3791], et al., of
Dalian Institute of Chemical Physics, Academia Sinica]

[Text] HY, CaHY, LaHY and the corresponding ultrastable treated USY, CaUSY,
LaUSY zeolites were studied by means of infrared spectroscopy. In comparison
with HY and USY, USYH obtained by further NH_4^+ ion exchange of USY was also
examined.

It was found that the intensity of $3700cm^{-1}$ band of MeUSY depended not only on
the content of Na+, but also on the content of other cations, such as Ca^{2+} and
La^{3+}. Spectra in the region of OH stretching vibration showed that the
presence of La^{3+} stabilized the skeletal OH groups in zeolites. The intensity
of spectral band around 1545 and $1455cm^{-1}$ and its change at different desorp-
tion temperatures of pyridine were examined for characterizing the quantity
and the strength of acidity of zeolites. it was revealed that HY, USY and
USYH behaved quite differently in this respect. Their Bronsted acid strength
are of three different levels and the Lewis acid strength of USYH is unexpec-
tedly high. A better corresponding relation between the cracking activity for
n-decane and Bronsted acid strength is found. These three zeolites samples,
in acidity, may be taken as representatives of zeolites investigated.

Discussion on the effect of ultrastable treatment, the properties of cations
and subsequent NH_4^+ exchange on the stability of zeolites, the nature and
accessibility of the acid sites was given. (Paper received 18 Sep 84.)

REFERENCES

(1) Scherzer, J., Bass, J. L. & Hunter, F. D., J. Phys. Chem., 79, 1194 (1975); J. Catal., 54, 405
(1976); J. Catal., 46, 100(1977).

(2) 余励勤,刘兴云,李宜文,石油炼制, No. 5, 10 (1982);催化学报, 1, 268 (1980).

(3) 张盈珍,尹桂林等,石油化工, 14, 354 (1985).

(4) Ward, J. W. in "Zeolite Chemistry and Catalysis", (Ed. Rabo, J. A.), ACS, Washington, Chapt.
3, 1976.

(5) Barthomeuf, D. & Beaumont, R., J. Catal., 30, 288 (1973).

(6) Dempsey, E., ibid., 33, 497 (1974).

(7) Barthomeuf, D., Rreprints (Div. Petrol. Chem. Amer. Chem. Soc.), 28, 875 (1983).

(8) Datka, J., J. Chem. Soc., Faraday Trans. I, 77, 2877 (1981).

DISTRIBUTION OF THE BIVALENT NICKEL ION IN ZSM-5 MOLECULAR SIEVE

[English abstract of article by Liu Zhenyi [0491 2182 5030], et al., of Department of Chemistry, Beijing University]

[Text] The catalytic behavior of ZSM-5 zeolite can be modified by both physical and chemical methods. Structural parameters of three-dimensional channel of ZSM-5 zeolite can be changed by physical method because of its structural flexibility, so its catalytic behavior is also changed. To elucidate the mechanism of the chemical modification, the structure of ZSM-5 zeolite after being exchanged with pressurized nickel was determined by polycrystal X-ray diffraction. It has been discovered that there are two positions of bivalent nickel ion outside the framework of ZSM-5 zeolite. One is that $Ni^{2+}(1)$ is located nearby the central point of the median line in the hexacycle facing the cavity of two channels and deviates to ca. 1.5Å from the wall of the channel. $Ni^{2+}(1)$ in such position has a direct influence upon the nearby electric charge distribution in the active center of ZSM-5 zeolite even though it is not inside the channel. Another is that $Ni^{2+}(2)$ is located in parallel to (100) direction of "Z" form channel and deviates to ca. 1.6Å from the center of decacycle. The existence of Ni^{2+} changes the effective gap in the opening of "Z" form channel; and, $Ni^{2+}(2)$ itself can be in contact with the reactants entered into the channel of zeolite and participates catalysis. (Paper received 27 Dec 84.)

REFERENCES

〔1〕 Chen, N. Y. & Garwood, W. E., *J. Catal.*, **52**, 453(1978).
〔2〕 张婉静等, 石油学报(石油加工), 1(1), 41(1985).
〔3〕 Chen, N. Y., Kaeding, W. W. & Dwyer, F. G., *J. Amer. Chem. Soc.*, **101**, 6783(1979)
〔4〕 周日新等, 石油化工, 11, 781(1982).
〔5〕 吴指南等, 石油化工, 12, 185(1983).
〔6〕 Olson, D. H. et al., *J. Phys. Chem.*, **85**, 2238(1981).
〔7〕 于勤等, 石油学报, 3(3), 83(1982).
〔8〕 Albinati, A. & Willis, B. T. M., *J. Appl. Cryst.*, **15**, 361(1982).

THE PROPERTIES OF OXYGEN SPECIES ON THE SURFACE OF V_2O_5/SiO_2 CATALYST

[English abstract of article by Zheng Xiaoming [6774 1420 2494], et al., of Department of Chemistry, Hangzhou University]

[Text] The TPD spectra of the surface oxygen of V_2O_5/SiO_2 catalyst have been obtained by using the high sensitive TPD-MS determination.

TPD spectra show obviously that the surface oxygen of V_2O_5/SiO_2 can be divided into three groups which possess different energies. The first group of surface oxygen is desorbed at 100-150°C, the second group is desorbed at 400-600°C, and the third at above 600°C. They correspond probably to the desorption of O_2^-, O^- and O^{2-} respectively in accordance with the ESR results. The area S_1 of the first peak is no more than 5-10 percent of the total peak area (S_1+S_2) of the catalyst, therefore, O^- is the main form of active oxygen on V_2O_5/SiO_2 catalyst. Dealing with the peak temperatures at different heating rates, the kinetic parameters of desorption species are obtained. The desorption activation energy of the first peak is 7.83 Kcal/mol, it concurs with the characteristic of weak-adsorbed O_2^-. The apparent activation energy of the second peak is as high as 154 Kcal/mol, because the desorption step has to break two bonds of $V-O^-$, and to overcome the big repelling force between two negative charges during the collisions of two $M-O^-$. (Paper received 1 Jul 85.)

REFERENCES

(1) Lunsford, J. H., *Adv. Catal.*, **22**, 265(1972).
(2) Lunsford, J. H., *Catal. Rev.-Sci. Eng.*, **8**, 135(1973).
(3) 田部浩三等, "金属酸化物和复合酸化物", 讲谈社, 东京, p. 136, 333, 1978.
(4) Sachtler, W. M. H. et al., *Catal. Rev.-Sci. Eng.*, **23**, 127(1981).
(5) Che, M. & Tench, A. J., *Adv. Catal.*, **31**, 77(1982).
(6) 岩本正和, 触媒(日), **26** (1), 30(1984).
(7) Shvets, V. A. et al., *J. Catal.*, **11**, 378(1968).
(8) Tarama, K. et al., *Bull. Chem. Soc. Japan*, **42**, 1161(1969).
(9) Shvets, V. A., Kazansky, V. B. et al., *J. Catal.*, **25**, 123(1972).
(10) Yoshida, S. et al., *Bull. Chem. Soc. Japan*, **47**, 1564(1974).
(11) Yoshida, S. et al., "Proceedings of the 5th International Congress on Catalysis", (Ed. Hightower J. W.), North-Holland, Amsterdam, p. 1049, 1972.
(12) Iwamoto, M. et al., *J. Phys. Chem.*, **82**, 2564(1978).
(13) 王吉祥, 谢筱帆, 催化学报, **1**, 229(1980).
(14) 邢起五, 郑小明, 金松寿, "集团结构适应理论文集", 第 1 卷, 第53页, 1984.

Chemistry

DETERMINATING THE ACTIVITY OF SOLID CATALYST S101 TYPE SULFURIC VANADIUM CATALYST
BY USING CD-2 TYPE INTERNAL RECYCLE GRADIENTLESS REACTOR

[English abstract of article by Tan Liye [3389 4539 2814]]

[Text] The principle and method for determinating solid catalyst activity
by using internal recycle gradientless reactor have been discussed in this
paper. The data of activity of S101 type sulfuric vanadium catalyst had been
determined. Thus correlated with tubular reactor method and recycle gradient-
less reactor method; and predicating the functions of pilot-plant reactor.

REFERENCES

[1] 陈誦英，石油化工，7 (1978), 290
[2] 谭立业，石油炼制，3 (1979), 14
[3] 谭立业、唐玉华，四川化工，2 (1982), 40
[4] 陈甘棠、梁玉衡，化学反应技术基础，科学出版社，1981
[5] 谭立业、唐玉华、罗开统*，应用 CD—2 型內循环无梯度反应器在 S101 型钒催化 剂上 研究
     SO_2 催化氧化动力学，1984

CHROMATOGRAPHIC SEPARATION OF PLATINUM METALS IN TWICE DEVELOPMENT

[English abstract of article by Luo Liangqiong [5012 5328 8825] and Zhang Chang [1728 1281]]

[Text] The chromatographic behaviour of platinum, palladium, rhodium, ruthenium, osmium iridium, gold, copper, cobalt and nickel on paper strips treated with N_{235} and N_{263} and eluted with HCl, HNO_3 and HNO_3-HCl mixed acid was investigated. On this basis, a two stepwise chromatographic method was proposed to separate the mixture of platinum metals, gold, copper, cobalt and nickel. Strip with stationary phase N_{263} was first developed with a mobile phase 4N HCl to separate cobalt, copper, nickel and rhodium, then a second mobile phase of 4N HNO_3-2N HCl was used to separate gold and five remained platinum metals. The method has successfully been used to separate and detect ten metals mentioned above.

REFERENCES

[1] 杨正伟、馬忠良、罗良琼、鉑系元素的反相紙色層（1979年，全国无机化学論文报告会論文）

[2] 罗良琼、赵文玉、童勇，铱、钌的萃取分配和紙色層（1979 年，全国无机化学論文报告会論文）

[3] S. Przeszlakowski et al, Talanta, 26 (1979), 1125

[4] S. I. Ginzburg et al, Analytical Chemistry of Platinum Metals, John Willy & Sons, 1975

[5] F. E. Beamish et al, Recent Advances in the Analytical Chemistry of the Noble Metals, 1966

[6] T. Braun et al, Extraction Chromatography, 1975

[7] 商家隆等，化学学报 29 (1963), 421

[8] 刘万一，分析化学 9 (1981), 51—3

AXIALLY DISSYMMETRIC BIARYLS

2. THE SYNTHESIS OF (+)- and (-)-10,10'-DIHYDROXY-9,9' -BIPHENANTHRYL.

[Text] Study of axially dissymmetric biaryls has recently been revived. Most of the work, however, was focused in derivatives of 1,1' -binaphthyl in terms of their syntheses and application to chiral recognition and various asymmetric syntheses[1]. We have been interested in finding synthesis and stereochemistry of higher analog of biaryls. In this article, we demonstrate a novel synthetic approach to both enantiomers of 10,10'-dihydroxy-9,9'-biphenanthryl [(1)- and (+)-6][5] was demonstrated. (Paper received Nov 85.)

REFERENCES

[1] (a). Cram, D.J., Trueblood, K.N., in *Topics in Current Chemistry*, **98**,(1981), 43

 (b). Cram, D.J, Cram, J.M., *Acc. Chem. Res.*, 11(1978), 8.

 (c). Noyori, R., Tomino, T., Tanimoto, Y., Nishizawa, M., *J. Am. Chem. Soc.*, 106(1984), 6709, 6717.

 (d). Miyamo, S., Handa, S., Shimizu, K., Tagami, K., Hashimoto, H., *Bull. Chem. Soc. Jpn.*, 57(1984), 1943.

 (e). Mazaleyrat, J.-P., Cram, D.J., *J. Am. Chem. Soc.*, 103(1981), 4585.

 (f). Olivero, A.G., Weidmann, B., Seebach, D., *Helv. Chim. Acta.*, 64(1981), 2485.

 (g). Miyashita, A., Takaya, H., Souchi, T., Noyori, R., *Tetrahedron*, 40(1984), 1245.

[2] (a). Badger, G.M., Drewer, R.J., Lewis, G.E., *J. Chem. Soc.*, 1962, 4268.

 (b). Yamada, S., Akimoto, H., *Tetrahedron Lett.*, 1968, 3967.

[3] Review see: Gschwend, H.W., Rodriguez, H.R., *Org. Reactns.*, 26(1980), 61.

[4] 许遵乐、黄文洪、鄢亮、谢颂凯, 有机化学, 1985, 475.

[5] Yamamoto, K., Tukushima, H., Okamoto, Y., Hatada, K., Nakazaki, M., *J. Chem. Soc., Chem. Commun.*, 1984, 1111.

[6] Horning, E.C., 有机合成, 中译本, 1955, 3, 82.

[7] Bacon, R.G.K., Rennison, S.C., *Chem. & Ind.*, 1966, 812.

[8] Jolly, W.L., 无机合成, 中译本, 11(1975), 72.

A STUDY OF THE SELECTIVITY OF SOLVENT EXTRACTION OF COBALT(II) AND NICKEL(II) AS THE MOLECULAR STRUCTURE OF THE EXTRACTABLE CHELATES

[English abstract of article by Yang Xueqiang [2799 1331 1730], et al.]

[Text] The composition and structure of extractable chelates and the reaction mechanism of extraction in the solvent extraction systems of cobalt(II) and nickel-(II) with commercial P_{204} di(2-ethylhexyl)phosphoric acid and P_{507} di(2-ethylhexyl)phosphonic acid were investigated.

The following substituted reaction was first found in the organic phase systems of cobalt(II) and nickel(II) with di(2-ethylhexyl)phosphoric acid.

$$Co(HA_2)_2(HA)(H_2O) + Ni(HA_2)_2(H_2O)_2 \rightleftharpoons Co(HA_2)_2(H_2O)_2 + Ni(HA_2)_2(HA)(H_2O)$$
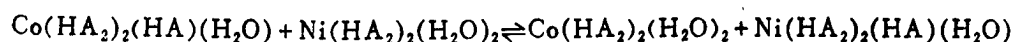
It has been proved that the selectivity of solvent extraction of cobalt(II) and nickel(II) depended remarkably on the molecular structure of the extractable chelates. (Paper received Nov 84.)

REFERENCES

[1] 高自立等，有色金属，1984，1，42.

[2] 沈静兰等，有色金属，1983，2，47.

[3] J.S.Preston, *Hydrometallury*, 9(1982), 2, 115-133.

[4] T.Sato et al., *J.Inorg. Nucl. Chem.*, 34(1972), 3721.

[5] J.E.Barnes et al. *J.Inorg. Nucl. Chenl.*, 38(1976), 1065-1067.

[6] 陈金榜等，高等学校化学学报，1983，3，281.

[7] 北京矿冶研究总院等，有色金属，1981，1，25.

AN INVESTIGATION INTO ADDITIVE-TYPE DIESEL ENGINE FUEL AND COMBUSTION

[English abstract of article by Xie Shiwen [6043 0013 2429] of Internal Combustion
Engine Research Institute]

[Text] The effect of the additive-type fuel on the expansion of light fuel
source and the improvement of the combustion of heavy fuel in high speed diesel
engines were studied.

The selectivity of additives and the relationship between the diesel performance
and values of 1, ψ, and φ of the additive-type fuel were explored. (Paper
received 4 Jun 85.)

REFERENCES

[1] J. E. Foulger, Chemical Additives as Part of Integrated Fuel Mana-
gement, MER, 1981—9 .

[2] Scandinavian Operators Claim Good Results with Clean Power Addi-
tive, Motor Ship, 62—734, 1981—9 .

[3] W. R. メイ，松本安弘，加藤裕之，《ガスクービソ添加剤》，[日] 燃料及
び燃焼，昭57年5月 (1982)，P17—22。

[4] G. Hanter, J. Scholl, et al, The Effects of Fuels on Diesel Oxidation
Catalyst Performace and the Physical, Chemical, and Biological charac-
ter of Diesel Particulate Emissions, SAE, Trans, 811192.

[5] 《ディーゼル機関の微粒子の焼却を促進する塩化物》，海外技術ハイライド，
1982. 10, Vol16, No.7。

[6] 绘畑义卫，《触媒にするディーゼル機関のススの酸化促進》，モークビクル，
1982.No.9，P48—51。

[7] 解世文，《车用柴油机燃料燃烧性能的非动力研究》，汽车技术，1984. No.11，
P37—41。

[8] 解世文，《柴油机燃料燃烧完全性的氧弹研究》，CICS会议论文 No.844072.
1981.11）。

TWO-DIMENTIONAL MATHEMATICAL MODELING FOR THE FIXED-BED REACTOR OF ETHYLBENZENE DEHYDROGENATION

[English abstract of article by Tong Zemin [0157 3419 3046] of Department of Chemical Technology, Beijing Petrochemical College]

[Text] A two-dimentional mathematical model was proposed for the design of ethylbenzene dehydrogenation fixed-bed reactor. The reactor was packed with Chinese-made Type-315 catalyst. Parameters were estimated based on a 2000 tons per year industrial reactor. The calculated outlet temperature and conversion were in good agreement with the data measured from industrial reactor. The calculated axial or radial temperature distribution, and conversion distribution were shown in diagrams. The biggest difference between radial temperature in the same axial position was 51°C. (Paper received 4 Nov 85.)

REFERENCES

[1] 蔡世干, 合成橡胶工业, 6[3],184(1983).

[2] 陈甘棠主编, "化学反应工程", 化学工业出版社, 234(1981).

[3] 王化淳、杨春生, 化学工程,[1], 33(1985).

[4] 北京燕山石化公司向阳化工厂, 内部资料.

[5] 赵中琦等, 催化学报, 6[2], 107(1983).

[6] 天津大学化学工程教研室, "化学工程", 第四册, 201(1976).

[7] Howard, F. Rase, "Chemical Reactor Design for Process Plants", Vol. II, 139 (1977).

[8] 兰州化学工业公司设计院编, 石油化工技术参考资料(33), "石油化工工业炉设计".

[9] Jenson, V.G., Jeffreys, G.V., "Mathematical Methods in Chemical Engineering", 2nd Ed., (1977).

STUDY OF THE REACTORS FOR THE THERMAL BULK POLYMERIZATION OF STYRENE

II. THE EFFECT OF MICROMIXING OF POLYMERIZATION

[English abstract of article by Feng Dibai [7458 0966 2672] of Lanzhou Petro-chemical Engineering Design Institute of SINOPEC]

[Text] The effect of micromixing on polymerization reaction speed and product quality of thermal bulk polymerization of styrene was studied with mathematical model of micromixing for polymerization reactors developed early. The results show that microsegregation speeds up the reaction and makes the reaction speed approach to that of piston flow reactor. The average molecular weight and its distribution of polystyrene obtained in microsegregation reactor are also between those of piston flow and maximum micromixing reactors. (Paper received 20 Sep 85.)

REFERENCES

〔 1 〕 冯地柏，合成橡胶工业，7〔1〕，13（1984）。

〔 2 〕 计其达，“聚合过程及设备”，化学工业出版社，88—89（1981）。

〔 3 〕 Hui,A.W.,et al.,J.Appl. Poly.Sci., 16〔3〕, 749（1972）.

〔 4 〕 冯康，百科知识，〔5〕，43（1985）。

〔 5 〕 冯地柏，合成橡胶工业，8〔4〕,240（1985）。

〔 6 〕 Danckwerts,P.V., "The Effect of Incomplete Mixing on Homogeneous Reactions" ,Chemical Reaction Engineering, 12th Meeting Europ.Fed. Chem.Engng. Amsterdam,（1957）.

〔 7 〕 Zwietering,TH. N.,Chem.Engng.Sci., 11〔1〕, 1（1959）.

〔 8 〕 Tadmor, Z.,Biesenberger,J. A.,I & EC Fund.,5〔3〕, 336（1966）.

〔 9 〕 Vollmert,B.著，孙以实译，“聚合物化学”（上），化学工业出版社,99(1980)。

MICROKINETIC STUDY OF BUTADIENE POLYMERIZATION WITH $MoCl_4$-$(i\text{-}Bu)_2AlO$⟨⟩CH_3 CATALYST SYSTEM

I. RATE EQUATION OF POLYMERIZATION AND DETERMINATION OF KINETIC PARAMETERS

[English abstract of article by Yang Yuwei [2799 3768 0251], et al., of Department of Polymer Engineering, Qingdao Institute of Chemical Technology]

[Text] The kinetic behavior of butadiene (Bd) polymerization with

$MoCl_4$- $(i\text{-}Bu)_2AlO$⟨⟩CH_3 catalyst was studied. The reaction order of monomer and catalyst was determined. The kinetic parameters, the efficiency of catalyst was determined. The kinetic parameters, the efficiency of catalyst, the concentration and the average life period of active center etc within the temperature range of 30-70°C were also obtained. The experimental results show that the rate of polymerization is first order with respect to both the concentrations of monomer and $MoCl_4$. The rate equation of polymerization can be expressed as follows:

$$-d[Bd]/dt = k_p a[MoCl_4][Bd]$$

The total activation energy for butadiene polymerization with

$MoCl_4$- $(i\text{-}Bu)_2AlO$⟨⟩CH_3 catalyst system is 17.4 kcal/mol, and the catalyst efficiency is found to be about 1.5 percent. The average life period of active center reduces with the rise of polymerization temperature. (Paper received 27 Jul 85.)

REFERENCES

〔1〕 倪少懦、高绪国、唐学明，高分子通讯，〔4〕，241；〔5〕，326（1983）。

〔2〕 杨玉伟、唐学明，四价钼催化体系合成高乙烯基聚丁二烯的研究．待发表。

〔3〕 杨玉伟、鞠远波、唐学明，合成橡胶工业，8〔5〕，330（1985）。

〔4〕 杨玉伟、李 迎、辛浩波、唐学明，合成橡胶工业，9〔2〕，101（1986）。

〔5〕 竹内安正，日本橡胶协会志（日文），〔8〕，43（1979）。

〔6〕 健谷勤，石油和石油化学（日文），〔9〕，100（1969）。

〔7〕 于广谦，"稀土催化合成橡胶文集"，科学出版社，49（1980）。

A NEW CROSSLINKING SYSTEM FOR MERCAPTAN-TERMINATED POLY(BUTADIENE-ACRYLONITRILE) LIQUID RUBBER

[English abstract of article by Jia Demin [6328 1795 3046], et al., of Materials Science Research Institute, South China Institute of Technology, Guangzhou]

[Text] Epoxy resin (Epon 828)/2-ethyl-4-methylimidazole (EMI-24) was used as a new crosslinking system for the mercaptan-terminated poly(butadiene-acrylonitrile) liquid rubber(MTBN). Kinetics of the crosslinking reaction investigated by means of JSR-curelastometer. The curing formulations, curing conditions and mechanical properties of cured MTBN were also investigated. The results show that this crosslinking system is effective for the crosslinking of MTBN. In contrast to Epon828/DMP-30 (2,4,6-tri,dimethylaminomethyl phenol), the conventional crosslinking system, the new one has faster curing speed at moderate curing temperatures and the cured products have better mechanical properties and longer pot life, etc. (Paper received 8 Jun 85.)

REFERENCES

〔1〕 Drake, R.S.,McCarthy, W.J., Rubber World, 159〔10〕, 121 (1968).

〔2〕 沈诗继、王孟钟，合成橡胶工业，7〔4〕，287 (1984).

〔3〕 长谷部磊彦、明石広光，日本橡胶协会志（日文），41〔10〕, 879 (1968).

〔4〕 梅野昌，日本橡胶协会志（日文），41〔10〕, 863 (1968).

〔5〕 日 本 橡 胶 协 会 志（日文），50〔8〕, 830 (1977).

〔6〕 Dea love, T.J., J.Appl. Polym .Sci ., 14, 1615 (1970).

EFFECT OF CURING AGENTS ON THERMAL-OXIDATIVE AGING PROPERTIES AND DAMPING COEFFICIENT OF EPDM-CIIR RUBBER BLENDS

[English abstract of article by Zhang Fenyu [1728 5358 3768], et al., of Changchun Institute of Applied Chemistry, Academia Sinica]

[Text] The EPDM-CIIR rubber blends were vulcanized with S-DCP (sulphur-dicumyl peroxide), GM-S (p-benzoquinone dioxime-sulphur) and 201 resin (brominated polymethyl phenol resin), respectively. Some properties and tan δ values of the vulcanizates were measured by rheovibron viscoelastomer, tensile tester and TDA. The results show that the rubber blend vulcanized with 201 resin has the best thermal-oxidation resistance and the change of the tan δ value is the least of all the vulcanizates. The activation energies have been calculated based on the relationship of log tan$\delta \sim T^{-1}$, and the values are 1.50, 0.82 and 0.40 kcal/mol, respectively for the three types of vulcanizates. (Paper received 4 May 85.)

REFERENCES

〔1〕 阮桂海，"丁基橡胶应用工艺"，化学工业出版社，（1980）。

〔2〕 W.霍夫曼著，王梦蛟译"橡胶硫化与硫化配合剂"，石油化学工业出版社，（1975）。

〔3〕 何曼君、陈维孝、董西侠，"高分子物理"，复旦大学出版社，（1982）。

〔4〕 Edwards.D.C., Rubb. Chem. Technol., 39, 581(1966).

〔5〕 井本稔等，日本橡胶协会志（日文），41, 583(1968).

〔6〕 根津佳代子，日本橡胶协会志（日文），41, 96(1968).

〔7〕 Studebaker.M.L and Beatty.J.R.,Rubb. Chem.Technol.,47, 803(1974).

THERMOTROPIC LIQUID CRYSTALLINE POLYMERS

-AROMATIC COPOLYESTERS CONTAINING MONOSUBSTITUTED BENZENE RINGS AND KINKING COMPONENTS

[English abstract of article by Xie Ping [6200 5493], et al., of Institute of Chemistry, Academia Sinica, Beijing]

[Text] The series of copolyesters were prepared from chloro-hydroquinone or methyl-hydroquinone, terephthalic acid and two kinds of comonomers, which could provide kinking and bending in chain: Oxy-4,4'-diphenol and isophthalic acid. The four-components copolyesters in certain range of compositions have low melting temperature, steady mesophase in a broad temperature range and fiber-forming tendency. Focuses on the relations of molecular composition-transitions-liquid crystallinity and fiber-forming tendency, and the morphologic features of mesophase. The general structure is as follows:
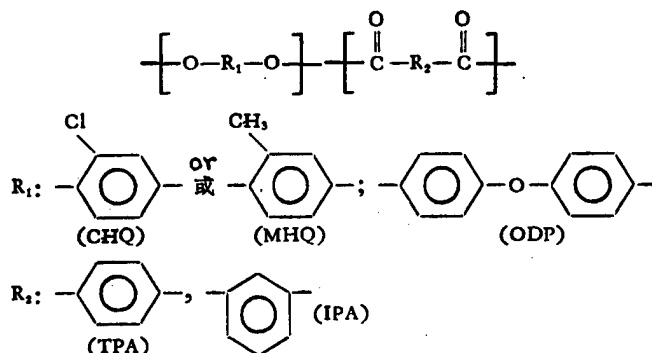
(Paper received 5 Mar 84.)

REFERENCES

[1] 谢萍、陆道惠、黄琦、郑树洪、宝净生，高分子通讯，1985，(4)，269.

[2] Kleinschuster. J. J., Pletcher. T .C., U. S. P. 4,066, 620, 1978.

[3] Lenz. R. W. and J. -I. Jin. *Macromol.*, 1981, 14, 1405—1411.

[4] Bosch. A. Ten., Maissa. P., Sixou. P., *Polym. Pre.*, 1983, 24, 246.

[5] Motoharu Fujii, Kyosuke Nagasaka, Jiroshimada and Hiromi Yamakawa., *Macromol.*, 1983, 16, 1613—1623.

[6] Vittorio Frosini, Auguto Marchetti, Silvano de petris., *Makromol. Chem., Rapid Commun.*, 1982, 3, 795—801.

[7] Janusz Grebowicz and bernhard Wunderlich., *J. Polym. Sci. Phys.*, 1983, 21, 141—150.

[8] Bata. L. "ADVANCES IN LIQUID CRYSTAL RESEARCH AND APPLICATIONS" (Proc. Third. Liq. Crys. conf.), 1979, 943.

DETERMINATION OF PHOSPHORUS AND FLUORINE IN POLYMERS AND ORGANIC COMPOUNDS WITH Nd3+

[English abstract of article by Xie Zhengqiu [6200 2973 4428] of Department of Chemistry, Wuhan University, Wuhan]

[Text] Procedures are developed for the determination of fluorine and phosphorus in polymers and organic compounds by titration with $Nd(NO_3)_3$-EDTA after decomposing the sample by O-flask. An amount of sample corresponding to approximately 1 mg of fluorine is decomposed and absorbed in an O-flask containing an excess of 0.01M Nd^{3+} $(NO_3)_3$. The absorbing liquid is boiled for 3 minutes. After being allowed to cool, a pH=5.5 buffer is added. In the presence of xylenol orange, the mixture is titrated with 0.01M EDTA. The procedure for determining phosphorus is the same as described above, but precipitation reaction of $NdPO_4$ is carried out in pH 5.5 after eliminating CO_2. If sample contains F and P, PO_4^{3-} in the solution containing F^- can be determined after eliminating F^- by adding HNO_3 and concentrating solution to dryness, and the percentage of F can be found after determining the total content of F and P. Determination procedure of total content is the same as F^-, but buffer is added while the mixture is hot. The maximum error of determining P is ±0.20 percent and F is ±0.30 percent except high fluorine or fully fluorinated compounds which give values approximately 0.50 percent lower than calculation. (Paper received 30 Mar 84.)

REFERENCES

[1] 能代 诚，铤田 富雄，分析化学(日)，**1977**, 26, 721.

[2] Осадчий В. Д., Маклакова А. В., Заводск. Лаборатория, **1977**, 43, 269.

[3] Nara, A., Kobayashi, N., Hasegawa, K., Honba, K. and Baba, S., *Microchem, J.*, **1975**, 20, 440.

[4] 穂積啓一郎、秋元直茂，分析化学(日)，**1971**, 20, 467.

[5] Friese, H. J., *Mikrochim. Acta*, **1981**, 1, 265.

[6] 陈耀祖、杜栋华，有机微量定量分析，科学出版社，**1978**, 214.

[7] Light, T. S., Manion, R. F., *Anal. Chem.*, **1969**, 41, 107.

[8] 王昌益、和海青，高分子通讯，**1980**, (5), 309.

[9] Hassan, S. S. M., *Mikrochim. Acta*, **1974**, 889.

[10] 刘惠英、何云陔、丁自荣、曾昭抡，化学学报(增刊)，**1981**, 153.

[11] Цыганова М. Ф., Новикова К. Ф., ЖАХ, **1969**, 24(2), 272.

[12] 云南省化工研究所有机微量分析小组，分析化学，**1976**, 4(6), 440.

[13] Püschel, R. und Wittmann, H., *Mikrochim. Acta*, **1960**, 670.

[14] Hunter, T. L., *Anal. Chim. Acta*, **1966**, 35, 398.

[15] Selig, W., *Z. Anal. Chem.*, **1969**, 247, 294.

[16] Bennewitz, R. und Tänzer, I., *Mikrochim. Acta*, **1959**, 835.

[17] Olson, E. C. and Shaw, S. R., *Microchem. J.*, **1961**, 5, 101.

[18] Lévy, R. und Debal, E., *Mikrochim., Acta*, **1962**, 224.

[19] 谢正秋、赵明焕、段九菊，高等学校化学学报，**1983**, 4(5), 646.

THERMAL STABILITIES OF SILICONE GUMS CONTAINING CYCLODISILAZANE IN THE BACKBONE

[English abstract of article by Li Qishan [2621 0366 1472] and Xie Zemin [6200 2344 3046] of Institute of Chemistry, Academia Sinica, Beijing]

[Text]   The thermal stabilities of silicone gums containing cyclodisilazane,

$$\left[\begin{array}{c} R \\ Si-N \\ R \end{array} \begin{array}{c} Me_2 \\ Si \\ \diagdown \\ Si \\ Me_2 \end{array} \begin{array}{cc} R & Me \\ N\ SiO(SiO)_x \\ R & Me \end{array} \right]_n$$

(SCD), R=Me, Ph, Were studied in comparison with methyl and phenyl silicone gum by the method of TGA. IGA. GC. and GC-MS. The initial temperature of the weight loss of SCD is 150-200°C higher than that of methyl silicone gum, the weight loss is 10-20 times less than that of methyl as well as phenyl silicone polymer. Based on both the GTA and the IGA data, the presence of cyclodislazane in SCD enhances the resistance of the main chain to degradation and the weight loss remains almost the same as the number (x) of Me_2SiO groups in SCD changes. Outstanding stability of this material makes them to be used potentially as high-temperature elastomers. According to analysis of the decomposed products a two steps mechanism of degration is proposed. (Paper received 3 Apr 84.)

REFERENCES

[1] 谢择民、李其山、王金亭、谢祖寿，高分子通讯，1979，(4)，216.
[2] Александрова, Ю. А. и Др., Высокомол. Соед., 1968, 10, 1078.
[3] Thomas, T. H., Hendrick, T. C., *J. Polym. Sci.,* A-2 1969, 7, 537.
[4] Knollmueller, K. O., Scott, R. N., *J. Polym. Sci.,* A-1, 1971, 9, 1071.
[5] Roller, M. N., Gillham, T. K., *J. Appl. Polym. Sci.,* 1973, 17, 2141.
[6] 李二成、谢择民、王金亭、徐广智、叶朝辉，波谱学杂志，1984，1(4)，353.

Computer Science

MULTIVARIATE GENERALIZED SPLINE APPROXIMATION TO SCATTERED DATA WITH CONTINUOUS BOUNDARY CONDITIONS THROUGHOUT A RECTANGLE

[English abstract of article by Guan Lutai [7070 1462 3141]]

[Text]   For multivarite generalized spline interpolation to scattered data and continuous boundary conditions, a suitable generalized blending spline function space is constructed. Existence, uniqueness, characteristics and the structure of the solution in such a space are established. The method can easily be carried out in a computer. (Paper received Dec 84.)

REFERENCES

[1] Li Yuesheng(李岳生), CAT* 55(1984), *Center for Approximation Theory*, Texas A&M University.

[2] Birkhoff,G & de Boor, *Approximation of Functions*, H.L.Garabedian ed., Elsevier, Amsterdam, 1965, 164—190.

[3] Birkhoff,G & H.L.Garabedian, *J.Math.Phys.*, 39(1960),258—268.

[4] Schumaker,L.L., *Approximation Theory* I,ed.by G.G.Lorentz, C.Chui & L.L.Schumaker, Academic Press,N.Y. 1976, 203-268.

[5] Duchon,J., *Rpt*.27, Univ, of Grenoble, 1976.

[6] Meinguet,J., *Polynomial and Spline Approximation*, ed.by Badrin Sahney, Canada, 1978.

[7] Dyn,L.& D.Levin, *R.A.I.R.O. Numerical Analysis*, 16(1982), 3, 201—209.

[8] Arthur, D.W., *J.Approximation Theory*, 12(1974), 396—411.

[9] Ritter, K., *Approximation with Special Emphasis on Spline Functions*, ed, by I.J.Schoenberg. Acad. Press, N.Y., 1969, 185—222.

[10] Mansfield, L.E., *SIAM J.Numer. Anal.*, 8(1971), 1.

[11] Laurent, P.J., *Approximation et Optimisation*, Hermann, Paris, 1972.

[12] 关履泰, 应用科学学报, 1983, 3, 193—201.

[13] 关履泰, 高等学校计算数学学报, 1982, 3, 268—278.

[14] M.阿佛里耳, 非线性规划（下）, 上海科学技术出版社, 1980.

[15] Fletcher, R,, *J.Inst, Math. Appl.*, 7(1971), 76—91,

SMOOTH BIHARMONIC SPLINES ON CIRCULAR DOMAIN

[English abstract of article by Lie Luoluo [7812 5012 5012]]

[Text] Two types of smooth biharmonic splines defined on circular domain are introduced. Characteristic conditions, existence and uniqueness of a solution are given. Smooth parameter is selected by iterative method and the solution can be obtained by solving a sequence of systems of linear algebraic equations which possess non-singular symmetric coefficient matrices. (Paper received Nov 84.)

REFERENCES

〔1〕 钱伟长、叶开源. 弹性力学，科学出版社，1980．

〔2〕 黄义，弹性力学基础及有限单元法，冶金工业出版社，1983．

〔3〕 A. H. 吉洪诺夫，A. A. 萨马尔斯基，数学物理方程，人民教育出版社，1963．

〔4〕 G. I. Marchuk, *Methods of Numerical Mathematics,* Springer-Verlag. New York, 1982.

SOFTWARE FOR SECTION-LINE DRAFTING OF COMPLICATED MECHANICAL FIGURES

[English abstract of article by Liu Chengfang [0491 6134 2455], et al., of Department of Mechanical Engineering]

[Text]   This paper proposes a method of designing the software for the section-line drafting in computer aided design and illustrates the engineering feasibility of drawing complicated mechanical figures with the shortest straight lines as well as the advantage of drafting speed.

This paper also presents a method model distinction in place of the conventional method of cutting figures to solve problems of the leap of the drafting-pen in the process of drafting and the section-line drafting of complicated objects with an open space in the center. (Paper received 6 Feb 85.)

REFERENCES

[1]   北京工业大学，微机应用研究室《微型计算机绘图系统》1983.10

[2]   范鸿玉、张莹《最优化技术基础》清华大学出版社，1982

[3]   金德安等《剖面线程序》浙江大学学报，1981.9.

[4]   《DXY—800》PLOTTER MANUAL 1983

[5]   《SR—6602 PLOTTER INSTRUCTION MANUAL》1983

/7358
CSO: 4009/1058

AI CONTROL AND ITS APPLICATION IN TEMPERATURE-CONTROLLING SYSTEM

[English abstract of article by Tu Xiangchu [3205 6272 0443] et al., of Beijing Polytechnic University]

[Text] A new approach to AI control is described, which possesses the marits of fuzzy control as well as that of conventional control and can carry out a series of experts' functions by means of an AI software. Results of laboratory tests and operations of a practical control system show that the qualities of the AI temperature-controller is excellent. A temperature-controlling system using this AI controller realizes a best quality of control: the temperature stability obtained is better than 0.0004K/h in the measuring range 13~120K. (Paper received Jan 85, finalized Nov 85.)

REFERENCES

〔1〕 汪培庄: 《模糊集合论及其应用》，上海科学技术出版社，第 1 版，p. 2, 1983。

〔2〕 涂序彦: 智能控制浅谈，自动化，No. 3, p. 6, 1984。

〔3〕 L. A. Zadeh: Fuzzy Sets, The Concept of a Linguistic Variable and Its Application to Approximate Reasoning, 〔陈国权译: 模糊集合、语言变量及模糊逻辑，科学出版社，第 1 版，p. 155 〔附录 I〕，1982年〕.

〔4〕 Tu Xiangchu: A simple and effective set-point regulator of artificial intelligence type, BUSEFAL, No. 15, pp. 105—116, 1983.

〔5〕 涂象初: Fuzzy 控制器在定值调节中的新应用途径，模糊数学，No. 2, pp. 65—72, 1984。

〔6〕 W. J. M. Kickert: Fuzzy Theories on Decision-Making, pp. 106—107, Martinus Nijhoff Social Science Division, Nertherland, 1978.

NEW COMPLETE DECODING OF TRIPLE-ERROR-CORRECTING BINARY BCH CODES

[English abstract of article by Feng Guiliang [7458 6311 5328] of Shanghai Institute of Computer Technology]

[Text] A new method is given for finding out roots of one type of nonlinear equations, which appears in Van der Horst and Berger's Complete decoding of triple-error-correcting binary BCH codes. When m is even, the new complete decoding of triple-error-correcting binary BCH codes with $n=2^m-1$ requires only extracting the roots of quadratic equations and calculating at most m times inner products of m-dimensional vectors over GF(2). The new complete decoding is very simple, and can be realized in practice even for moderate m. (Paper received Aug 84, finalized Nov 84.)

REFERENCES

[1] D. C. Gorenstein, W. W. Peterson and N. Zierler: Infor. and Control, Vol. 3, pp.291—294,1960.

[2] C. R. P. Hartmann: IEEE Trans., Vol. IT-17, pp. 765—766,1971.

[3] E. F. Assmus and H. F. Mattson: IEEE Trans , Vol IT-22, pp. 348—349,1976.

[4] J. A. Van der Horst and T. Berger: IEEE Trans., Vol IT-22, pp. 138—147,1976.

[5] T. Helleseth: IEEE Trans., Vol. IT-24, pp.257—257;1978.

[6] F. J. Macwilliams and N. J. A. Sloane: The Theory of Error-Correcting Codes, North-Holland, New York, pp. 110—110, 1977.

[7] 冯贵良: 电子科学学刊, Vol 5, No. 6, pp. 343-348,1983.

CMOS/SOI DEVICES FABRICATED ON Ar+ LASER RECRYSTALLIZED POLYSILICON FILMS

[English abstract of article by Shen Zongyong [3088 1350 7167], et al., of Shanghai Institute of Metallurgy, Academic Sinica]

[Text] CMOS/SOI devices are fabricated on Ar+ laser recrystallized polysilicon islands on SiO_2 isolating layers. Both N-channel and P-channel MOSFET exhibit good output characteristics. The low field electron and hole mobilities of MOSFET with a channel length of 4μm are 510cm^2/V.s and 142cm^2/V.s respectively. 6-stage CMOS inverters have fine static and transient characteristics. 9-stage CMOS ring oscillators with P-channel transistors of (W/L)=112μm/6μm) and N-channel transistors of (W/L)=52μm/6μm) are fabricated. The minimum propagation delay is 2.8ns/stage, and the minimum power delay product is 2.6pJ/stage. These speed performance of CMOS/SOI devices are superior to those of the same CMOS devices fabricated on bulk silicon. (Paper received Dec 84, finalized Jun 85.)

REFERENCES

[1] H. W. Lam, A. F. Tasch, T. C. Holloway: IEEE Electron Dev. Lett., Vol. EDL-1, No. 10, p. 206, 1980.

[2] H. W. Lam, R. F. Pinizzotto, A. F. Tasch: J. Electrochem. Sec., Vol. 128, p. 1981, 1981.

[3] T. I. Kamins, B. P. Von Herzen, IEEE Electron Dev. Lett., Vol. EDL-2, No. 12, p. 313, 1981.

[4] B. Y. Tsaur, J. C. C. Fan, R. L. Chapman, M. W. Geis, D. J. Silversmith, R. W. Mountain: IEEE Electron Dev. Lett., Vol. EDL-3, p. 398, 1982.

[5] 邹世昌、沈宗雍、林成鲁、倪如山、林梓鑫、姚良骐、朱桂枫: 电子学报 Vol. 11, No. 5, p. 1, 1983.

[6] 林成鲁、沈宗雍、邹世昌: 微细加工技术, No. 1, p. 7, 1985.

[7] H. J. Leamy et al.: Appl. Phys. Lett., Vol. 40, No. 7, p. 598, 1982.

[8] F. Fang, C. L. Lin, Z. Y. Shen, S. C. Tsou: Nuclear Instruments and Methods in Physics Research, Vol. B7/8, p. 348—351, 1985.

A NOVEL InGaAs PHOTOTRANSISTOR BY CaO EMITTER

[English abstract of article by Su Liman [5685 6849 2581] of Beijing Electron Tube Factory]

[Text] A novel InGaAs phototransistor is proposed. CdO has the properties of high conductivity ($\sigma = 5 \times 10^3 \Omega^{-1} cm^{-1}$) and wide forbidden gap ($E_g(\Gamma) = 2.5 eV$), thus it is used as the wide emitter for the transistor. Experimental results show that the transistor has a wide spectral response ($\lambda = 0.5 \sim 1.6 \mu m$). A current gain $h_{fe} = 10$ ($V_{cE} = 3V$), $I_c = 1mA$) is obtained. Other results including I-V characteristic of the emitter junction, $h_{fe} - I_c$ characteristic and dark current behavior are also presented. (Paper received Oct 84, finalized Jul 85.)

REFERENCES

[1] L. M. Su: Phys. Inst. Ser., Vol.65, p. 417, 1983.

[2] P. D. Wright, R. J. Nelson, T. Cella: Appl. Phys. Lett., Vol. 37, p. 192, 1980.

[3] M. Tobe, Y. Amemiya, S. Sasaki et al.: Appl. phys. Lett., Vol. 37, p. 73, 1980.

[4] M. Miyato, K. Miyake, Y. Yamaguchi: Appl. Phys. Lett., Vol. 37, p. 180, 1980.

[5] F. P. Koffyberg: Phys. Rev. B, Vol. 13, No. 10, p. 4470, 1976.

[6] 苏里曼: 半导体技术, No. 1, pp. 1~5, 1985.

[7] H. Beneking, L. M. Su: Electron. Lett., Vol. 18, p. 25, 1982.

DESIGN OF BAND-PASS FILTERS WITH WIDE-BAND USING THREE PARALLEL-COUPLED LINES

[English abstract of article by Liao Chengen [1675 2110 1869] of Northwest Tele-communication Engineering Institute, Xian; and Han Xiaolu [7281 2556 6922] of The 23rd Research Institute of Ministry of Electronic Industry, Shanghai]

[Text] The design principle is analysed for band-pass filters using three paral-lel coupled-lines and the related design curves are given. This kind of filter has many advantages such as large bandwidth, easy to design and manufacture, and gives satisfactory performance. The design examples of S-band stripline band-pass filters are given. The test results is in good agreement with calcu-lated results. (Paper received Jul 84, finalized Jul 85.)

REFERENCES

[1] 廖承恩, 鞠殿武: 一种新型宽带微带线带通滤波器, 第三次微波通信年会暨学术交流 会, 1983年10月21日。

[2] William J. Getsinger: Coupled rectangular bars between parallel plates, IRE Trans., vol. MTT-10, No. 1, pp. 65—72, Jan. 1962.

[3] George L. Matthaei, Leo Young, and E. M. T. Jones: Microwave Filters, Impedance-Matching Net-works and Coupling Structures, McGraw-Hill Inc., pp.190—193, 217—221, 1964.

VOLTAGE RESPONSE AND RF IMPEDANCE TO EXTERNAL RADIATION FOR SUPERCONDUCTING WEAK LINKS

[English abstract of article by Wu Binruo [6762 1755 5387] of Chengdu Institute of Radio Engineering, Department of Optical and Electronic Technology]

[Text] Based on the analytical solution of RSJ model with the existence of external radiation, a method for finding voltage response and RF impedance of superconducting weak links is proposed and discussed. Taking the lowest approach, the analytical expressions of the voltage response and RF impedance are obtained with this method. The results show that the impedance varies continuously on the IVC from the 0th current step to the 1st step. The analytical impedance expressions within the range of the 1st current step are deduced for the first time. (Paper received Nov 84, finalized Apr 85.)

REFERENCES

[1] H. Kanter, F. L. Vernon, Jr: J. Appl. Phys., Vol. 43, No.7, p.3174, 1972.
[2] F. Auracher, T. Van Duzer: J. Appl. Phys., Vol. 44, No.2, p.848, 1973.
[3] F. Auracher, T. Van Duzer: Proc. Applied Superconductivity Conference, p.603, 1972.
[4] 姚希贤: 物理学报, Vol.27, No.5, p.569,1978.
[5] 姚希贤: 物理学报, Vol.28, No.3, p.416,1979.
[6] 西北大学低温物理科研组: 超导隧道效应及其应用, p. 57, 1982(中国制冷学会)。

EARTHQUAKE RESPONSE ANALYSIS OF LARGE ANTENNA STRUCTURE

[English abstract of article by Chen Jianjun [7115 1696 6511] and Zeng Yugeng [2582 0151 1649] of Northwest Telecommunication Engineering Institute, Xian]

[Text] Large antennas consist of a great many different kinds of elements generally, such as truss, beam, plate, shell and so on. In this paper, a wheel-track form antenna structure is discreted into multi-degree-of-freedom (2694) system and its response to deterministic earthquake is calculated by means of the finite element method. By this method, the first five natural frequencies, structure modes, displacement response history of all nodes and various maximum stress responses of all elements are obtained. Finally, some views and propositions concerning large antenna structure are put forward. (Paper received Nov 84, finalized Jun 85.)

REFERENCES

〔1〕 R. L. Wiegel (ed): Earthquake Engineering, 1970. (中国科学院工程力学研究所译：《地震工程学》，科学出版社，1978)

〔2〕《地震工程概论》编写组编著：《地震工程学》，科学出版社，1977.

〔3〕 王光远著：《建筑结构的振动》，科学出版社，1978.

〔4〕 李国豪主编：《工程结构抗震动力学》，上海科学技术出版社，1980.

〔5〕 何钜如、邵世勤编著：《松潘强震记录的谱分析》，地震出版社，1979.

〔6〕 C. S. Desai, J. F. Abel: Introduction to the Finite Element Method, 1972. (江伯南、尹泽勇译；《有限元素法引论》，科学出版社，1978)

〔7〕 华东水利学院编：《弹性力学问题的有限单元法》(修订版)，水利电力出版社，1977.

〔8〕 曾余庚：天线结构谱摄分析，西北电讯工程学院资料室，1976.

〔9〕 陈建军、曾余庚：桁架结构随机地震响应分析，西北电讯工程学院学报，4,pp53-61,1984.

〔10〕 Meirovitch, Leonard: Elements of Vibration Analysis, McGraw-Hill, Inc., New York, 1975.

〔11〕 James W. Mar, Harold Liebowitz: Structure and technology for large raido and radar telescope systems, The Masschusetts Institute of Technology, 1969.

〔12〕 Eiich, Tomonori: Earthquake effects on steel tower for microwave antennas atop building, Review of the Electrical Communication Laboratory, Vol, 23, pp. 301—315, 1975.

A NEW METHOD FOR CIRCUITS DESIGN CENTERING--CENTER RANDOM MOVE

[English abstract of article by Yu Xiaoyong [0060 7522 0516], et al., of Guizhou Polytechnical Institute, Guiyan]

[Text] A new method for circuits design centering is described. By assuming normal distribution and identical variances, its convergence is discussed using stochastic approximation theory. Since it requires only Monte Carlo analysis and not sensitivity calculation, it is equally applicable to linear and non-linear circuits and simple to implement. Examples show that this algorithm performs well and is insensitive to nonconvexity and nonconnectivity of the region of acceptability. (Paper received Sep 84, finalized Nov 84.)

REFERENCES

[1] R. K. Brayton et al.: Proc. IEEE, Vol. 69, pp. 1334—1364, 1981.
[2] K. S. Tahim et al.: IEEE Trans., Vol. CAS-26, pp. 768—774, 1979.
[3] R. S. Soin et al.: IEE Proc., G., Vol. 127, pp. 260—269, 1980.
[4] E. Wehrhahn & R. Spence: IEEE Proc. ISCAS'84, pp. 1424—1438.
[5] A. Ruszczynski et al.: IEEE Trans., Vol. AC-28(1983), pp. 1097—1105, 1983.
[6] M. A. Styblinski et al.: Electr. Lett., Vol. 19, pp. 300—302, 1983.
[7] 于晓勇: MCA-Newton法进行电路合格率估计及最优中心设计，电子科学学刊待发表，1984.
[8] D. Agnew: IEE Proc. G., Vol. 127, pp. 270—277, 1980
[9] M. A. Styblinski et al.: IEEE Proc. ISCAS'81, pp. 554—557.

TWO OXYGEN DONORS IN ANNEALING NTD CZ Si

[English abstract of article by Meng Xiangti [1322 4382 2251] of Qinghua University]

[Text]   The formation and annealing behavior of the thermal donor (TD) and new donor (ND) in NTD CZ Si are studied by Hall effect, electrical resistivity and IR absorption measurements.   The apparent TD concentration is decreased obviously and the ND formation can be promoted by neutron irradiation.   The main cause of ND formation in NTD CZ Si is that the oxygen atoms aggregate in the disordered region due to radiation enhancing diffusion to form large size complicated silicon oxygen complex.   (Paper received Sep 83, finalized Sep 85.)

REFERENCES

[1] 孟祥提, 杜光庭, 刘开敏; 核科学与工程, Vol. 2, No. 2, p. 172, 1982。

[2] H. M. Liaw et al.: Semiconductor Silicon, J. Electrochem. Soc., PV-77-2, p.116, 1977.

[3] J. W. Cleland et al.: Neutron-Transmutation-Doped Silicon, Plenum Press, New York and London, p. 55, 1981.

[4] 孟祥提等; 清华大学核能技术研究所年报, P.90, 1980; 半导体技术, No. 2, p. 14, 1982。

[5] 孟祥提等; 第三届全国集成电路和硅材料学术年会论文集, p. 100, 1983。

[6] C. S. Fuller et al.: Phys. Rev., Vol. 99, p. 833, 1954.

[7] P. Capper et al.: J. Appl. Phys., Vol. 48, No. 4, p. 1648, 1977.

[8] W. Kaiser: Phys. Rev., Vol. 105, p. 1751, 1957; W. Kaiser et al.: Phys. Rev., Vol.112, No. 5, p. 1546, 1958.

[9] K. Graff et al.: 同[2], P. 575, 1977.

[10] R. C. Newman et al.: J. Phys. C: Solid State Phys., Vol. 16, p. L667, 1983.

[11] D. Helmreich et al.: ibid[2], p. 626, 1977.

[12] 许振嘉 等; 物理学报, Vol. 31, No. 10, p. 1362, 1982。

[13] L. C. Kimerling et al.: Appl. Phys. Lett., Vol. 39, No. 5, p. 410, 1981.

[14] Michio Tajima et al.: Japan J. Appl. Phys., Vol. 19, No. 12, P. L755, 1980.

[15] Akihiro Kanamori et al.: J. Appl. Phys., Vol. 50, No. 12, p. 8095, 1979.

[16] Kiyoshi Yasutake et al.: Japan J. Appl. Phys., Vol. 19, No.9, p. L544, 1980.

[17] 许振嘉等; 电子学报, Vol. 11, No. 2, p. 16, 1983; 电子学报, Vol. 9, No. 6, p. 58, 1981。

[18] V. Cazcarra et al.: J. Appl. Phys., Vol. 51, No. 8, p. 4206, 1980.

[19] J. W. Corbett et al.: Phys. Rev., Vol. 135, p. A1381, 1964.

[20] K. Hölzlein et al.: Appl. Phys. A: Solids and Surface, Vol. A34, No. 3, p. 155, 1984.

[21] 许振嘉等; 半导体学报, Vol. 3, No. 6, p. 450, 1982。

[22] Fumio Shimura et al.: Appl. Phys. Lett., Vol. 37, No. 5, p. 483, 1980.

[23] V. D. Akhmetov et al.: Phys. Stat. Sol.(a), Vol. 75, No. 2, p. 601, 1983.

[24] I. D. Konozenko et al.: Radiation Damage and Defects in Semiconductors, Inst. of Physics, London and Bristol, p. 289, 1973.

Engineering

THE RESPONSE ANALYSIS OF VIBRATION SYSTEMS TO NONZERO MEAN RANDOM EXCITATION

[English abstract of article by Wang Hexiang [3769 0735 4382] et al., of Department of Engineering Mechanics]

[Text] An equivalent linearization method for obtaining the response of nonlinear multi-degree-of-freedom dynamic systems to nonstationary Gaussian excitation with nonzero mean is presented. Using the property of Gaussian vector processes, the closed formulas of the coefficients of the equivalent linear system are obtained. The linear coefficients obtained are as simple as those of the Atalik and Utku method in mathematical form. A method to treat stochastic dynamic equation of complicated structure by means of modal truncation method and to compute response statistics of dynamic system in the time domain is presented. One numerical method to compute mean and covariance equations of stochastic dynamic system is presented. (Paper received Apr 85.)

REFERENCES

[1] T. K. Caughey, Adv. appl. Mech., 11(1971)

[2] W. D. Iwan and I. N. Yang, J. appl. Mech., 39 (1972)

[3] S. T. Atalik and S. Utku, Earthq. Engng. Struct. Dynamics, 4(1976)

[4] W. D. Iwan and A. B. Mason, Int. J. Nonlinear Mech., 15, 2(1980)

[5] R. E. Nickell, Computer Methods in Applied Mechanics and Engineering, 7 (1976)

[6] L. D. Ofmeister, Computer and Structure, 8(1978)

[7] 郑兆昌，《应用数学和力学》，4，4(1983)

[8] 蔡坚，清华大学工程力学系硕士论文，1984.9.

[9] B.C. 普加切夫：《随机函数理论及其在自动控制中的应用》（中译本），科学出版社，1966.

[10] 王照林等编：《现代控制理论基础》，国防工业出版社，1981

[11] 郑兆昌、程保荣，《海洋工程》，2(1984)

[12] 王和祥、张宪宏、蔡坚，《地震工程与工程振动》，4 (1985)

ANALYSIS OF THE FLASHOVER CRITERION OF POLLUTED INSULATOR UNDER DC VOLTAGE

[English abstract of article by Guan Zhicheng [7070 1807 2052], et al., of Department of Electrical Engineering]

[Text] The volt-ampere characteristics of the arc developing along the surface of polluted insulator and the surface conductivity of remainder pollution layer were measured. The effective surface conductivity γ_e was proposed and the method to determine it was presented. A new method to calculate the DC flashover criterion of polluted insulator was proposed. Experimental data of some insulators are in agreement with the calculated results. (Paper received Feb 85.)

REFERENCES

[1] F. Obenaus, Disch. Electrotechnik, 12, 4(1958), 135—136

[2] L. L. Alston, et al., PIEE, 110, 7(1963), 1260—1266

[3] A. M. Rahal, et al., IEEE, PAS—98, 6(1979), 2223—2231

[4] R. Wilkins., PIEE, 116, 3(1969), 457—465

[5] B. F. Hampton., PIEE, 111, 5(1964), 985—990

[6] 关志成：《染污绝缘子临闪前泄漏电流和污闪电压之间关系的研究》，清华大学硕士研究生论文，1981

[7] 关志成：《在交、直流电压下染污绝缘子闪络条件的分析计算和试验研究》，清华大学博士研究生论文，1984

FAULT LOCATION OF FLUID TRANSPORT PIPELINE BASED ON MODELLING AND ESTIMATION METHODS

[English abstract of article by Tao Luowen [7118 3157 2429], et al., of Department of Automation]

[Text] The normal operation of long-distance oil, gas, water or slurry transport pipeline may be troubled by faults such as blockage and leakage. A new method based on modelling and estimation is proposed to locate the faults by a microcomputer and two pressure transducers, both set at one end of the pipe. By analyzing the impulse response of the estimated model, the location of the blockage or leakage (not less than 10 percent) can be determined to an accuracy of 0.5 percent. This method has been verified in an experimental liquid transport pipeline. (Paper received Jan 85.)

REFERENCES

[1]   Butler, N. C., **Process Engineering**, 10, 7(1982), 31—35

[2]   Isermann, R., **Automatica**, 20(1984), 387

[3]   Siebert, H., **Process Automation**, 2(1981), 90

[4]   陶洛文：《以辨识为基础的长输管线故障定位》，硕士学位论文，清华大学自动化系，1984

[5]   Wylie, E. B. and V. L. Streeter: **Fluid Transients**, McGraw-Hill Book Co., New York, 1978

[6]   Sharp, B. B.: **Water Hammer**, Edward Arnold Ltd., London, 1981

FATIGUE ANALYSIS OF SPECIMENS WITH COMPLICATED STRESS FIELD

[English abstract of article by Yan Yongnian [7346 3057 1628], et al., of Department of Mechanical Engineering and Zhou Chuntian [0719 2504 3944], et al., of Department of Engineering Mechanics]

[Text] The fatigue test of specimens with complicated stress field and its analysis show that the intensity of stress field method can be used for correct judgement for the dangerous part of component with complicated stress field and for the estimation of its fatigue life with appropriate accuracy. (Paper received Nov 84.)

REFERENCES

[1] 郑楚鸿：《高周疲劳设计方法——应力场强法》，清华大学工学博士学位论文，1984,3

[2] H. O. Fuchs, R. I. Stephens: **Metal Fatigue in Engineering,** John Wiley & Sons, 1980

[3] 周春田，勾秋静：《循环载荷下缺口板弹塑性应变分布测定》，清华大学材力实验室，1983

[4] R. A. Smith and K. J. Miller, **Int. J. Mech. Sci.,** 19, (1977), 11—22

[5] N. E. Dowling, **Fracture Mechanics,** ASTM STP677, (1979), 247—273

[6] 颜鸣皋 : **Some Microscopic Features and Mechanisms of Fatigue Behaviour in Metals,** 1st China—U. S. A. Bilateral Metallurgical Conference, 1981, 11

[7] D.布洛克：《工程断裂力学基础》，王克仁等译，科学出版社，1980,5

[8] Huseyin Sehitoglu, **Eng. Fracture Mech.,** 18, 3(1983), 609—621

[9] 徐灏：《疲劳强度设计》，机械工业出版社，1981

DECORATIVE COATING OF TiN IN GOLDEN COLOR ON CERAMIC SUBSTRATES BY CHEMICAL VAPOR DEPOSITION

[English abstract of article by Cai Zuoqian [5591 0155 0051], et al., of Department of Chemistry]

[Text]   Experiments were carried out to produce TiN coating in golden color on ceramic substrate by CVD technique using $TiCI_4$, NH_3, N_2 and H_2.   The region of proper deposition temperature is at 800°C to 850°C.   Satisfactory lustrous coating of TiN in golden color was obtained when the amount of the flow of gas reactants got smaller.   The composition of the coating deposited on ceramics is close to stoichiometric TiN, i.e. the value of atomic ratio N/Ti is approximate to 1:1.   The lattice parameter α_0 equals to 4.241Å.   The lightness reached the level of gold.   Because of its high hardness, the TiN coating gives a higher wear resistant than the gold coating with a high chemical stability.   (Paper received Mar 85.)

REFERENCES

[1] Г.В.Самсонов, Т.С. Верхоглядова, Журнал Сгруктурhoй Химии, 2 (1961),617

[2] Robert C. Weast; CRC Handbook of Chemistry and Physics, 63rd (1982—1983)

[3] 池永勝，工業材料,32,3(1984),51

[4] John R. Peterson, J. Vac. Sci. Technol, 11(1974), 715

[5] W. Schintlmeister, O. Pacher and K. Pfaffinger, J. Electrochem. Soc., 123 (1976), 924

[6] W. Schintlmeister and O. Pacher, J. Vac. Sci. Technol., 12(1975), 743

[7] P. J. M. Van der Straten and G. Verspui, Philips Tech. Rev., 40, 7(1982), 204—210

[8] H. O. Pierson, Thin Solid Films, 40(1977), 41

[9] 日本专利，公開特許公報，昭 57-108260(82,108260)

[10] W. Junghans und R. Wilberg, H. Liebmann und H. Schmidt, Silikattechnik, 33, (1982), 365

[11] 张克铉，蔡作乾，《物理》，13,12 (1984),732-736

[12] A. Kato and N. Tamari, J. Cryst. Growth, 29(1975), 55—60

THE INVERSE SYSTEM METHOD AND ITS APPLICATION

[English abstract of article by Li Chunwen [2621 2504 2429] and Feng Yuankun [7458 0337 3824] of Department of Automation]

[Text] A new method, called inverse system method, is proposed for the synthesis of a class of multivariable analytic nonlinear control systems. It consists of two parts: constructing at first an "α integral inverse system" which can be realized by state feedback from the inverse of the original system, so that a "pseudo-linear system" is formed through precompensation of the α integral inverse system and a linear relation exists between its input and its output; then, designing the controller of the pseudo-linear system by the well known linear system theories, e.g., decoupling, pole assignment, linear quadratic optimal and robust regulator, etc. The inverse system method was used in the design of the dynamic control system of robot manipulator. Some digital simulation results given in the paper prove that the inverse system method is effective. (Paper received Mar 85.)

REFERENCES

[1] J.Marshik,《第一届 IFAC 会议论文集选集》，（中译本），上海科技出版 社，1963

[2] 韩京清，《全国控制理论及其应用学术交流会议论文集》，科学出版社，1979

[3] H. Nijmeijer, IEEE Trans. Automat. Contr., Ac-28, 8(1983), 861—862

[4] S. N. Singh, IEEE Trans. Automat. Contr., Ac-25 (1980), 1237—1239

[5] L. M. Silverman, IEEE Trans. Automat. Contro., Ac-14 (1969), 270—276

[6] R. M. Hirschorn, IEEE Trans. Automat. Contr., Ac-24 (1979), 855—865

A FAST AC-AF ALGORITHM FOR SOLVING THE CONSERVATIVE TRANSONIC 3D POTENTIAL EQUATION EMPLOYING NON-ORTHOGONAL CURVILINEAR COORDINATES AND NON-ORTHOGONAL VELOCITY COMPONENTS

[English abstract of article by Zhang Jialin [1728 1367 7792] of Institute of Engineering Thermophysics, Academia Sinica]

[Text] A conservative full-potential equation of 3D transonic flow in a turbo-machine has been derived with the tensor method and expressed with respect to nonorthogonal curvilinear coordinates, and a full implicit artificial com-pressibility--approximate factorization scheme to calculate the flow field has been developed in this paper. The new algorithm has been used to compute the 3D transonic flow field within the axial-flow single-stage compressor rotor tested by DFVLR. Comparisons between the computed flow field and the DFVLR data have been made. Results demonstrate that fast convergence can be achieved by the presented algorithm and that the agreement with the measure-ments obtained with an advanced laser velocimeter is quite good.

CALCULATION OF THREE-DIMENSIONAL FLOW WITH JET-WAKE MODEL IN CENTRIFUGAL PUMPS

[English abstract of article by Liu Diankui [0491 3013 7608] of Institute of Engineering Thermophysics, Academia Sinica]

[Text] Expanding the slip factor which comes from a lot of experimental data into three dimensional flow, a calculation method of Jet-Wake model which is based on Prof. Wu's theory is presented here.

A redesign of a centrifugal pump impeller has been done to verify the method. The experimental results show that the efficiency of the pump is increased by 4 percent. Therefore, the method is useful to improve one dimensional design method which is used widely abroad and at home up to now.

COMPUTATION METHODS OF INVERSE AND SEVERAL MIXED AERODYNAMIC PROBLEMS FOR
TRANSONIC CASCADES

[English abstract of article by Wang Zhengming [3769 2973 2494] of Institute
of Engineering Thermophysics, Academia Sinica]

[Text] The computation methods of the inverse and several mixed aerodynamic
problems for transonic cascades are presented. The calculations are completed
directly on the physical plane by the stream function equation. The correspon-
ding boundary conditions of these problems are transferred into the boundary
conditions expressed by stream function with the help of the relations of
the basic equations. The methods presented have a clear physical concept
and use similar manners of iteration for different problems. The calculations
of some examples for the transonic inverse problem indicate this method is
very effective. An example is given of a shockless supercritical cascade
designed successfully by the transonic inverse code.

A NEW METHOD FOR SOLVING AERODYNAMIC HYBRID PROBLEM OF PROFILE CASCADE ON S_1 STREAM SURFACE OF REVOLUTION BY EMPLOYING STREAM FUNCTION EQUATION EXPRESSED WITH NON-ORTHOGONAL COORDINATE SYSTEM

[English abstract of article by Chen Naixing [7115 0035 5281] and Li Weihong [2621 5898 4767] of Institute of Engineering Thermophysics, Academia Sinica]

[Text] A new method is developed in the present paper for solving an aerodynamic hybrid problem of profile cascade on S_1 stream-surface of revolution by employing stream function equation on non-orthogonal coordinate system. For this kind of problems the shape of a portion of the blade profile is unknown. The remainder is determined by a giving prescribed velocity distribution. Four examples of blade cascades have been carried out to examine this method. It is shown that the calculation method presented herein can be used as a powerful tool together with aerodynamic optimization method for blade cascade design.

A MATHEMATICAL MODEL FOR CALCULATION OF EFFECTS OF AIR HUMIDITY FUEL COMPOSITION AND GAS DISSOCIATION ON ENGINE PERFORMANCE AND ITS ACTUAL APPLICATION

[English abstract of article by Gu Yonggen [7357 3057 2704] of Nanhua Powerplant Research Institute Zhuzhou, Hunan, China]

[Text] This paper presents a mathematical model for computation of the effects of air humidity, fuel composition and gas dissociation on gas turbine engine performance. The programmed model was also successfully applied to a computer program for simulation of gas turbine engine performance, called a 'TURBOFLEXI'. The results from it is in good agreement with the published data.

VARIATIONAL PRINCIPLES (VP$_S$) & GENERALIZED VP$_S$ FOR 3-D TRANSONIC FLOW WITH SHOCK WAVES IN A ROTATING TURBO-IMPELLER (II)

[English abstract of article by Liu Gaolian [0491 7559 5114] of Shanghai Institute of Mechanical Engineering]

[Text] As a further development of Ref. [1] two VP families for 3-D transonic potential-, Beltrami- and rotational flows with shocks in rotors in terms of stream functions are established. Functional variations with variable domain are used with success to handle unknown discontinuities (shocks, free trailing vortex sheets etc.), converting the matching conditions across them (including the Rankine-Hugoniot shock relations) into natural ones. A sound theoretical basis is thus provided for the FE analysis of transonic flow.

APPLICATIONS OF DOUBLE FILM HEAT FLUX GAUGES IN HEAT TRANSFER TEST OF TURBINE

[English abstract of article by Cao Yuzhang [2580 3768 3864] of Beijing Institute
of Aeronautics and Astronautics, China]

[Text] This paper presents applications of double film heat flux gauges in
the experimental study of turbine heat transfer and discussions of the data
obtained from MIT turbine blowdown facility. The result shows that the small
fluctuation of temperature on the measured surface at high frequency will
cause the large fluctuation of heat transfer rate.

EXPERIMENTAL STUDY ON COMBUSTION OF FLAME OF COAL-WATER MIXTURE

[English abstract of article by Lu Deshou, et al., of Zhejing University]

[Text] The results of the preliminary CWM combustion experiments carried out in a tunnel testing furnace with its thermal rate of 4.187×10^6 watt are presented. The CWM with the coal concentration of 64 ~ 68 percent (in Weight) and viscosity of 700 ~1100 cp can be smoothly transported and well atomized, and can be dependably ignited and stably burned when the combustion air temperature is between ambient and 330°C, with the conversion efficiency up to 98 percent. The experimental result; of blue gas temperature blue gas composition and combustible matter burn-nut within the furnace are also given in the paper.

/7358
CSO: 4009/94

ON THE NTH ORDER WAVE INTERACTION THEORY

[English abstract of article by Tan Weihan [6223 4850 5060] of Shanghai Institute of Optics and Fine Mechanics, Academia Sinica]

[Text] The nth order wave interaction theory investigated in this paper should be considered as a continuation of the "exact solution to solitary wave equations of light interaction with two-level atomic systems" in the earlier paper[1]. In literature[4,5] the third order wave equations originate from the research of three-wave interaction. But the nth order wave equations considered now are derived from the n-dimensional vector functions which satisfy two nonlinear equations, and the general solutions can be expressed in terms of the upper hemiplane analytical solutions and the lower hemiplane analytical solutions. These results include the 2nd and the 3rd order solutions as a special example.

FREE-ELECTRON LASERS WITH TAPERED WIGGLERS: A DISCUSSION ON THE CASE WITH
AXIAL MAGNETIC FIELD

[English abstract of article by Wang Yuandian [3769 0337 3013] of Institute
of Space Physics, Academia Sinica]

[Text] It is pointed out in this paper that in order to increase efficiency
of free-electron lasers with axial magnetic field, tapered wigglers can be
applied. At the same time, general formulae for calculation of the parameters
of the tapered wigglers have been derived, too. A comparison has been made
between the two cases with and without axial magnetic field.

A NEWLY DESIGNED PULSED AND OPTICALLY-PUMPED FIR LASER

[English abstract of article by Pan Chengzhi [3382 2110 1807], et al., of Beijing Research Institute of Vacuum Electron Devices]

[Text] A pulsed and optically-pumped FIR laser with a mesh coupling and a stable cavity has been designed. Its cavity length can be adjusted. 5 FIR laser lines at 205.3μm, 163.9 μm, 65.1μm and 233μm emitted from Ch_3OH and 309.23μm from HCOOH have been obtained.

FREQUENCY STABILIZED DYE LASER OSCILLATOR-AMPLIFIER SYSTEM FOR HIGH RESOLUTION
SPECTROSCOPY

[English abstract of article by Xia Jingfang [1115 2417 5364] of Laser Physics
Lab., Dept. of Physics, Fudan University]

[Text] This paper describes a frequency stabilized dye laser oscillator-ampli-
fier system for high resolution spectroscopy. It uses frequency doubled output
of a Q-switched Nd:YAG laser to pump a system that amplifies the output of
a frequency stabilized CW dye laser to provide near Fourier transform limited
pulses of 1 MW peak intensity. A new method for laser frequency stabilization
is also presented.

NARROW BANDWIDTH TUNNING OF RHODAMINE 6G DYE PUMPED BY XeCl EXCIMER LASER

[English abstract of article by Shangguan Cheng [0006 1351 6134], et al., of Shanghai Institute of Optics and Fine Mechanics, Academia Sinica]

[Text] In this paper the experimental study for narrow bandwidth tunning of ethyenglycol solution of rhodamine 6G pumped by a XeCl excimer laser is report-ed. The tunable range from 572.7nm to 612.9 nm with linewidth of 0.004 nm has been obtained. The conversion efficiency is 16.0 percent. The experimen-tal results of other seven dyes are also presented.

/7358
CSO: 4009/89

CHARACTERISTICS OF PICOSECOND PULSES GENERATED FROM SYNCHRONOUSLY PUMPED DYE
LASER SYSTEM--THE THIRD ORDER EXPANSION OF GAIN OF MODE-LOCKED EQUATION AND
ITS SOLUTION

[English abstract of article by Bao Xiaoyi [7637 2556 3015] and Guan Xinan
[7070 0207 1344] of Department of Physics, Nankai University]

[Text] In this paper, we present the third order expansion of gain of mode-
locked equation, and solved the equation with Lagrange multiplier method. The
results provide simple analytical expressions for the pulsewidth, pulse inten-
sity and delay (which is the advance of the pump pulse relative to the dye
pulse) in synchronously pumped dye laser. They can explain satisfactorily
some experimental results[4].

STIMULATED RAMAN SCATTERING OF UNPOLARIZED LONG PULSE XeCl EXCIMER LASER
RADIATION IN H_2

[English abstract of article by Lou Qihong [2869 4388 3163] et al., of Shanghai
Institute of Optics and Fine Mechanics, Academia Sinica]

[Text] Stimulated Raman scattering (SRS) experiments in hydrogen were performed
with a collimated beam from an X-ray preionization discharge XeCl laser operating
at 308 nm. The photodiode output profile S_1, S_2 and S_3 stoken lines were obser-
ved. The reduction of beam spread angle and pulse duration of SRS were analysed
theoretically.

TWO-PASS AMPLIFICATION ATOMIC IODINE LASER AMPLIFIER

[English abstract of article by Chen Shisheng [7115 2514 0524] of Shanghai Institute of Optics and Fine Mechanics, Academia Sinica]

[Text] In this paper, we report the experimental results of a two-pass amplification atomic iodine laser amplifier. For an iodine amplifier working under the condition lower than those in the saturation region, two-pass amplification can increase the efficiency of the iodine laser amplifier obviously. Besides, we found that He is the best among He, Ar, SF_6 usually used as buffer gases in iodine lasers. It has obvious advantages especially in reducing the beam deformation produced by optical pumping and in holding beam direction.

MANIFESTATION OF ROTATIONAL NONEQUILIBRIUM IN A CW DF CHEMICAL LASER

[English abstract of article by Sang Fengting [2718 7685 0080] et al., of Dalian Institute of Chemical Physics, Academia Sinica]

[Text] The rotational nonequilibrium phenomenon in a CW DF chemical laser was experimentally studied. The dual-peak character in the output spectral intensity profile was observed with a fast mixing nozzle for the first time. The same phenomenon does not occur with slow mixing nozzles, nor with HF as lasant.

/7358
CSO: 4009/90

PROBLEMS ON GENERATION OF CONTINUOUSLY TUNABLE VUV COHERENT RADIATION BY FOUR WAVE-MIXING

[English abstract of article by Li Binxue [2621 1755 1331] and Huang Yongkai [7806 3057 2818] of Shanghai Institute of Optics and Fine Mechanics, Academia Sinica]

[Text] The theory and experimental results on acquiring VUV coherent sources by four wave-mixing process are briefly described. An analysis of the important aspects for effective generation of VUV coherent radiation by FWM is presented.

A LOW JITTER TWO CHANNEL DISCHARGE PUMPED EXCIMER LASER

[English abstract of article by Hu Xuejin [5170 7185 6855] et al., of Anhui Institute of Optics and Fine Mechanics, Academia Sinica]

[Text] A two channel fast discharge pumped excimer laser was designed. The jitter time between two output laser beams was measured as ±1 ns at the operation pressure of 1 atm, and ±5 ns at 2 atm, respectively. The output energy of each channel was 80-100 mJ, the maximum was approximately 150 mJ.

EXPLANATION AND DISCUSSION ON THE REPORTED EXPERIMENTAL RESULTS OF CHARACTERISTICS OF PICOSECOND PULSE GENERATED FROM SYNCHRONOUSLY PUMPED DYE LASER SYSTEM

[English abstract of article by Bao Xiaoyi [7637 2556 3015] and Guan Xinan [7070 0207 1344] of Department of Physics, Nankai University]

[Text] In this paper, we give the simple analytic expressions of picosecond pulses in synchronfously pumped dye laser, and also some discussion and explanation based on the above theoretical results. This theory proved especially that for the pulsewidth and average power of synchronously pumped dye laser there exists an optimum value.

EXCURSION OF ALIGNED LASER BEAM THROUGH ATMOSPHERE ABOVE WATER SURFACE AND LAND

[English abstract of article by Ma Jian [7456 1696] and Tang Wu [0781 2976] of Shanghai Institute of Laser Technology, and Shen Shanxiong [3088 3790 7160] et al., of Department of Physics, East Teachers University]

[Text] Laser beam excursion through atmosphere above the water surface and the land if presented. The results show that the beam excursion curves of the two paths have similar outline and cycle, and are similar to those of the temperature except of their phase ahead of $0.17 \sim 0.21\pi$. The amount of beam excursion through the land path h_L in vertical direction in one cycle 24 hrs is greater than that of the water path h_w, and h_L/h_w equals to $1.14 \sim 1.40$.

A SIMPLE NEUTRON-GAMMA DISCRIMINATING SYSTEM

[English abstract of article by Liu Zhongming [0491 0022 2494] et al., of Shanghai Institute of Nuclear Research, Academia Sinica]

[Text] A simple neutron-gamma discriminating system is described. A detector and a pulse shape discriminator are suitable for the neutron-gamma discriminating system. The influence of the constant fraction discriminator threshold energy on the neutron-gamma resolution properties is shown. The neutron-gamma timing distributions from an ^{241}Am-Be source, 2.5MeV neutron beam and 14MeV neutron beam are presented.

Keywords: neutron-gamma discriminating system   resolution property timing distribution

A STUDY ON THE SURFACE DAMAGE OF R-IBE CRYSTALS BY RBS-CHANNELING TECHNIQUE

[English abstract of article by Cao Dexin [2580 1795 2450], et al., of Shanghai Institute of Nuclear Research, Academia Sinica]

[Text] This paper reported the study on the surface damage, and its annealing of R-IBE (reaction ion beam etched) crystal by RBS-channeling technique. The topography of the etched surface was observed by SEM.

The experimental results show that the reactive ion beam etching with CF_4 results in a surface damage layer and the amount of the damage increases with increasing the energy of the ion beam.

Keywords: reaction ion beam etching   damage   thermal annealing channeling technique

THE INFLUENCES OF THE THICKNESS OF CARBON STRIPPING FOIL ON THE CHARGE STATE
DISTRIBUTION

[English abstract of article by Sun Yunmin [1327 7301 2404] and Shao Mingzhu
[6730 2494 3796] of Institute of Modern Physics, Academia Sinica]

[Text] This paper describes an experiment about the effect of the thickness
of stripping carbon foils on the charge state distribution of carbon and neon
which are extracted from 1.5m classical cyclotron. The energies of the par-
ticles are 72 MeV and 140 MeV respectively. The results show that the thicker
foils were used, the more number of the high charge state particles were obtained
after stripping.

Keywords: thickness of carbon stripping foil charge state distribution

A LIQUID SCINTILLATION NUCLEAR ACTIVITY METROLOGY INSTRUMENT

[English abstract of article by Wang Zhangzhi [3769 4545 2535], et al., of Shanghai Institute of Nuclear Research, Academia Sinica]

[Text] A new precise instrument for determination of the absolute disintegration of β, α emitter solutions by the method of liquid scintillation counting is described. The instrument includes a triple phototube liquid scintillation detector and three output counting channels which are used for the number of triple coincidences N_C, the number of sum of double coincidences N_D and the number of sum of single phototube counting N_E separately. This instrument is based on the principle of extrapolating the triple to double coincidence ratio (TDCR) to unity.

Examples of application of the instrument for ^{3}H and ^{14}C are given.

The instrument has two main advantages: 1. Higher accuracy. The overall measurement uncertainty (3σ), for ^{3}H, ^{63}Ni, ^{35}S and ^{14}C etc. is in 0.5-1.5 percent. 2. Easy to operate. The measurement time is much less than usual metrology instrument.

Keywords: liquid scintillation counting   activity metrology   TDCR

ELECTRIC QUADRUPOLE INTERACTIONS IN In$_{0.95}$ Ag$_{0.045}$ Ga$_{0.005}$ ALLOY

[English abstract of article by Zhu Shengyun [2612 0581 0061], et al., of Institute of Atomic Energy, Academia Sinica]

[Text] The temperature dependence of the quadrupole interaction of ^{111}Cd in In$_{0.95}$Ag$_{0.045}$ Ga$_{0.005}$ alloy is determined by the time differential perturbed angular correlation (TDPAC) method from 80 to 422K. The electric field gradients produced by the lattice in the alloy are derived. The temperature dependence of the electric field gradient follows the $T^{3/2}$law: $V_{zz}(T)=V_{zz}(0)$ $(1 - B^{3/2})$ with a slop $B=7.48(47)\cdot10^{-5}K^{-3/2}$. The FWHM's of the electric field gradient are 0.1147(259), 0.0924(340) and 1.344 (175) at 80, 298 and 422 K, respectively. This indicates that the characteristics of the lattice structure of the alloy are better at 80 and 298 K than at 422K.

Keywords: TDPAC method   quadrupole interaction   electric field   gradient $T^{3/2}$law

A CEMS STUDY OF THE ION IMPLANTED LAYER OF SMALL BUBBLE DIAMETER GARNET MATERIAL

[English abstract of article by Wang Lixuan [3769 4539 5503], et al., of Shanghai Institute of Nuclear Research, Academia Sinica]

[Text] This paper describes an ^{57}Fe conversion electron Mossbauer spectrascopic study of small bubble diameter material. The nominal composition of the film is $(YLuBi)_3- (FeGa)_5 O_{12}$. After a dosage of 5×10^{13} to 1×10^{14} cm^{-2} 100 keV Ne^+ implantation, peaks of 2 and 5 of CEMS are emerged, indicating that the magnetization vector M_S of the surface layer of the film is toward the film plane. It was found that the stress induced magnetic plannar anisotropy owing to the dosage of ion implantation is not necessary to be very large. While $d = 2 \times 10^{14} cm^{-2}$, only paramagnetic spectra are obtained but the and d site spectrum is distinguishable. When $d \geqslant 7 \times 10^{13} cm^{-2}$, hard bubbles are suppressed. High temperature 1050°C annealling is required to restore the hyperfine field to the value in the as-grown state, however, peaks 2 and 5 are present in the spectra and hard bubbles are still suppressed.

Keywords: CEMS   ion implantation   garnet material   small bubble diameter

A DEVICE OF DOUBLE CONTROL OF VOLTAGE REGULATION AND BREAKDOWN PREVENTION
OF VAN DE GRAAFF ACCELERATOR

[English abstract of article by Fan Zhifang [5400 1807 2455] of Institute
of High Energy Physics, Academia Sinica]

[Text] The principle of a double control and breakdown prevention device
is described. The operational performances are described. It has been proved
experimentally that this device can effectively prevent the accidentally termi-
nal voltage rising that may result a destructive breakdown. With the help
of the device, the energy of accelerated particles has been increased from
2.0 MeV to 2.88 MeV, the regulation of beam is also made much more convenient
and safer, and the voltage stability has been improved noticeably.

/7358
CSO: 4009/92

INFLUENCE OF α-NUCLEUS ALAS POTENTIAL ON THE ^{40}Ca(α,p)^{43}Sc REACTION

[English abstract of article by Bao Xiumin [7637 4423 2404], et al., of Institute of Atomic Energy, P.O. Box 275, Beijing]

[Text] To clarify the ambiguities of the explanations of the ALAS (α-nucleus anomalous large angle scattering), (α,p) reactions are used to test several α-anomalous potentials, which have well explained the ALAS. The differential cross sections of ^{40}Ca(α,p)^{43}Sc reaction to ground state (7/2−), 0.472 MeV (3/2−) and 1.179 MeV (3/2−) state are measured, the energy of α particles is 25.8 MeV. An additional peak around 110° region is observed. DWUCK4 program is modified for calculations using α-anomalous potentials. It is found that for the lower and higher partial waves of the incident channel wave function, the imaginary ι-dependent potential can provide a reasonable description, but the WS^2 , $WS^2(s)$, $WS^{2.65}$ and WS^5 type potentials cannot give the correct behaviour for the lower partial waves, so it is unable to reproduce the angular distributions of (α, p) reactions.

Key words (α, p) reaction, ^{40}Ca, DWBA calculation.

THE MASS DISTRIBUTION IN 14.9 MeV NEUTRON-INDUCED FISSION OF 238U

[English abstract of article by Liu Conggui [0491 1783 6311], et al., of Institute of Atomic Energy, P.O. Box 275, Beijing]

[Text] The mass distribution for the 14.9 MeV neutron-induced fission of ^{238}U is measured using Ge(Li) γ ray spectrum method. The absolute measurement of fission rate is carried out by a double ionization chamber. The absolute activities of fission products are determined by a Ge(Li) detector. Thirty-nine mass chain yields and one cumulative yield are obtained in the region A=84-151. Among them thirteen yields are measured relatively to the yields of ^{132}Te or ^{140}Ba. The yields measured make up about 131.97 percent of the total of 200 percent expected from fission. The present results are compared with other measurements. As reported by others previously, a fine structure is observed at the mass number of 134, in other mass region no clear evidence could be found.

COMMENTS ON THE NEW NEUTRINO "BALANCE": A DISCUSSION OF THE FEASIBILITY OF USING THE ELECTRON CAPTURE PROCESS IN ^{158}Tb, ^{157}Tb AND ^{163}Ho FOR NEUTRINO MASS DETERMINATION

[English abstract of article by Qing Chengrui [1987 2110 3843], et al., of Institute of Theoretical Physics, Academia Sinica, P. O. Box 2735, Beijing]

[Text] It is pointed out that there are two main difficulties for neutrino mass determination in the K electron capture in ^{158}Tb$\rightarrow$^{158}Gd (1187). One of them is that the atomic structure must be calculated with high precision, and the other is that the maximum energy of photons E_γ^{max} accompanied with the capture must be determined independently. However, it is possible to determine the neutrino mass with accuracy about 10-30 eV by using the M1, M2, N1, electron capture in ^{163}Ho (7/2-)$\rightarrow$^{163}Dy (5/2-) or the L1, L2, M1, M2 electron capture in ^{157}Tb$\rightarrow$^{157}Gd (5/2-) if the newly measured Q values of them are correct. Particularly, with the aid of the L1, L2, M1, M2 electron capture in ^{157}Tb$\rightarrow$^{157}Gd(3/2-), neutrino mass can be determined independent of the nuclear matrix and the electron wave functions.

Key words Neutrino mass, Electron capture, ^{157}Tb, ^{158}Tb, ^{163}Ho.

THREE CRYSTAL PAIR SPECTROMETER

[English abstract of article by Zeng Xiantang [2582 2009 1016], et al., of Institute of Atomic Energy, P.O. Box 275, Beijing]

[Text] Using a HPGe (ϕ4.3×2.5cm) as the central detecter and two cylindrical NaI(T1) (ϕ12.5×10.0cm) as the outside detectors, a three crystal pair spectro-meter is built up. In order to increase double escaping efficiency and improve energy resolution, the central HPGe is mounted transversely, so that γ rays are incident upon the side of HPGe cylinder. The spectrometer is operated in single mode below 3 MeV and in pair mode above 2 MeV. For ^{24}Na 2.754 MeV γ ray double escaping peak, the ratio of the peak to adjacent continual background is 8.5 in single mode, 350 in pair mode, the actual improvement factor is 41. The influence of annihilation photon "window" over the shape of double escaping peak is tested.

Key words Pair spectrometer.

DEPTH PROFILING OF TRITIUM IN TITANIUM TRITIDE TARGETS

[English abstract of article by Zhao Guoqing [6392 0948 1987], et al., of Fudan University, Shanghai]

[Text] Depth profiles of tritium in titanium tritide targets are determined by using Rutherford backscattering technique and Bragg's additivity rule of the stopping cross sections for T-Ti targets. For backscattering spectra of 2 MeV ^{4}He$^+$ ions from two T-Ti targets, atom ratios of tritium to titanium at the surface of samples are calculated to be 1.50 ± 0.10 and 0.94 ± 0.08 respectively. Depth distributions of atom ratio of T/Ti in a region of 8000Å under the surface of samples are nearly uniform with a discrepancy of ±3 percent. The detection limit of T in the T-Ti targets is ~40 at percent. The depth resolution of this analytical method is about 300Å at the surface region.

ON THE THEORY OF A KIND OF PROBABILISTIC METRIC SPACES WITH APPLICATIONS

[English abstract of article by Zhang Shisheng [1728 4258 3932]]

[Text] Our purpose is to introduce the concept of C-probabilistic metric spaces. By virtue of its some basic properties, we obtain some new fixed point theorems. (Paper received 25 Apr 84.)

REFERENCES

[1] B.Schweizer, A.sklar, Probabilistic Metric Spaces, North-Holland, New york, Amsterdam, Oxford, 1982.

[2] 张石生 中国科学, A辑, 1983,495—504.

[3] V.M.Sehgal, A.T.Bharucha-Reid, Mathematical Systems Theory, 62(1972), 97—I02..

COMPACTNESS IN FUZZY UNIT INTERVAL

[English abstract of article by Dian Jianwei [0368 1696 0251]]

[Text] Set L be a completely distributive lattice which has a smallest element 0, a largest element $1(0 \neq 1)$ and a reverse order involution $\alpha \rightarrow \alpha'$ ($\alpha \in L$).

Let $L^c = \{\Psi \in L : \Psi$ is comparable to each $\alpha \in L\}$. Then, i) the fuzzy unit interval is α-compact, for all $\alpha \in L;^c$ ii) I(L) may be a non-α^*-compact space, if L be ortho-complementary and $0 < \alpha \leqslant 1$. (Paper received 21 Dec 83.)

REFERENCES

[1] Hutton, B., J.Math.Anal.Appl., 50(1975), 74—79

[2] Gantner, T.E., Steinlage, R.C. and Warren, R.H., J.Math.Anal.Appl., 62(1978) 547—562

[3] 刘应明，科学通报（数、理、化专辑），(1980),33—35

Metallurgy

THE ELECTRICAL RESISTANCE STUDY OF AMORPHOUS ALLOY $Fe_{80} B_{20}$ IN THE PROCESSES OF CRYSTALLIZATION AND STRUCTURAL RELAXATION

[English abstract of article by Wang Yunxin [3769 6663 2450], et al.]

[Text] The change of resistance in the process of ascending temperature for metallic glass $Fe_{80}B_{20}$ was measured as a function of temperature by four-terminal method. Both structure relaxation process (lower temperature region) and crystallization process (high temperature region) were observed. In the process of structure relaxation, $\Delta p/p$ varies with temperature as T^{-1}, but deviates linear in the temperature range of 450~550K and the maximum deviative of $\Delta p/p$ from T^{-1} is about 0.5%p(R.T)

The amorphous/crystalline transformation takes place in two stages and in distinct regions of temperature. The isothermal crystallization kindics was studied in these two distinct regions of temperature and the crystallization activation energy is 3.0ev and 1.0ev respectively. (Paper received Oct 85.)

REFERENCES

[1] 林德明等，贵金属，2(1981), 4, 24.

[2] F. J. Ohkawa, *J. Phys. SOC. Japan*, 44(1978), 1105.

[3] D.A.Newetal, *J. Appl. Phys.*, 50(1979), 1654.

[4] N. Banerjee et al., *Phys. Rev.*, 24(1981), 6801.

[5] J. Orehotsky, *J. Appl. Phys.*, 50(1979), 7612.

STRENGTHENING AND TOUGHENING MECHANISMS OF MARAGING STAINLESS STEEL

[English abstract of article by Cao Yang [2580 7122], et al., of Dept. of Materials Science and Engineering]

[Text] The strengthening and toughening mechanism of maraging stainless steel after thermo mechanical treatment (TMT) has been investigated with steel 00Cr12Ni9Cu2TiNbBeRE. According to experimental data and theoretical analysis, the quantitative relationships are obtained both between yield strength and parameters of TMT, and between yield strength and microstructural parameters. By means of energy-analysis, an expression of the impact toughness and micro-structural parameters has been given. Hence the microstructural factors controlling strength and toughness are precipitate, martensitic microstructure and cellular substructure. A theoretical foundation has finally been obtained for the design of treatments' processing. (Paper received 1 Apr 85.)

REFERENCES

[1] Anti-Corrosion, Methods and Marterials, Vol.1, No.2, (1966), 7.

[2] Crawford, W. M.; Contractor, G. P., JISI, Vol.207, No.12, (1969), 1642.

[8] Caton, R. L., Cobalt, Vol.6, No.55, (1972), 92.

[4] Cadowaki, E. P., Mct. Eng. Quart., Vol.2, No.2, (1972), 47.

[5] 许清池；陈复民；李困俊；姚家鑫；高后秀；秦世麒，仪表材料，Vol.15, No.1, (1984), 14.

[6] 曹 阳，形变热处理对 $00Cr12Ni9Cu2TiNbBeRE$ 马氏体时效不锈钢组织和性能影响的研究，天津大学硕士论文，1984.

[7] McMahon, J.; Thomas, G., Third Intern. Conf. on Strength of Metals and Alloys, 'Microstructure and Design of Alloys' , Vol.1, 1973, P.180.

[8] May, I. L.; Schetky, L. M., Copper in Iron and Steel, JOHN WILEY & SONS, 1982, P.21.

[9] Honeycomb, R. W.; Pickering, F. B., Metall. Trans., Vol.3, No.5, (1972), 1099.

[10] 冈田康孝；邦武立郎，鉄と鋼，Vol. 67, No.6, (1981), 791.

[11] Norström, L. - Å., Scand. J. Mctallurgy, Vol.5, No.4, (1976), 159.

[12] Bergström, Y.; Josefsson, Å., Scand. J. Metallurgy, Vol.3, No.4, (1974), 259.

[13] Naylor, J. P., Metall. Trans., Vol. 10A, No.7, (1979), 861.

[14] Gleiter, H., Acta Mctall., Vol.15, No.8, (1967), 1223.

[15] Gleiter, H.; Hornbogen, E., Mater. Sci. Eng., Vol.2, No.6, (1968), 285.

[16] Kelly, A., Intern. Mater. Rev., Vol.18, №1, (1973), 31.

[17] Kocks, U. F., Acta Metall., Vol.6, №1, (1958), 85.

[18] 赵志业，金属塑性变形与轧制理论，冶金工业出版社，1980，*P*.28.

[19] 肖纪美，金属的韧性与韧化，上海科学技术出版社，1980，*P*.260.

RELATIONSHIP BETWEEN HEAVY METAL POLLUTION AND WATER PRODUCTIVITY IN XIAMEN ESTUARINE HARBOR

[English abstract of article by Wu Yuduan [0702 3842 4551], et al., of Xiamen University]

[Text] Based upon the results of simulation experiments and annual observation on the effect of Cr, Cu, Hg, Zn, on diatom (Chaetoceros spp., Skeletonema costatum, and Melosira sulcata) growth, many physico-chemical parameters are found to play a considerable role in the toxicity and accumulation of metal in organisms especially in laboratory experiment. The Mesopic level in water environment is related to phytoplankton growth, whereas the higher nutrient level could have a negative impact on diatom production. Several metals mentioned above coexist in the investigated region and exert an antagonistic effect.

We employed the mathematical statistics-orthogonal design in simulation experiments of 6 parameters (Cr, Cu, Hg, Zn, O.M., N/P) with three levels per parameter system for diatom culture. It showed that (1) the range of content of heavy metals is as follows: Cr 10-30, Cu 0.5-50, Hg 0.02-1.5, Zn 20-100 and (2) the optimal nutrient contents: N 100-250, P 25-40, O.M. 100,000 (all in ppb).

We observed these parameters, total phosphorus content, ratio of T-N/T-P (in atom) and Chlorophyl content in the investigated region for one year, and found that ranges of these data were 24-35ppb-P, 10-18T-N/T-P, and 10-20 mgm^{-3} Chlorophyl (cell numbers of phytoplankton are about 10^6 cells/L) in all probability. (Paper received 8 Jul 84.)

REFERENCES

[1] Betz, M., 1977. Investigations on the simultaneous uptake and release of mercury by *Dunaliella tertialecta. Mar. Biol.* 41(1): 89—97.

[2] Fisher, N. S. and J. G. Fabris, 1982. Complexation of Cu, Zn, and Cd by metabolites excreted from marine diatom. *Mar. Chem.* 11(3): 245—255.

[3] Fisher, N. S., 1981. Heavy metals and marine phytoplankton correlation of toxicity and sulphydroyl binding. *J. Phycol.* 17(2): 108.

[4] Fisher, N. S. and D. Frood, 1980. Heavy metals and marine diatoms: influence of DOC on toxicity and selection for metal tolerance among four species. *Mar. Biol.* 59(2): 85—93.

[5] Gaering, J. J., D. Boisseau and D. Mattor, 1977. Effects of Copper on silicic acid uptake by a marine phytoplankton population: CEPEX. *Bull. Mar. Sci.* 27(1): 58—65.

[6] Hollibaugh, J. T., 1980. A comparison of the acute toxicities of ten heavy metals to phytoplankton for Saunich Inlet, B. C. Canada. *Estua. Coast. Mar. Sci.* 10(1): 93—105.

[7] Kuiper, J., 1982. Ecotoxicological experiments with marine plankton communities in plastic bags. *In*: Marine Mesocosms. Grice, G. D. and M. R. Reeve ed. Charpter 13, Springer-Verlag N. Y. Inc. pp. 357—384.

[8] Malone, T. C., 1982. Factors influencing the fate of sewage-derived nutrients in the lower Hudson estuary and N. Y. Bight. *In*: Ecological Stress and the N. Y. Bight: Science and Management. Mayer, G. F. ed. Estuarine Research Federation Columbia, S. Carolina. pp. 389—412.

[9] Patin, S. A. 1982. Effect of pollutants on cultured unicellular marine algae. *In*: Pollution and the Biological Resources of the Oceans. Charpter 6, Butterworth Scientific. pp. 80—109.

[10] Rueter, Jr. J. G. and F. M. M. Morel 1981. The interaction between Zinc deficiency and copper toxicity as it affects the silicic acid uptake mechanisms in *Thalassiosira pseudonana. Lim. Ocean.* 26(1): 67—73.

[11] Rueter, Jr. J. G., S. W. Chisholm and F. M. M. Morel, 1981. Effects of copper toxicity on silicic acid uptake and growth in *Thalassiosira pseudonana*. *J. Phycol.* **17**(3): 270—278.

[12] Sunda, W. G. and R. R. L. Guillard, 1976. The relationship between cupric ion activity and the toxicity of copper to phytoplankton. *J. Mar. Res.* **34**(1): 34—40.

[13] Thoms, W. H., J. T. Hollibaugh, D. L. R. Seibert et al, 1980. Toxicity of a mixture of ten metals to phytoplankton. *Mar. Ecol. Prog. Ser.* **11**(3): 213—220.

[14] Yamada, M., 1982. Effects of industrial effluents containing organic material such as dyestuff on the growth of several species of marine phytoplankton. *Bull. Jap. Soc. Sci. Fish.* **48**(10): 1453—1456.

CHARACTERISTICS OF TIDAL CURRENT AND SEDIMENTATION OF SUSPENDED LOAD ON TIDAL MUD FLAT IN JIANGSU PROVINCE

[English abstract of article by Shang Renshun [1728 1804 7311] of Nanjing University]

[Text] The prograding tidal mud flat in Jiangsu Province is perhaps the widest and longest in China. It belongs to the open (north part) or semi-open (south part) tidal flat and is of moderate-high tidal range.

Four profiles of tidal mud flat in Jiangsu Province were dealt with. A 25-hours survey of the whole tide hydrography was carried out for each profile. Based on these investigations, the characteristics of tidal current and concentration of suspended sediment on tidal mud flat were analyzed. The distribution of concentration of suspended sediment was different from that of current velocity along the profiles, the concentration of suspended sediment was highest near low water line but decreased toward the sea and the high water line, however the velocity decreased from offshore to high water line. The tidal current was rectilinear in offshore tidal channel, but rotary on tidal mud flat; and the direction of residual transport of water and sediment on upper intertidal zone contrasted strikingly with that on lower intertidal and subtidal zone.

The lag mechanism could explain some features, but not all the main phenomena of sedimentary processes taking place on tidal flat in Jiangsu Province unless introducing wave and storm surge effect. It is notable that the horizontal residual circulation of water and suspended load is present on tidal flat. As a result, the wide tidal mud flat is divided into a series of longshore cells which form individual dynamic units. (Paper received 9 Oct 84.)

REFERENCES

[1] 任美锷、张忍顺、杨巨海，1984。江苏王港地区淤泥质潮滩的沉积作用。海洋通报 3(1): 40—54。

[2] 任美锷、张忍顺、杨巨海等，1983。风暴潮对淤泥质海岸的影响。海洋地质与第四纪地质 3(4): 1—24。

[3] 张忍顺，1984。苏北黄河三角洲及滨海平原的成陆过程。地理学报 39(2): 173—184。

[4] Bayliss-Smith, T. P., R. Healey, R. Lailey et al., 1979. Tidal flows in salt marsh creek, *Estuar. Coast. Sci.* 9: 235—255.

[5] Carling, P. A., 1982. Temporal and spatial variation in intertidal sedimentation rates. *Sedimentology* 29(1): 17—23.

[6] Collins, M. B., C. L. Amos and G. Evans, 1981. Observation of some sediment-transport processes over intertidal flat. *Sediment* 5: 81—98.

[7] Göhren, H., 1976. Currents in tidal flats during storm surges. Proc. of the 15th Coastal Engineering Conf. New York, American Society of Civil Engineers. vol. 2, pp. 959—970.

[8] Häntzschel, W., 1939. Tidal flat deposits, Holocene Tidal Sedimentation (Ed. Klein, G. dev.), DH and R. pp. 14—24.

[9] Inman, D. L., and B. M. Brush, 1973. The coastal challenge. *Science* 181: 20—32.

[10] Kestner, F. J. T., 1975. The Loose-boundary regime of the Wash. *The Geograph. J.* 141(3): 388—414.

[11] Pethick, J. S., 1980. Velocity surges and asymmetry in tidal channel. *Estuar. Coast. Mar. Sci.* 11 (3): 331—345.

[12] Postma, H., 1954. Hydrography of the Dutch Wadden Sea. *Arch. Néerl. Zool.* 10: 405—511.

[13] Postma, H., 1961. Transport and accumulation of suspended matter in the Dutch Wadden Sea. *Netherlands J. Sea Res.* 1(1/2): 148—190.

[14] Postma, H., 1967. Sediment transport and sedimentation in the Estuarine Environment. Estuarine (Ed. by H. Lauff). AAS. pp. 158—179.

[15] Postma, H., 1982. Hydrography of the Wadden Sea: Movements and Properties of Water and Particulate Matter. Printed in the Netherlands. Chapt. 2, pp. 18—19; 34—47.

[16] Ren Meie, Zhang Renshun and Yang Juhai, 1983. Sedimentation on tidal mud flat of Wanggang Area, Jiangsu Province, China. *Collected Oceanic Works* 6(2): 84—108.

[17] Straaten, K. N. J. U. Van and Ph. H., Kuenen, 1958. Tidal action as a cause for clay accumulation. *J. Sed. Petrol.* 28: 406—413.

[18] Wells, J. T., 1978. Suspension and transportation of fluid mud by Solitory-Like waves. Proc. of 16th Coastal Engineering Cof. New York, American Society of Civil Engineers. vol. 2, pp. 1932—1952.

[19] Wells, J. T., 1983. Dynamics of coastal fluid muds in low-, Moderate-, and high-tidal range environment. *Can. J. Fish. Aquat. Sci.* 40(Suppl. 1): 130—142.

A PRELIMINARY STUDY ABOUT SEPARATION AND FORECAST OF THE CURRENT MASS TRANSPORT

[English abstract of article by Shen Lingyun [3088 0407 0061] of Nanjing Chemical Technological School, and Zhao Baoren [6392 0202 0088] of Institute of Oceanology, Academia Sinica, Qingdao]

[Text] It is presumed that the mass transport of current is composed of constant current and wind drift current, of which the mass transport of the constant current is invariable in a short period, and that the wind factor and current deviation angle of the wind drift mass transport vary with wind direction. The wind factor with current deviation angle of mass transportation can therefore be decomposed into north wind factor with current deviation angle and east wind factor with current deviation angle. In general the above four elements of the wind drift mass transport as well as two constant current elements are called the six elements of current mass transport.

With three sets of observations of wind and current vectors and depth and density made at different times and by solving six linear algebraic equations, the six elements of mass transport can be obtained. From the obtained formula for the wind factors and current deviation angles of the mass transport it is shown that the orbit of the current vectors is an ellipse when the wind direction varies.

All the previous methods for the separation of the wind drift current are confined to current vectors. We introduce the concept of current mass transport for the separation of the drift current. The previous methods for separations of the wind drift current are special cases of the present method. Without the influence of density, it turns to volume separation method, yet with the volume transport of the unit thickness only, it turns to the method of the separation of wind drift current ellipse. In the deep sea area far from coast, when the wind factor and current deviation angles are independent of wind direction a cycle will be found. So the present method can be regarded as a generalization of all previous methods of residual current separation.

As an example, the wind factors and the current deviation angles are calculated and tabled for every layer and for all the 16 azimuths of the station A near the coast in the northern East China Sea. According to the wind forecast, the wind drift current can be predicted by the tables and simple calculation. This method is useful for predicting the current in the lake also.

Comparing the predicted residual current with measured one, they are in good agreement. The errors are 22 percent for the magnitudes and 31° for directions of the residual current in average, respectively. (Paper received 21 Nov 84.)

REFERENCES

[1] 赵保仁,1982。确定近岸风海流椭圆的一个简单方法。海洋科学 1982(2)41—43。

[2] 赵保仁,1982。局地风对黄海和东海近岸浅海海流影响的研究。海洋与湖沼 13(6): 479—490。

[3] Nansen, F., 1902. The Norwegian North Polar Expedition 1893—1896. Vol. III, pp. 358—359.

[4] Sverdrup, H. U., 1936. The Wind-Drift of the Norwegian North Polar Expedition with the "Mond" 1918—1925. pp. 18—19.

AN EMPIRICAL FORMULA FOR SCATTERING PROPERTY OF FILM FOR PSEUDOCOLOR ENCODING OF IMAGE

[English abstract of article by Chen Zexian [7115 3419 0341] and Su Xianyu [5685 7359 3254]]

[Text] Real-time pseudocolor effect resulted from scattering of film emulsion is described. The scattering properties of Chinese-made medical X-ray film is studied, and an empirical formula for describing the properties is given. The experimental result is in a good coincidence with theoretical analysis. The real-time pseudocolor enhancement technique is used for processing of medical X-ray photograph, the resulting output hue curve and some other results are given. (Paper received 27 Sep 84.)

REFERENCES

[1] H.K.Liu, J.W.Goodman, S.P.I.E., 83(1976), 125.
[2] F.T.S.Yu, A.Tai and H.Chen, J.Opt., 9(1978), 269.
[3] T.H.Chao, S.L.Zhuang, F.T.S.Yu, Opt.Lett., 5(1980), 230.
[4] 郭履容等, 光学学报, 4(1984), 145.
[5] R. Arizaga, N. Bolognini, H. J. Babal, E. E. Siere and M. Garavaglia, Opt.Commun., 43(1982), 12.
[6] J.A.Mendez and M.Nieto-vesperinas, Appl.Opt., 22(1983), 2068.
[7] P.Beckmann and A.Spizzichino, The Scattering of Electromagnetic Waves from Rough Surfaces, Pergamon, New York, 1963.
[8] H.M.Smith, Appl. Opt., 11(1972), 26.

A DOUBLE CORRELATION TECHNIQUE FOR COUNTING RED BLOOD CELLS

[English abstract of article by Zhong Yongbi [6988 3057 4310], et al.]

[Text] The optical double correlation is a new technique not using a holographic matched filter. The principle applied to erythrocyte counting and the experimental system are described. The experimental results are given. The experimental results are in agreement with the theoretical analysis. (Paper received 2 Nov 84.)

REFERENCES

[1] J.E.Ward, F.P.Carlson and J.D.Heywood, IEEE Trans.Biom.Eng.BME-21(1974), 12.

[2] S.Jutamulia, H.Fujii and T.Asakura, Opt Commun., 43(1982), 7.

[3] 赵霖, 张洪钧, 物理学报, 31(1981), 143.

THEORETICAL STUDY ON STABILIZATION OF F_2^+ CENTERS BY O^{--} IN LIF CRYSTALS

[English abstract of article by Ruan Yongfeng [7086 3057 0023] and Wan Liangfeng [8001 5328 7364] of Department of Physics]

[Text] This paper studies the stabilization of F_2^+ centers by O^{--} in LiF crystals. According to the pattern of energy cycle suggested in this paper the stable energy is calculated by means of HWW model, point charge model and quantum-mechanics perturbation method. The results show that O^{--} reduces the electron affinity energy of F_2^+ centers on the one hand and increases their binding energy on the other hand. It is because of this dual nature that the stability of F_2^+ centers rises in LiF crystals doped with oxygen. The theoretical value of the stable energy given is in good agreement with the experimental one in the condition of chosen parameter. So far no similar work has been reported. (Paper received 12 Mar 86.)

REFERENCES

[1] Б.Д.Лобонов и др., Изв. ВУЗ, физика, 4, 81, (1978)

[2] 阮永丰 万良风 郭绍章，《掺氧LiF晶体中F_2^+心稳定性的实验研究》，发表于《中国激光》第10卷第5期第269页（1983年）及《Chinese physics》(edited by American Institute of Physics) Vol.3, No.4, P.1014

[8] В.А.Архангельская и др.,Квантовая Электроника, 7,1141, (1980)

[4] 郑立行等，《LiF晶体中F_3^+心的形成》，全国第七届晶体生长与材料会议论文，1985年10月，烟台

[5] R. C. Herman, M. C. Wallis, R. F. Wallis, Phys. Rev., 103, 87, (1956)

[6] M. A. Aegerter & F. Lüty, Phys. Stat. Sol. (b), 43, 227, (1971)

[7] 何铨，《F_2^+心电子的能态》，上海市物理学会1983年物理学应用研究成果交流报告会论文，1983年7月

[8] J. H. Crawford, J. Phys. Chem. Sol., 31, 399, (1969)

[9] 唐敖庆等，《量子化学》，科学出版社出版，（1982年）

[10] J.C. Slater, 《Quantum Theory of Molecules and Solids》Vol.1, App.6

[11] W. Kolos, L. Wolniewize, J. Chem. Phys., 43, 2429; (1965) and 45, 509 (1966)

[12] D.R. Bates, Ledsham and Stewart, Phil. Trans. Roy. Soc. (London), A246, 215, (1954)

[13] И.А. Парфпанович и др., Изв. Академии наук СССР, Сер. Физ. 43, 1125, (1979)

[14] Axel Meyer, R. F. Wood, Phys, Rev., 133, A1436, (1964)

[15] L. F. Mollenauer, "Color Center Lasers", in 《Methods of Experimental Physics》Vol.15, Part B, edited by Tang. C. L., New York, (1979)

END